Universidade de São Paulo
Instituto de Física

De teorias de *higher gauge* abelianas a fases quânticas da matéria

Lucas Nixon Queiroz Xavier

Orientador: Prof. Dr. Paulo Teotônio-Sobrinho

Tese de doutorado apresentada ao Instituto de Física da Universidade de São Paulo, como requisito parcial para a obtenção do título de Doutor em Ciências.

Banca Examinadora:
Prof. Dr. Paulo Teotônio-Sobrinho - Orientador (IFUSP)
Prof. Dr. Julio Antonio Larrea Jimenez (IFUSP)
Prof. Dr. Hugo Luiz Mariano (IME USP)
Prof. Dr. Eduardo Peres Novais de Sá (UFABC)
Prof. Dr. Eliezer Batista (UFSC)

São Paulo
2022

FICHA CATALOGRÁFICA
Preparada pelo Serviço de Biblioteca e Informação
do Instituto de Física da Universidade de São Paulo

University of São Paulo
Physics Institute

From abelian higher gauge theories to quantum phases of matter

Lucas Nixon Queiroz Xavier

Supervisor: Prof. Dr. Paulo Teotônio-Sobrinho

Thesis submitted to the Physics Institute of the University of São Paulo in partial fulfillment of the requirements for the degree of Doctor of Science.

Examining Committee:
Prof. Dr. Paulo Teotônio-Sobrinho - Supervisor (IFUSP)
Prof. Dr. Julio Antonio Larrea Jimenez (IFUSP)
Prof. Dr. Hugo Luiz Mariano (IME USP)
Prof. Dr. Eduardo Peres Novais de Sá (UFABC)
Prof. Dr. Eliezer Batista (UFSC)

São Paulo
2022

Acknowledgements

Abstract

Topological phases of matter are gapped quantum phases of matter that cannot be described by Landau's theory of symmetry breaking. In 2-dimensions, the standard examples of Hamiltonian models of topological order are given by Kitaev's *Quantum Double Models* (QDMs). In [1], a generalization of Abelian QDMs for any D-dimensional space was introduced through *Abelian higher gauge theories* (AHGT). These theories require as input a geometrical chain complex describing the discretization of the underlying space and a generalization of a particular example of a higher gauge group in the form of a group chain complex. The Hamiltonian models built based on Abelian higher gauge theories are examples of topological order. In this framework, to find examples of models that go beyond topological order, it is necessary to modify some of the underlying assumptions of Abelian higher gauge theories. In this thesis, we study how some modifications in an AHGT affects the physics of the resulting quantum phases of matter. By modifying the geometrical chain complex, we find that the resulting Hamiltonian models describe quantum phases with *subsystem symmetries*. In particular in 3-dimensions, this modification results in a *subsystem symmetry enriched topological phase* [2]. Moreover, by introducing classical external fields that resemble some of the dynamical quantum degrees of freedom encountered in an AHGT, we find that the resulting Hamiltonian models describe quantum phases whose ground states measure geometric properties of the underlying space. In particular, the ground states depend on *shortest paths* of the manifold and can thus be used to compute shortest paths between points in the space.

Keywords.- Gauge Theories, Topological Order, Quantum Phases of Matter

Resumo

Fases topológicas da matéria são fases quânticas da matéria com *gap* que não podem ser descritas pela teoria da quebra de simetria de Landau. Em 2-dimensões, os exemplos padrões de modelos Hamiltonianos de ordem topológica são dados pelos *Modelos Duplo Quânticos* (MDQs) de Kitaev. Em [1], uma generalização de MDQs Abelianos para qualquer espaço D-dimensional foi introduzida por meio do uso de *teorias de higher gauge Abelianas* (THGA). Essas teorias são construídas com base em um complexo de cadeias geométrico, que descreve a discretização do espaço, e uma generalização de um exemplo particular de um grupo de *higher gauge* na forma de um complexo de cadeias de grupo. Os modelos Hamiltonianos construídos com base em teorias de *higher gauge* Abelianas são exemplos de ordem topológica. Para encontrar exemplos de modelos que vão além de ordem topológica, é necessário modificar algumas das hipóteses por trás das teorias de *higher gauge* Abelianas. Nesta tese, estudamos como algumas modificações em uma THGA afetam a física das fases quânticas da matéria resultantes. Modificando o complexo de cadeias geométrico, obtivemos modelos Hamiltonianos que descrevem fases quânticas com *simetrias de subsistema*. Em particular, em 3-dimensões, essa modificação resulta em uma *fase topológica enriquecida por simetrias de subsistema* [2]. Além disso, introduzindo campos externos clássicos que se assemelham a alguns graus de liberdade quânticos encontrados em uma THGA, obtivemos modelos Hamiltonianos que descrevem fases quânticas da matéria cujos estados fundamentais medem propriedades geométricas do espaço subjacente. Mais especificamente, tais estados fundamentais dependem de *caminhos mínimos* da variedade, e portanto podem ser utilizados para calcular caminhos mínimos entre pontos no espaço.

Palavras-chave.- Teorias de Gauge, Ordem Topológica, Fases Quânticas da Matéria

Contents

Chapter 1

Introduction

The classification of phases of matter through symmetry groups is known as *Landau's theory* [3, 4]. It describes with great precision what happens to various physical systems, from water phase transitions to the formation of crystalline structures, from magnetic materials to superconductors and superfluids. However, the discovery of the *fractional quantum Hall effect* (FQHE) [5, 6, 7] showed that not every phase of matter can be described by Landau's paradigm. In the FQHE, different quantum phases of matter have the same symmetries and no local measurement can distinguish the phases. That is, there is no local order parameter that can be used to characterize each phase. The states in the FQHE are *topological phases of matter*, and the FQHE is an example of a system with *topological order* [8, 9].

Although there is no precise definition of what is topological order, systems that possess it tend to present certain common characteristics. An important property of systems with topological order is the presence of degenerate ground states that form a subspace of the total Hilbert space. The dimension of this subspace, known as the *ground state degeneracy GSD*, is a *topological invariant* of the underlying space [8, 10]. For example, in 2-dimensions, if we define a quantum system with topological order over a surface of genus g, the dimension of the ground state subspace will be a function of g. The *Toric Code*, which we will discuss in depth in chapter 2, has $GSD = 4$ when defined over a 2-torus and $GSD = 1$ when defined over a sphere. In contrast, the 2-dimensional Ising model has the same number of ground states ($GSD = 2$) when defined over a sphere or over a 2-torus.

Moreover, the ground states of a system with topological order exhibit *long-range entanglement* [11]. Long-range entangled states are so different from product states that they cannot be transformed into product states by local unitary transformations. In a sense, there are quantum

correlations among the degrees of freedom of the system at all length scales. Another characteristics of systems with topological order is that they possess a *topological entanglement entropy*. That is, suppose we divide a system with topological order into two regions, A and B, and calculate the *entanglement entropy* S_A of the ground state. The entanglement entropy S_A is defined as the von Neumann entropy of the reduced density matrix ρ_A of A, that is,

$$S_A = -\text{Tr}\left(\rho_A \log \rho_A\right), \tag{1.0.1}$$

and it gives a notion of how pure the state ρ_A is. The higher S_A is, more entangled is the state ρ_A. By doing that, we see that S_A is the sum of two terms. The first term depends on the boundary ∂A, and is in fact the the so-called *area law* of entanglement entropy [12]. The other term is a constant that depends on the topology of both A and ∂A [13, 14, 1]. This term, called *topological entanglement entropy*, indicates the presence of non-local correlations among the degrees of freedom of the system.

Another characteristics of systems with topological order in $(2+1)$-dimensions is the presence of *anyons*. These are *quasiparticles* with exotic statistics. For instance, the permutation of two bosons changes the system's wave function by a factor of $e^{2\pi i} = 1$, while the permutation of two fermions generates a phase factor of $e^{\pi i} = -1$. The permutation of anyons, on the other hand, generates a phase factor of $e^{i\phi}$, where $0 < \phi < \pi$. Moreover, the permutation of two *non-Abelian anyons* generates a rotation on the wave function by an unitary matrix U. The presence of anyons makes systems with topological order potential platforms for the realization of *fault-tolerant quantum computation* [15, 16].

Topological order and symmetry can coexist, giving rise to quantum systems with different physics both from pure topological order and pure symmetry-breaking order. Systems with topological order and global symmetries present phases known as *symmetry-enriched topological phases* (SET). A system is in a SET phase if, by breaking the symmetry, the system remains in a topological phase [17, 18, 19, 20]. The FQHE states are examples of SET phases, with a global $U(1)$ charge conservation symmetry.

A great number of systems with topological order are given by *lattice gauge theories* [21]. In 2-dimensions, there exists a classification of topological order in terms of *string net models* [22]. Such models are lattice gauge theories based on *fusion categories* [23]. In 3-dimensions however, there is no general way of constructing models with topological order. Examples such as *fracton* phases, which we will discuss shortly, show that the physics of topological order can

be much richer in higher dimensions. To access these different behaviors, there is a need to use different mathematical tools more suited to higher dimensions. This has motivated plenty of research groups to search for higher-dimensional generalizations beyond gauge theories to construct models of topological order.

A possibility is to make use of generalizations of the group structure and study models based on n-groups (see appendix B). These algebraic structures are generalizations of groups to higher dimensions based on a geometric point of view of the group operations. For example, a 2-group has two kinds of products, a horizontal one and a vertical one, satisfying a particular consistency relation. We can make use of 2-groups [24] to construct *higher gauge theories* [25]. This allows us to build lattice higher gauge theory models with topological order in higher dimensions. In [26] and independently in [27, 28], an exactly solvable model of topological order in 3-dimensions was built based on 2-groups. In [1], a general way of constructing exactly solvable lattice Abelian higher gauge theory models with topological order in D-dimensions was introduced. This formalism allows to find a general formula for the GSD in any dimension D in terms of topological invariants of the underlying manifold. Moreover, using this formalism, a general formula for the *topological entanglement entropy* in any dimension D can be derived in terms of topological invariants of the underlying space [1].

Recently, there were discovered new types of long-range entangled quantum phases of matter with properties that differ from the ones presented by topological phases. In these new quantum phases, ground states cannot be identified by measurements of local operators, just as in topological phases. However, their ground state degeneracy depends on the system size, which means that the GSD is not a topological invariant. Moreover, such phases host quasiparticles with mobility restrictions. That is, these quasiparticles can only move along some subspace of the system, such as a curve or a plane. Some of them, called *fractons*, are completely immobile, in the sense that if we try to move a fracton, more excitations are created in the lattice and the energy of the system is increased. These new quantum phases of matter are known as *fracton phases* [29, 30, 31, 32, 33].

In this thesis, we analyse how modifications in some assumptions in the general formalism introduced in [1] affect the physics of the resulting quantum Hamiltonian models. In particular, we analyse how modifications to the geometrical and group degrees of freedom impact the dynamics of the derived Hamiltonian models. We find that changes in the geometrical inputs to an Abelian higher gauge theory result in gauge theories with *subsystem symmetries*. These

are symmetries that act only over a subspace of the manifold. These gauge theories are used to build what we call *fractonlike* models. These are models in which the ground state degeneracy has a subextensive dependence on the system size. Moreover, in these models, there are excitations of the *fracton* type. Namely, there are some excitations which are immobile, in the fracton sense. However, in fractonlike models, local perturbations that break subsystem symmetries can be employed to destroy the subextensive ground state degeneracy. As an example of fractonlike model in $3D$, we construct one of the first examples of *subsystem symmetry-enriched topological phase* [2] found in the literature. This phase reduces to the $3D$ *Toric Code* when subsystem symmetry is broken.

Furthermore, by changing the dynamics of the degrees of freedom of Abelian higher gauge theories, we construct models whose long-range entangled ground states depend on *geometric* properties of the manifold. In such models, the ground states can be used to *find shortest paths* between subspaces of the manifold. By introducing an appropriated coupling constant, an Abelian higher gauge theory in any spatial D-dimensions can be constructed such that its dual theory finds the *shortest path* between two predetermined vertices in the lattice. Therefore, these models can be considered as *quantum codes* to find minimal distances in a lattice.

The rest of this thesis is divided into three chapters. In chapter 2, we motivate the construction of the general formalism introduced in [1] by reviewing Kitaev's *Quantum Double Models*. In section 2.1, we review the physical properties of the standard example of a Quantum Double Model, which is the Toric Code. In section 2.2, we review the general theory of Quantum Double Models, focusing in finding a general formula for the ground state degeneracy of any Quantum Double Model and showing its dependence on the topology of the underlying manifold.

In chapter 3, we review the general formalism of Abelian higher gauge theories introduced in [1]. In section 3.1 the main aspects of the theory are revisited and in section 3.2 some examples of models are exhibited.

In chapter 4, the main results of the thesis are described. First, in 4.1.3, the procedure to construct subsystem symmetry-enriched topological phases from Abelian higher gauge theories is outlined and some examples in $2D$ and in $3D$ are given. Particular focus is given to a $3D$ model, which is an intuitive model of subsystem-symmetry enriched topological phase. In section 4.2, Hamiltonian models of quantum phases based on Abelian higher gauge theories whose ground states measure geometric properties of the space are built. Some examples that

resemble familiar models are given in $2D$ and $3D$. Finally, a model whose ground state finds the shortest path between two points in a lattice is described.

In chapter 5, we present overview of the results found in this thesis and point to some open problems and next steps to be addressed in future works.

Chapter 2

Quantum double models

The formalism of Abelian Higher Gauge Theories generalizes to any spatial dimensions a class of models in $(2+1)d$ called the *Quantum Double Models* (QDM) [15, 34, 35, 36]. These models are Hamiltonian realizations of lattice gauge theories in $(2+1)d$ that exhibit topological order. Also, the ground state of such models behaves like error correcting codes, which makes them interesting from the quantum computation point of view [37]. Before we introduce the general formulation of QDM with arbitrary finite gauge groups G, let's build intuition by reviewing a standard example: the *Toric Code* [38, 15].

2.1 Toric code

The Toric Code is the standard example of an exactly solvable Hamiltonian realization of a lattice gauge theory describing a topological phase of matter. It is also an important example of an error correcting code in topological quantum computation. In this section, we discuss its main physical properties as a model of topological order.

2.1.1 The model

Consider a 2-dimensional manifold M discretized by a regular square lattice K. The lattice K is composed by a set of vertices K_0, a set of links K_1 and a set of plaquettes K_2. A *qubit* degree of freedom sits at every link $l \in K_1$ of the lattice. That is, there is a local Hilbert space $\mathcal{H}_l$, for each $l \in K_1$, whose basis is the set $\{|0\rangle_l, |1\rangle_l\}$. The total Hilbert space $\mathcal{H}$ of the system is given

by the tensor product

$$\mathcal{H} = \bigotimes_{l \in K_1} \mathcal{H}_l. \tag{2.1.1}$$

The dynamics of this qubit system is governed by the Hamiltonian

$$H = -\sum_{v \in K_0} A_v - \sum_{p \in K_2} B_p. \tag{2.1.2}$$

For each vertex $v \in K_0$, the operator $A_v : \mathcal{H} \to \mathcal{H}$ is the identity operator everywhere except around the vertex v, where it is given by

$$A_v = \frac{1}{2} \left(\bigotimes_{l \in \text{star}(v)} \mathbb{1}_l + \bigotimes_{l \in \text{star}(v)} \sigma_l^x \right), \tag{2.1.3}$$

where, for $l \in K_1$, the Pauli matrix σ_l^x acts over a qubit by flipping it:

$$\sigma_l^x \left| 0 \right\rangle_l = \left| 1 \right\rangle_l, \ \sigma_l^x \left| 1 \right\rangle_l = \left| 0 \right\rangle_l.$$

For each plaquette $p \in K_2$, the operator $B_p : \mathcal{H} \to \mathcal{H}$ is the identity operator everywhere except at the plaquette p, where it is given by

$$B_p = \frac{1}{2} \left(\bigotimes_{l \in \partial p} \mathbb{1}_l + \bigotimes_{l \in \partial p} \sigma_l^z \right), \tag{2.1.4}$$

where, for each $l \in K_1$, the Pauli matrix σ_l^z acts over a qubit by measuring it:

$$\sigma_l^z \left| 0 \right\rangle_l = \left| 0 \right\rangle_l, \ \sigma_l^x \left| 1 \right\rangle_l = - \left| 1 \right\rangle_l.$$

Before we proceed, let's describe an intuitive way to understand how the Toric Code is related to lattice gauge theories using a familiar model. Consider the *transverse field Ising model* on a 2-dimensional regular square lattice. It is defined by placing spin-1/2 degrees of freedom at the vertices of the lattice. The Ising Hamiltonian is usually given by

$$H_{Ising} = -J \sum_{\langle v, v' \rangle} \sigma_v^z \sigma_{v'}^z - g \sum_v \sigma^x, \tag{2.1.5}$$

where J and g are coupling constants (the Ising interaction strength and the transverse magnetic field, respectively). However, it will be convenient for us if we rotate the Pauli operators by $\pi/2$ around the y-axis, which is equivalent to changing $x \leftrightarrow z$. This is an unitary transformation and as such will not change the physical properties of the model. Then, let's consider the Hamiltonian

$$H_{Ising} = -J \sum_{\langle v,v' \rangle} \sigma_v^x \sigma_{v'}^x - g \sum_v \sigma_v^z. \tag{2.1.6}$$

The Ising model (2.1.6) has a global $\mathbb{Z}_2$ symmetry, given by the operator

$$U = \bigotimes_v \sigma_v^z. \tag{2.1.7}$$

For $J >> g$, there are two ground states of the system. They are formed by all spins pointing to the same direction, either $+x$ or $-x$. Since these states are not symmetric under the global $\mathbb{Z}_2$ symmetry, we say they are *symmetry breaking states*. If the system is in such a state, we say it is in a *symmetry breaking quantum phase*. In contrast, for $J << g$, the unique ground state of the system is composed by all spins in a superposition of the states $|0\rangle$ and $|1\rangle$. This state is *symmetric* under the global $\mathbb{Z}_2$ symmetry. If the system is in such state, we say it is in a *symmetric quantum phase*.

Note that the system has no *local* $\mathbb{Z}_2$ symmetry. In particular, the Ising interaction doesn't commute with σ_v^z for any single site v. To construct a model with local symmetry, we need to *gauge* the $\mathbb{Z}_2$ symmetry by introducing a $\mathbb{Z}_2$ *gauge field*.

Thus, we place spin-1/2 degrees of freedom at the *links* of the square lattice. Pauli operators acting over such spins are denoted as τ_l^μ, for any link l and $\mu = x, y, z$. We minimally couple the *matter* degrees of freedom at the vertices to the *gauge field* at the links by changing the Ising interaction as

$$\sigma_v^z \sigma_{v'}^z \rightarrow \sigma_v^z \tau_l^z \sigma_{v'}^z, \tag{2.1.8}$$

for any vertices v, v' such that they are nearest neighbors and any link l that connects the two

vertices v, v'. This term is now invariant under the *local* $\mathbb{Z}_2$ symmetry given by the operator

$$A'_v = \sigma_v^z \bigotimes_{l\in\text{star}(v)} \tau_l^z, \tag{2.1.9}$$

for each vertex v in the lattice.

We constrain the gauge field dynamics in such a way that its flux around a plaquette must be zero. In the continuum limit, this is equivalent to saying that the gauge field is such that there is no magnetic field. Since magnetic field costs energy, this is a reasonable condition. This constraint is enforced by adding to the Hamiltonian the operator

$$B_p = \bigotimes_{l\in\partial p} \tau_l^x. \tag{2.1.10}$$

Thus, the gauged Hamiltonian is given by

$$H_{gauged} = -J \sum_{\langle v,v'\rangle} \sigma_v^z \tau_l^z \sigma_{v'}^z - g \sum_v \sigma_v^z - \sum_p B_p. \tag{2.1.11}$$

Now, in the symmetric phase ($J << g$), we can ignore the first term and study the Hamiltonian

$$H_{gauged} = -g \sum_v \sigma_v^z - \sum_p B_p. \tag{2.1.12}$$

If we also impose that physical states $|\psi\rangle$ must be invariant under the gauge (local) symmetry, we have that

$$\sigma_v^z \bigotimes_{l\in\text{star}(v)} \tau_l^z |\psi\rangle = |\psi\rangle \,,$$

i.e.,

$$\bigotimes_{l\in\text{star}(v)} \tau_l^z |\psi\rangle = \sigma_v^z |\psi\rangle \,.$$

Then, in the subspace of physical states, we can replace σ_v^z by $A_v = \bigotimes_{l\in\text{star}(v)} \tau_l^z$. In this subspace, the gauged Hamiltonian is

$$H_{gauged} = -\sum_v A_v - \sum_p B_p, \tag{2.1.13}$$

where we set $g = 1$ for convenience. By rotating the link spins by $\pi/2$ around the y axis, we

have finally that H_{gauged} is equivalent to the Toric Code Hamiltonian. Thus, the Toric Code can be seen as the gauged $2D$ transverse field Ising model in the symmetric phase constrained to the subspace of locally $\mathbb{Z}_2$-symmetric states.

Back to the Toric Code, let's analyse its physical properties. The operators A_v and B_p are both projectors for all $v \in K_0$ and all $p \in K_2$. In fact,

$$A_v^2 = \frac{1}{4}\left(\bigotimes_{l\in\text{star}(v)} \mathbb{1}_l + \bigotimes_{l\in\text{star}(v)} \sigma_l^x\right)\left(\bigotimes_{l\in\text{star}(v)} \mathbb{1}_l + \bigotimes_{l\in\text{star}(v)} \sigma_l^x\right)$$

$$= \frac{1}{4}\left(\bigotimes_{l\in\text{star}(v)} \mathbb{1}_l + \bigotimes_{l\in\text{star}(v)} \sigma_l^x + \bigotimes_{l\in\text{star}(v)} \sigma_l^x + \bigotimes_{l\in\text{star}(v)} \mathbb{1}_l\right)$$

$$= \frac{1}{2}\left(\bigotimes_{l\in\text{star}(v)} \mathbb{1}_l + \bigotimes_{l\in\text{star}(v)} \sigma_l^x\right)$$

$$= A_v,$$

$\forall v \in K_0$, where we used the fact that $(\sigma_l^x)^2 = \mathbb{1}_l$ for all $l \in K_1$. The same can be shown for B_p, i.e.,

$$B_p^2 = B_p, \forall p \in K_2.$$

This means that an eigenvalue λ of these operators can only be either $\lambda = 0$ or $\lambda = 1$. Moreover, A_v and B_p commute for all $v \in K_0$ and all $p \in K_2$. In fact, for $A_{v'}$ and $B_{p'}$ such that the plaquette $p' \in K_2$ doesn't have $v' \in K_0$ as one of its vertices, as in figure 2.1.1, this is an obvious statement. And for A_v and B_p such that p has v as one of its vertices, like in figure 2.1.1, we have

$$A_v B_p = \frac{1}{4}\left(\bigotimes_{l\in\text{star}(v)} \mathbb{1}_l + \bigotimes_{l\in\text{star}(v)} \sigma_l^x\right)\left(\bigotimes_{l\in\partial p} \mathbb{1}_l + \bigotimes_{l\in\partial p} \sigma_l^z\right)$$

$$= \frac{1}{4}\left(\bigotimes_{l\in\text{star}(v)} \mathbb{1}_l \bigotimes_{l\in\partial p} \mathbb{1}_l + \bigotimes_{l\in\text{star}(v)} \mathbb{1}_l \bigotimes_{l\in\partial p} \sigma_l^z + \bigotimes_{l\in\text{star}(v)} \sigma_l^x \bigotimes_{l\in\partial p} \mathbb{1}_l + \bigotimes_{l\in\text{star}(v)} \sigma_l^x \bigotimes_{l\in\partial p} \sigma_l^z\right).$$

The only possibly non-commuting term is the last one. We have that

$$\bigotimes_{l\in\text{star}(v)} \sigma_l^x \bigotimes_{l\in\partial p} \sigma_l^z = (\sigma_{l_1}^x \otimes \sigma_{l_2}^x \otimes \sigma_{l_3}^x \otimes \sigma_{l_4}^x \otimes \mathbb{1}_{l_5} \otimes \mathbb{1}_{l_6})(\mathbb{1}_{l_1} \otimes \mathbb{1}_{l_2} \otimes \sigma_{l_3}^z \otimes \sigma_{l_4}^z \otimes \sigma_{l_5}^z \otimes \sigma_{l_6}^z)$$
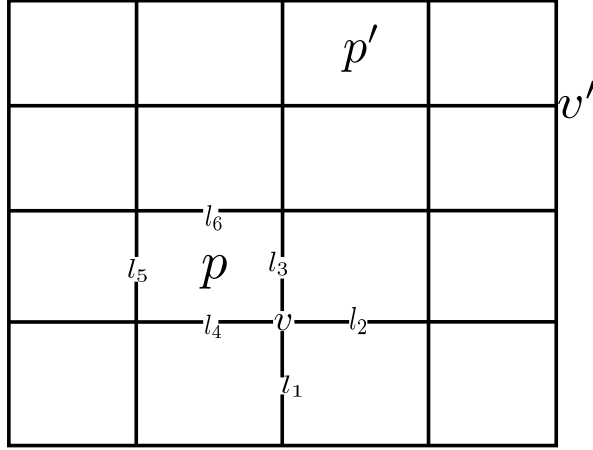
Figure 2.1.1: Plaquette and vertex operators that act over common links commute.

$$= \sigma_{l_1}^x \mathbb{1}_{l_1} \otimes \sigma_{l_2}^x \mathbb{1}_{l_2} \otimes \sigma_{l_3}^x \sigma_{l_3}^z \otimes \sigma_{l_4}^x \sigma_{l_4}^z \otimes \mathbb{1}_{l_5} \sigma_{l_5}^z \otimes \mathbb{1}_{l_6} \sigma_{l_6}^z$$

$$= \mathbb{1}_{l_1} \sigma_{l_1}^x \otimes \mathbb{1}_{l_2} \sigma_{l_2}^x \otimes \left(-\sigma_{l_3}^z \sigma_{l_3}^x \right) \otimes \left(-\sigma_{l_4}^z \sigma_{l_4}^x \right) \otimes \sigma_{l_5}^z \mathbb{1}_{l_5} \otimes \sigma_{l_6}^z \mathbb{1}_{l_6}$$

$$= \bigotimes_{l \in \partial p} \sigma_l^z \bigotimes_{l \in \mathrm{star}(v)} \sigma_l^x,$$

and thus

$$A_v B_p = B_p A_v.$$

This means that each term in the Hamiltonian (2.1.2) can be simultaneously diagonalized and thus the model is exactly solvable. Next we discuss the spectrum of the Toric Code, starting with its ground states, and show why it is a model of topological order.

2.1.2 Ground state properties

From now on, we consider the case in which M is a 2-torus, i.e., the $2D$ lattice has periodic boundary conditions. As shown in 2.1.1, a basis of simultaneous eigenstates $\mathcal{B} = \{|\psi\rangle\}$ of A_v and B_p, $\forall v \in K_0, p \in K_2$, is also a basis of eigenstates of the Hamiltonian (2.1.2). Any state $|\psi\rangle \in \mathcal{B}$ is such that

$$A_v |\psi\rangle = \lambda |\psi\rangle \text{ and } B_p |\psi\rangle = \lambda' |\psi\rangle, \forall v \in K_0, p \in K_2,$$

where $\lambda, \lambda' \in \{0, 1\}$. Let $N_v = |K_0|$ be the number of vertices, $N = |K_1|$ the number of links and $N_p = |K_2|$ the number of plaquettes in the lattice. For a state $|\psi\rangle \in \mathcal{B}$ which has eigenvalue $\lambda = 0$ for n vertex operators A_v and m plaquette operators B_p and eigenvalue $\lambda = 1$ for $N_v - n$

vertex operators A_v and $N_p - m$ plaquette operators B_p, we have that

$$H \ket{\psi} = E(n, m) \ket{\psi},$$

where the energy $E(n, m)$ is given by

$$E(n, m) = n + m - (N_v + N_p). \tag{2.1.14}$$

In the 2-torus, the Euler relation takes the form $N_p + N_v - N = 0$, which can be used to rewrite the energy $E(n, m)$ as

$$E(n, m) = n + m - N. \tag{2.1.15}$$

From (2.1.15), we can see that the ground state has energy $E(0, 0) = -N$, and it is given by the configurations in which all vertex and plaquette operators have eigenvalue $\lambda = 1$. Thus, the ground state subspace of the Toric Code is the space

$$\mathcal{H}_0 = \{\ket{\psi} : A_v \ket{\psi} = B_p \ket{\psi} = \ket{\psi}, \forall v \in K_0, p \in K_2\}.$$

We are left with finding explicitly the ground states of the Toric Code. To do so, consider the state

$$\ket{\psi_0} = N \prod_{v \in K_0} A_v \bigotimes_{l \in K_1} \ket{0}_l, \tag{2.1.16}$$

where N is some normalization constant. This state is know as the *loop gas*, for reasons we will discuss soon. For now, let's show that this is a ground state of the Toric Code Hamiltonian. This is accomplished by showing that $A_v \ket{\psi_0} = B_p \ket{\psi_0} = \ket{\psi_0}$, for all vertices and plaquettes in the lattice. We have that, for any $p \in K_2$,

$$B_p \ket{\psi_0} = N B_p \prod_{v \in K_0} A_v \bigotimes_{l \in K_1} \ket{0}_l$$

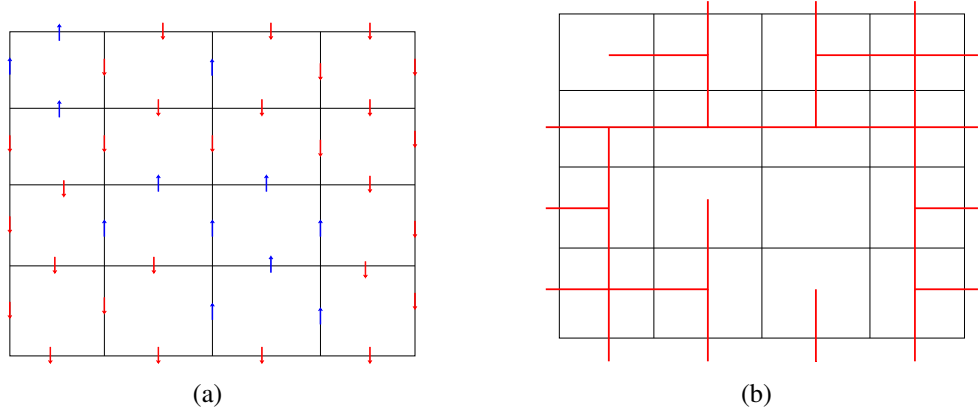$$= N \prod_{v \in K_0} A_v B_p \bigotimes_{l \in K_1} \ket{0}_l$$

Figure 2.1.2: In (a) we show a Toric Code state. In (b), the same state is presented in graphical notation, where links in the state $|-1\rangle$ are crossed by dual red links.

$$= N \prod_{v \in K_0} A_v \bigotimes_{l \in K_1} |0\rangle_l$$

$$= |\psi_0\rangle \, ,$$

where we used the fact that A_v commutes with B_p for every vertex and plaquette and that $\sigma_l^z |0\rangle_l = |0\rangle_l$ for every link. Likewise, for any $v' \in K_0$,

$$A_{v'} |\psi_0\rangle = N A_{v'} \prod_{v \in K_0} A_v \bigotimes_{l \in K_1} |0\rangle_l$$

$$= N \left(A_{v_1} ... A_{v'} A_{v'} ... A_{v_{N_p}} \right) \bigotimes_{l \in K_1} |0\rangle_l$$

$$= N \left(A_{v_1} ... A_{v'} ... A_{v_{N_p}} \right) \bigotimes_{l \in K_1} |0\rangle_l$$

$$= |\psi_0\rangle \, ,$$

where we used the fact that A_v is a projector for any v. Thus, $|\psi_0\rangle$ is indeed a ground state of the Toric Code.

Before we proceed, we introduce a graphical notation to represent the Toric Code states in the lattice. In this notation, a link hosting a qubit in the $|-1\rangle$ state is crossed by a *red dual link*, as illustrated in figure 2.1.2.

We now introduce the *string operators*

$$X_{\gamma^*} = \bigotimes_{l \in \gamma^*} \sigma_l^x, \tag{2.1.17}$$

13

where γ^* is a path in the dual lattice, and

$$Z_\gamma = \bigotimes_{l \in \gamma} \sigma_l^z, \tag{2.1.18}$$

where γ is a path in the lattice (see 2.1.3). The string operator X_{γ^*} flips qubits at links that cross a path γ^* in the dual lattice, while the string operator Z_γ measures qubits along a path γ in the direct lattice. Noting that dual red links cancel each other when crossing the same direct link, we can represent the action of X_{γ^*} in graphical notation by drawing a dual red curve along γ^*:

$$X_{\gamma^*} \left| \begin{array}{c} \end{array} \right\rangle = \left| \begin{array}{c} \end{array} \right\rangle. \tag{2.1.19}$$

Let γ^* be a closed path in the dual lattice and consider the state

$$|\psi_{\gamma^*}\rangle = X_{\gamma^*} |\psi_0\rangle. \tag{2.1.20}$$

This state is also a ground state of the Toric Code. In fact, it is straightforward to see that $A_v |\psi_{\gamma^*}\rangle = |\psi_{\gamma^*}\rangle$, for any $v \in K_0$, because A_v commutes with X_{γ^*} for any v. Now, consider the product $B_p X_{\gamma^*}$ for any $p \in K_2$. The only possibly non-commuting term in this product is

$$\bigotimes_{l \in \partial p} \sigma_l^z \bigotimes_{l \in \gamma^*} \sigma_l^x.$$

Since γ^* is closed, if it encounters the plaquette p. it must pass through two of its boundary links, meaning that we will always have two products

$$... \otimes \sigma_l^z \sigma_l^x \otimes ... \otimes \sigma_{l'}^z \sigma_{l'}^x \otimes ...$$

which we can anti-commute, yielding

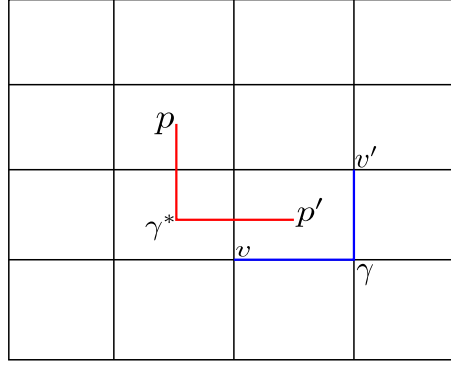$$... \otimes \sigma_l^x \sigma_l^z \otimes ... \otimes \sigma_{l'}^x \sigma_{l'}^z \otimes ...$$

Figure 2.1.3: Example of possible direct (in blue) and dual (in red) paths that can parameterize the operators X and Z.

and thus

$$\bigotimes_{l\in\partial p} \sigma_l^z \bigotimes_{l\in\gamma^*} \sigma_l^x = \bigotimes_{l\in\gamma^*} \sigma_l^x \bigotimes_{l\in\partial p} \sigma_l^z,$$

i.e., $B_p X_{\gamma^*} = X_{\gamma^*} B_p$. Therefore, $B_p |\psi_{\gamma^*}\rangle = |\psi_{\gamma^*}\rangle$ for any $p \in K_2$, and the state $|\psi_{\gamma^*}\rangle$ is also a ground state of the Toric Code. It remains to know if $|\psi_{\gamma^*}\rangle$ and $|\psi_0\rangle$ are in fact different states.

Consider the path of dual links γ^* that surround a vertex v. These dual links intercept the links in star(v), as shown in figure 2.1.4. Making an abuse of notation, we denote the dual path $\gamma^* = \text{star}(v)$ and the string operator associated to it as $X_{\text{star}(v)}$. It is then straightforward to see that we can write the vertex operator A_v as

$$A_v = \frac{1}{2} \left(\bigotimes_{l\in\text{star}(v)} \mathbb{1} + X_{\text{star}(v)} \right). \tag{2.1.21}$$

The state $|\psi_0\rangle$ can then be written as the sum

$$|\psi_0\rangle = N \left(\mathbb{1} + \sum_{v\in K_0} X_{\text{star}(v)} + \sum_{v,v'\in K_0} X_{\text{star}(v)} X_{\text{star}(v')} + ... \right) \bigotimes_{l\in K_1} |0\rangle_l. \tag{2.1.22}$$

Note that, as illustrated in equation (2.1.19), the action of X_{γ^*} can be represented in graphical notation by drawing a dual red curve in the lattice along γ^*. Thus, the action of $X_{\text{star}(v)}$ can be represented by drawing a *dual red loop* around the vertex v. The state (2.1.22) can be thus represented as

$$|\psi_0\rangle \propto \left| \begin{array}{c} \end{array} \right\rangle + \left| \begin{array}{c} \end{array} \right\rangle + \left| \begin{array}{c} \end{array} \right\rangle + \left| \begin{array}{c} \end{array} \right\rangle + ... \tag{2.1.23}$$
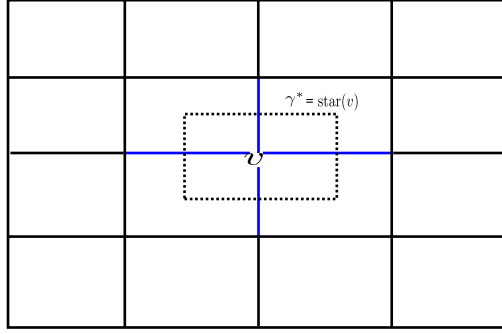
15

Figure 2.1.4: The set of links star(v) (highlighted in blue) is crossed by the closed dual path γ^*.

This is why this state is known as the *loop gas state*. It is given by the superposition of every possible dual red loop one can draw in the lattice.

From (2.1.22), it is clear that the state $|\psi_{\gamma^*}\rangle$ is the same as the state $|\psi_0\rangle$ whenever the dual closed path γ^* can be decomposed as a product of paths of the kind star(v), i.e., whenever we can write

$$|\psi_{\gamma^*}\rangle = X_{\gamma^*}|\psi_0\rangle = X_{\text{star}(v)}X_{\text{star}(v')}X_{\text{star}(v'')}\ldots|\psi_0\rangle\,.$$

In the 2-torus, the only two closed paths we can draw that cannot be decomposed as a product of star(v)'s are the two *non-contractible* paths α and β of figure 2.1.5. Thus, we can conclude that there are four linearly independent ground states of the Toric Code in the 2-torus. They are

$$|\psi_0\rangle = N \prod_{v\in K_0} A_v \bigotimes_{l\in K_1} |0\rangle_l\,, \tag{2.1.24}$$

$$|\psi_1\rangle = X_\alpha |\psi_0\rangle\,, \tag{2.1.25}$$

$$|\psi_2\rangle = X_\beta |\psi_0\rangle\,, \tag{2.1.26}$$

$$|\psi_3\rangle = X_\alpha X_\beta |\psi_0\rangle\,, \tag{2.1.27}$$

and the ground state subspace $\mathcal{H}_0$ has dimension

$$\dim(\mathcal{H}_0) = 4. \tag{2.1.28}$$

The existence of distinct ground states of the Toric Code in the 2-torus relies on the fact that we can draw *non-contractible* loops over the surface of the torus, which renders it a *topologically non-trivial* surface. In fact, we can define the Toric Code over any 2-dimensional surface of *genus* g. Since the number of non-contractible loops in a surface of genus g is $2g$, the dimension of the ground state subspace of such a model, often called its *ground state degeneracy*
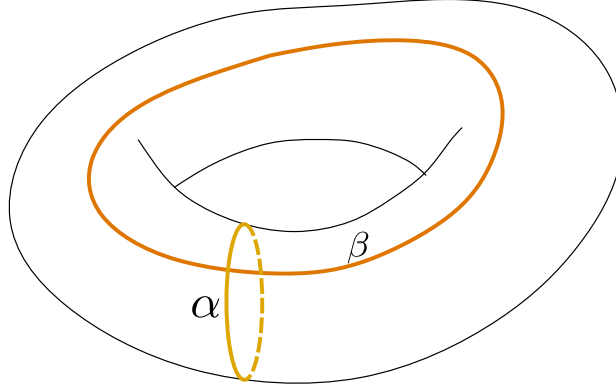
Figure 2.1.5: The non-contractible paths α and β on a 2-torus.

(GSD), is equal to

$$GSD = \dim(\mathcal{H}_0) = 2^{2g}. \tag{2.1.29}$$

A topological ground state degeneracy is one of the main characteristics of topological order [8].

2.1.3 Excited states

From (2.1.15), we see that excited states of the Toric Code have vertex and/or plaquette excitations with eigenvalues $\lambda = 0$. Let's see how we can create such excitations.

Let $l \in K_1$ be a link joining the vertices $v', v'' \in K_0$ and consider the state

$$|e_{v'}, e_{v''}\rangle = \sigma_l^z |\psi_0\rangle, \tag{2.1.30}$$

where $|\psi_0\rangle$ is the ground-state defined in (2.1.16) (any ground-state of the Toric Code would also work for our purposes). This state is an eigenstate of the operator B_p with eigenvalue $\lambda = 1$ for any plaquette $p \in K_2$. It is also an eigenstate of the operator A_v with eigenvalue $\lambda = 1$ for most of the vertices $v \in K_0$. However, for the operators $A_{v'}$ and $A_{v''}$, $|e_{v'}, e_{v''}\rangle$ has eigenvalue $\lambda = 0$. To see this, note that σ_l^z anti-commutes with σ_l^x. Thus,

$$A_{v'}\sigma_l^z |\psi_0\rangle = \frac{1}{2}\left(\bigotimes_{l \in \text{star}(v')} \mathbb{1}_l + \bigotimes_{l \in \text{star}(v')} \sigma_l^x\right)\sigma_l^z |\psi_0\rangle$$
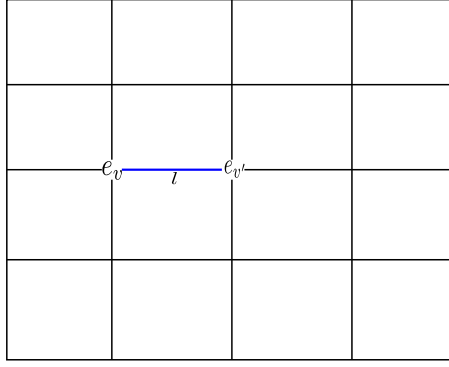
17

Figure 2.1.6: Charge quasiparticles at vertices v and v' created by the action of σ_l^z over the link l (in blue).

$$= \frac{1}{2}\sigma_l^z \left(\bigotimes_{l \in \text{star}(v')} \mathbb{1}_l - \bigotimes_{l \in \text{star}(v')} \sigma_l^x \right) |\psi_0\rangle$$

$$= \frac{1}{2}\sigma_l^z \left(|\psi_0\rangle - |\psi_0\rangle \right) = 0,$$

because

$$\bigotimes_{l \in \text{star}(v')} \sigma_l^x |\psi_0\rangle = X_{\text{star}(v')} |\psi_0\rangle = |\psi_0\rangle,$$

as we noted previously. The same can be shown for $A_{v''}$, concluding that indeed

$$A_{v'} |e_{v'}, e_{v''}\rangle = A_{v''} |e_{v'}, e_{v''}\rangle = 0. \qquad (2.1.31)$$

This means that the state $|e_{v'}, e_{v''}\rangle$ is an *excited state* of the Toric Code. The energy of this state is

$$E(2,0) = 2 - N. \qquad (2.1.32)$$

It is common to think of the state $|e_{v'}, e_{v''}\rangle$ as a pair of *quasiparticles* $e_{v'}$, $e_{v''}$, usually called *charges*, living at the vertices v' and v'' of the lattice (see figure 2.1.6). Given an open path γ starting at the vertex v' and ending at the vertex v'' of the lattice, we can create a pair of charge quasiparticles $e_{v'}$ and $e_{v''}$ by applying a string operator Z_γ to any ground-state of the Toric Code:

$$|e_{v'}, e_{v''}\rangle = Z_\gamma |\psi\rangle, \qquad (2.1.33)$$

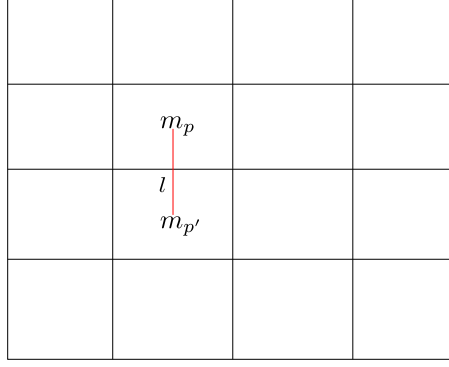for any $|\psi\rangle \in \mathcal{H}_0$.

Figure 2.1.7: Flux quasiparticles at plaquettes p and p' created by the action of σ_l^x over the link l (dual red link).

Now, let $l \in K_1$ be a link shared by two plaquettes $p', p'' \in K_2$ and consider the state

$$|m_{p'}, m_{p''}\rangle = \sigma_l^x |\psi_0\rangle. \tag{2.1.34}$$

This state has eigenvalue $\lambda = 0$ for the plaquette operators $B_{p'}, B_{p''}$, while having eigenvalues $\lambda = 1$ for all the other operators in the Toric Code Hamiltonian. The way to see this is analogous to the case of the charge quasiparticles, and also relies on the fact that σ_l^x anti-commutes with σ_l^z. The excited state $|m_{p'}, m_{p''}\rangle$ has energy

$$E(0,2) = 2 - N. \tag{2.1.35}$$

Just as in the case of the charge quasiparticles, the state $|m_{p'}, m_{p''}\rangle$ also carries a quasiparticle interpretation: it is the state of a pair of *flux quasiparticles* living at the plaquettes p' and p'' of the lattice, as in figure 2.1.7. In fact, given any open dual path γ^* in the dual lattice, starting at a plaquette p' and ending at a plaquette p'', we can create a pair of flux quasiparticles $m_{p'}$ and $m_{p''}$ by applying a string operator X_{γ^*} to any ground-state of the Toric Code:

$$|m_{p'}, m_{p''}\rangle = X_{\gamma^*} |\psi\rangle, \tag{2.1.36}$$

where $|\psi\rangle \in \mathcal{H}_0$.

It is worth noting that, since the energy of a state depends only on the number of quasiparticles present, the quasiparticles of the Toric Code can move around freely without any energy costs. This is a problem when considering the Toric Code as a platform for a quantum memory. To explain a bit further, it is possible to encode quantum information in the 2-qubit system
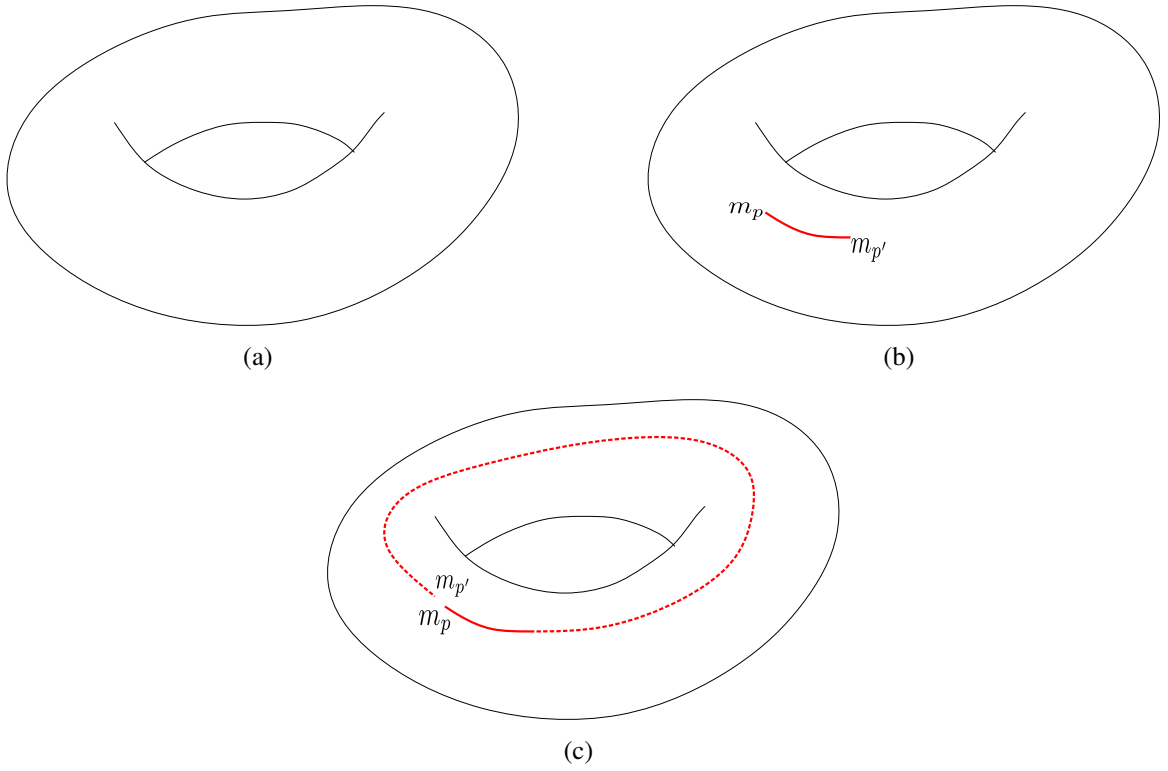
Figure 2.1.8: (a) The Toric Code state $|\psi_0\rangle$. (b) Thermal fluctuations create a pair of flux quasiparticles connected by a dual red path. (c) If the quasiparticles are annihilated by closing the dual red path as shown in this figure, the system undergoes the quantum phase transition $|\psi_0\rangle \to |\psi_2\rangle$.

that is the ground-state of the Toric Code. Because of the topological order, local perturbations would not affect the ground-states, and thus it would not change the encoded information, making it a robust quantum memory. However, thermal fluctuations could create pairs of quasiparticles, which would fluctuate around the lattice and possibly enforce a transition between ground-states, scrambling the memory (see figure 2.1.8). This is a so-called *logical error*, and it cannot be efficiently corrected [37].

Another important property of the excitations of the Toric Code is their *fusion rules*. The fusion of two particles can be thought of as the result of putting two particles at the same point in space. It is easy to see that, since Pauli operators square to the identity operator, the fusion of two charge quasiparticles equals the vacuum, and the same happens for flux quasiparticles. We express this by writing

$$e \times e = 1, \; m \times m = 1,$$

where e represents a charge quasiparticle and m represents a flux quasiparticle. The fusion of a charge quasiparticle and a flux quasiparticle does not results in a vacuum. Instead, it can
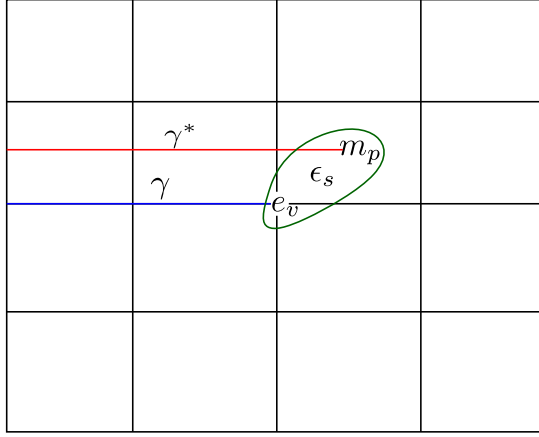
Figure 2.1.9: Dyon created by the fusion of a flux and a charge.

be interpreted as a new quasiparticle, the *dyon*. The dyon can be created from the vacuum as follows:

$$|\epsilon_s, \epsilon_{s'}\rangle = Z_\gamma X_{\gamma^*} |\psi\rangle, \tag{2.1.37}$$

where $|\psi\rangle \in \mathcal{H}_0$ and γ and γ^* are as in figure 2.1.9. Dyons are located at *sites $s = (v, p)$*, which are pairs of adjacent plaquettes and vertices. Since dyons are the result of fusion between charges and fluxes, we write

$$e \times m = \epsilon.$$

One last important property of Toric Code quasiparticles is their *statistics* under particle exchange. Suppose we exchange two charge quasiparticles as in figure 2.10(a). We can see that to make the exchange, we have to apply to the system's state the operator Z_γ where γ is a closed path in the lattice. Note that, since Z_γ is equal to $Z_{\gamma'}$, where γ' is a product of different plaquette boundaries ∂p and since $B_p \propto \mathbb{1} + Z_{\partial p}$ for any $p \in K_2$, Z_γ can be written as a combination of B_p's and identity operators. Thus, it acts as the identity over the system's state. Then, the exchange between two charge quasiparticles does not generates any additional phase factor to the system's wave function, meaning that charge quasiparticles are bosons. The same argument can be applied to flux quasiparticles, which are then bosons as well. As for dyons, note that, since charges and fluxes are bosons, the statistics of dyons is determined by the mutual statistics between fluxes and charges. Then, suppose we make a charge go around a flux, as in figure 2.10(b). This means that we act with the operator Z_α over the state $|\epsilon\rangle = X_{\gamma^*} Z_\gamma |\psi\rangle$, where $|\psi\rangle$ is a vacuum state. It is straightforward to see that Z_α anti-commutes with X_{γ^*}, and
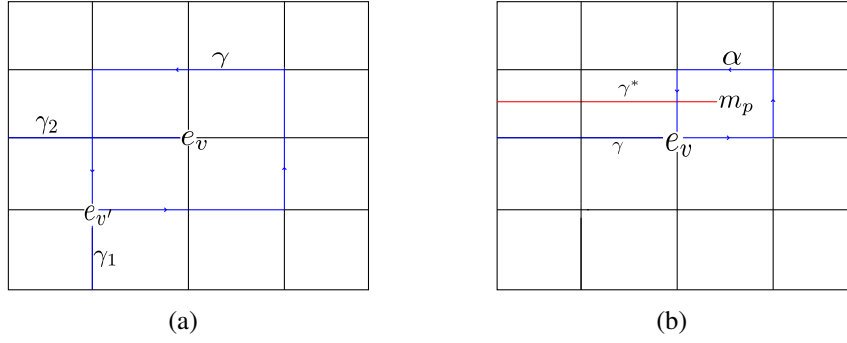
Figure 2.1.10: (a) The exchange of two charge quasiparticles. Since no phase factor results from this operation, charges are bosons. (b) The exchange of a charge and a flux. Since Z and X operators anti-commute, this operation results in a -1 phase factor, and thus dyons are fermions.

thus the state acquires a phase of $-1 = e^{i\pi}$. Therefore, dyons are fermions.

All quasiparticles of the Toric Code have usual statistics, i.e., they are either bosons or fermions. They are trivial examples of *Abelian anyons*. The presence of emergent anyons are a strong indicative of topological order [8]. As we will see next, *non-Abelian anyons* can be found in Quantum Double Models. Non-Abelian anyons can be employed as a platform for fault-tolerant quantum computation [37, 15].

2.2 Quantum double models

The Quantum Double Models with arbitrary gauge group G are the standard example of topological order with the presence of non-Abelian anyons. In this section, we review these models and discuss its main physical properties, emphasising its topological ground-state degeneracy.

2.2.1 The model

Let G be a finite (possibly non-Abelian) group. Let $\mathbb{C}G$ be the *group algebra* based on G, that is, the complex vector space of formal linear combinations of elements of G with complex coefficients. A natural basis for $\mathbb{C}G$ is given by the set $\{|g\rangle : g \in G\}$. This basis can be made orthonormal by defining the inner product between basis vectors as

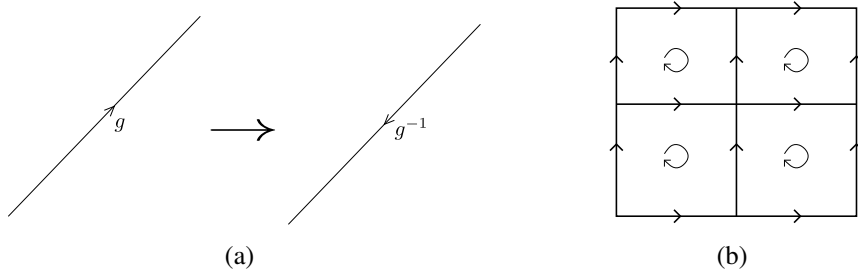$$\langle g|h\rangle = \delta(g, h), \tag{2.2.1}$$

Figure 2.2.1: (a) To make the model orientation-independent, reversing a link orientation also inverts the degree of freedom associated to it. (b) Orientation convention we adopt for the definition of the QDM.

$\forall g, h \in G$, where

$$
\delta(g, h) = \begin{cases} 0, & \text{if} \quad g \neq h, \\ 1, & \text{if} \quad g = h \end{cases}.
$$

Let M be a 2-dimensional oriented manifold discretized by an oriented square lattice $K = K_0 \cup K_1 \cup K_2$, where K_0 is the set of vertices, K_1 is the set of links and K_2 is the set of plaquettes. To each link $l \in K_1$, we associate a Hilbert space $\mathcal{H}_l = \mathbb{C}G$ which is the group algebra of G. This means that at each link $l \in K_1$ sits a state $|g\rangle_l \in \mathcal{H}_l$. The total Hilbert space of the system is given by

$$
\mathcal{H} = \bigotimes_{l \in K_1} \mathcal{H}_l.
$$

To make the model independent of the lattice orientation, we establish that whenever the orientation of a link is reversed, the degree of freedom g associated to that link transforms as $g \to g^{-1}$ (see figure 2.1(a)). We fix the orientation of the lattice as in figure 2.1(b).

Given a $g \in G$ and a $l \in K_1$, let $L_l^g : \mathcal{H}_l \to \mathcal{H}_l$ and $R_l^g : \mathcal{H}_l \to \mathcal{H}_l$ be operators such that, for any $|h\rangle_l \in \mathcal{H}_l$,

$$
L_l^g |h\rangle_l = |gh\rangle_l, \tag{2.2.2}
$$

$$
R_l^g |h\rangle_l = |hg\rangle_l, \tag{2.2.3}
$$

i.e., they are *right and left multiplication* operators. Also, for a $g \in G$ and $l \in K_1$, let $T_l^g : \mathcal{H}_l \to \mathcal{H}_l$ be an operator such that, for any $|h\rangle_l \in \mathcal{H}_l$,

$$
T_l^g |h\rangle_l = \delta(g, h) |h\rangle_l. \tag{2.2.4}
$$

23

These operators will be used to construct the Hamiltonian of the Quantum Double Model. To find the algebra of these operators, let $a, g, h \in G$, $l \in K_1$ and $|a\rangle_l \in \mathcal{H}_l$. We have that

$$L_l^g L_l^h |a\rangle_l = |g(ha)\rangle_l = |(gh)a\rangle_l = L_l^{gh} |a\rangle_l \,,$$

$$R_l^g R_l^h |a\rangle_l = |(ah)g\rangle_l = |a(hg)\rangle_l = R_l^{hg} |a\rangle_l \,,$$

that is,

$$L_l^g L_l^h = L_l^{gh}, \tag{2.2.5}$$

$$R_l^g R_l^h = R_l^{hg}. \tag{2.2.6}$$

Also, it is clear that

$$T_l^g T_l^h = T_l^h T_l^g. \tag{2.2.7}$$

Moreover,

$$L_l^g T_l^h |a\rangle_l = \delta(h, a) |ga\rangle_l = \delta(gh, ga) |ga\rangle_l = T_l^{gh} L_l^g |a\rangle_l \,,$$

$$R_l^g T_l^h |a\rangle_l = \delta(h, a) |ag\rangle_l = \delta(hg, ag) |ag\rangle_l = T_l^{hg} R_l^g |a\rangle_l \,,$$

$$L_l^g R_l^h |a\rangle_l = |gah\rangle_l = R_l^g L_l^h |a\rangle_l \,,$$

i.e.,

$$L_l^g T_l^h = T_l^{gh} L_l^g, \tag{2.2.8}$$

$$R_l^g T_l^h = T_l^{hg} R_l^g, \tag{2.2.9}$$

$$L_l^g R_l^h = R_l^g L_l^h. \tag{2.2.10}$$

Thus, the operators (2.2.2), (2.2.3) and (2.2.4) obey the *Quantum Double Algebra* of the group G, often denoted by $D(G)$. For a proof of this statement, see [39].

Now, let $v \in K_0$ and $g \in G$. We define the operator $A_v^g : \mathcal{H} \to \mathcal{H}$ as

$$A_v^g = L_{l_1}^g \otimes L_{l_2}^g \otimes R_{l_3}^{g^{-1}} \otimes R_{l_4}^{g^{-1}}, \tag{2.2.11}$$

where l_1, l_2, l_3, l_4 are the links in K_1 that touch v and the operator acts like the identity out-
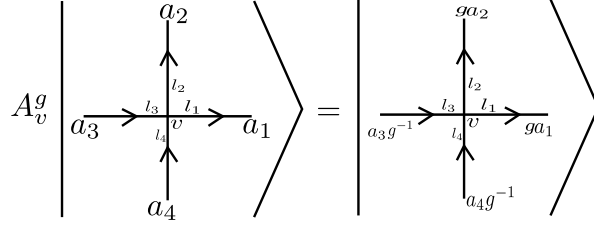
Figure 2.2.2: Action of A_v^g operator over an arbitrary state.

side this region (see figure 2.2.2). The operator (2.2.11) acts as a *local gauge transformation*, transforming links degrees of freedom locally around a vertex by a group operation.

Let $p \in K_2$ and $g \in G$. We define the operator $B_p^g : \mathcal{H} \to \mathcal{H}$ as

$$B_p^g = \sum_{\{b_i\}_{i=1}^4} \delta(b_1 b_2 b_3^{-1} b_4^{-1}, g) T_{l_1}^{b_1} \otimes T_{l_2}^{b_2} \otimes T_{l_3}^{b_3} \otimes T_{l_4}^{b_4}, \qquad (2.2.12)$$

where the sum is over all possible group elements b_1, b_2, b_3, b_4 and l_1, l_2, l_3, l_4 are the links that form the boundary of p. The operator (2.2.12) measures the *holonomy* around a plaquette.

The Hamiltonian of the Quantum Double Model is given by

$$H_{QDM} = -\sum_{v \in K_0} A_v - \sum_{p \in K_2} B_p, \qquad (2.2.13)$$

where

$$A_v = \frac{1}{|G|} \sum_{g \in G} A_v^g, \qquad (2.2.14)$$

and

$$B_p = B_p^e, \qquad (2.2.15)$$

where $e \in G$ is the group identity.

Before we proceed, consider the case in which $G = \mathbb{Z}_2$. The Hilbert space of the system is a product of the local spaces

$$\mathcal{H}_l = \text{Span}_{\mathbb{C}}\{|+1\rangle, |-1\rangle\}.$$

Since the group is Abelian, right and left multiplication coincide. Consider the left multiplication L_l^g for some $l \in K_1$. There are only two possible such operators, $L_l^{-1} = \sigma_l^x$ and $L_l^1 = \mathbb{1}_l$.

25

Thus, the operator (2.2.14) is given by

$$A_v = \frac{1}{2}\left(A_v^1 + A_v^{-1}\right)$$

$$= \frac{1}{2}\left(\mathbb{1}_{l_1} \otimes \mathbb{1}_{l_2} \otimes \mathbb{1}_{l_3} \otimes \mathbb{1}_{l_4} + \sigma_{l_1}^x \otimes \sigma_{l_2}^x \otimes \sigma_{l_3}^x \otimes \sigma_{l_4}^x\right).$$

Likewise, it can be shown that

$$B_p = \frac{1}{2}\left(\mathbb{1}_{l_1} \otimes \mathbb{1}_{l_2} \otimes \mathbb{1}_{l_3} \otimes \mathbb{1}_{l_4} + \sigma_{l_1}^z \otimes \sigma_{l_2}^z \otimes \sigma_{l_3}^z \otimes \sigma_{l_4}^z\right),$$

and thus the Quantum Double Model with gauge group $G = \mathbb{Z}_2$ is the Toric Code.

The operators (2.2.14) and (2.2.15) are commuting orthogonal projectors. To check this, let $v \in K_0$. We have that

$$(A_v)^2 = \frac{1}{|G|^2}\sum_{g,h \in G} A_v^g A_v^h,$$

where

$$A_v^g A_v^h = L_{l_1}^g L_{l_1}^h \otimes L_{l_2}^g L_{l_2}^h \otimes R_{l_3}^{g^{-1}} R_{l_3}^{h^{-1}} \otimes R_{l_4}^{g^{-1}} R_{l_4}^{h^{-1}}.$$

From equations (2.2.5) and (2.2.6), we have that

$$A_v^g A_v^h = L_{l_1}^{gh} \otimes L_{l_2}^{gh} \otimes R_{l_3}^{(gh)^{-1}} \otimes R_{l_4}^{(gh)^{-1}},$$

and thus we must consider the sum

$$\sum_{g,h \in G} L_{l_1}^{gh} \otimes L_{l_2}^{gh} \otimes R_{l_3}^{(gh)^{-1}} \otimes R_{l_4}^{(gh)^{-1}}.$$

By letting $k = gh$, we can write this sum as

$$\sum_{g,k \in G} L_{l_1}^k \otimes L_{l_2}^k \otimes R_{l_3}^{k^{-1}} \otimes R_{l_4}^{k^{-1}}$$

$$= |G|\sum_{k \in G} L_{l_1}^k \otimes L_{l_2}^k \otimes R_{l_3}^{k^{-1}} \otimes R_{l_4}^{k^{-1}}.$$

$$= |G|\sum_{k \in G} A_v^k.$$

Thus,

$$(A_v)^2 = \frac{1}{|G|^2}|G|\sum_{k \in G} A_v^k = A_v.$$

Likewise, it can be show that, given $p \in K_2$,

$$(B_p)^2 = B_p.$$

To check that A_v and B_p commute for every $v \in K_0$ and $p \in K_2$, choose a vertex v and a plaquette p. If v does not touch p, the operators commute. If v touches p, we have that (see figure 2.2.3)

$$A_v B_p = \frac{1}{|G|}\sum_{g \in G}\sum_{b_i}\delta(b_1 b_2 b_3^{-1} b_4^{-1}, e)(L_{l_1}^g T_{l_1}^{b_1}) \otimes T_{l_2}^{b_2} \otimes T_{l_3}^{b_3} \otimes (L_{l_4}^g T_{l_4}^{b_4}) \otimes R_{l_5}^{g^{-1}} \otimes R_{l_6}^{g^{-1}}.$$

From equation (2.2.8), we have that

$$A_v B_p = \frac{1}{|G|}\sum_{g \in G}\sum_{\{b_i\}}\delta(b_1 b_2 b_3^{-1} b_4^{-1}, e)(T_{l_1}^{gb_1} L_{l_1}^g) \otimes T_{l_2}^{b_2} \otimes T_{l_3}^{b_3} \otimes (T_{l_4}^{gb_4} L_{l_4}^g) \otimes R_{l_5}^{g^{-1}} \otimes R_{l_6}^{g^{-1}}$$

$$= \frac{1}{|G|}\sum_{g \in G}\sum_{\{b_i\}}\delta(g^{-1} b_1' b_2 b_3^{-1} b_4'^{-1} g, e)(T_{l_1}^{b_1'} L_{l_1}^g) \otimes T_{l_2}^{b_2} \otimes T_{l_3}^{b_3} \otimes (T_{l_4}^{b_4'} L_{l_4}^g) \otimes R_{l_5}^{g^{-1}} \otimes R_{l_6}^{g^{-1}}$$

$$= \frac{1}{|G|}\sum_{g \in G}\sum_{\{b_i\}}\delta(b_1' b_2 b_3^{-1} b_4'^{-1}, e)(T_{l_1}^{b_1'} L_{l_1}^g) \otimes T_{l_2}^{b_2} \otimes T_{l_3}^{b_3} \otimes (T_{l_4}^{b_4'} L_{l_4}^g) \otimes R_{l_5}^{g^{-1}} \otimes R_{l_6}^{g^{-1}}$$

$$= B_p A_v,$$

where we made the change of variables $b_i' = gb_i$ for $i = 1, 4$. Thus,

$$[A_v, B_p] = 0, \ \forall v \in K_0, p \in K_2. \tag{2.2.16}$$

Therefore, since each term in (2.2.13) can be simultaneously diagonalized, Quantum Double Models for arbitrary gauge groups G are exactly solvable. In the following section, we start the analysis of the spectra of these models, with special attention to its topological ground-states.

2.2.2 Ground-state properties

Much like in 2.1.2, here we can also state that a basis of simultaneous eigenstates $\mathcal{B} = \{|\psi\rangle\}$ of the operators (2.2.14) and (2.2.15), $\forall v \in K_0, p \in K_2$, is also a basis of eigenstates of the
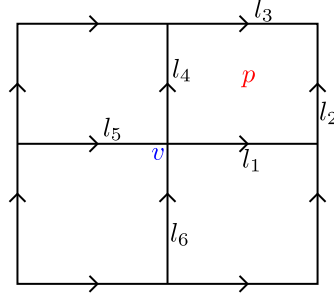
Figure 2.2.3: Plaquette and vertex operators that act over common links commute in the QDM.

Hamiltonian (2.2.13). This means that any state $|\psi\rangle \in \mathcal{B}$ is such that

$$A_v |\psi\rangle = \lambda |\psi\rangle \text{ and } B_p |\psi\rangle = \lambda' |\psi\rangle, \forall v \in K_0, p \in K_2,$$

where $\lambda, \lambda' \in \{0, 1\}$. Let $N_v = |K_0|$ be the number of vertices, $N = |K_1|$ the number of links and $N_p = |K_2|$ the number of plaquettes in the lattice. For a state $|\psi\rangle \in \mathcal{B}$ which has eigenvalue $\lambda = 0$ for n vertex operators A_v and m plaquette operators B_p and eigenvalue $\lambda = 1$ for $N_v - n$ vertex operators A_v and $N_p - m$ plaquette operators B_p, we have that

$$H |\psi\rangle = E(n, m) |\psi\rangle,$$

where the energy $E(n, m)$ is given by

$$E(n, m) = n + m - (N_v + N_p). \tag{2.2.17}$$

We can see that the ground-state has energy $E(0, 0) = -(N_v + N_p)$, and it is given by the configurations in which all vertex and plaquette operators has eigenvalue $\lambda = 1$. Thus, the ground-state subspace of the Quantum Double Model is the space

$$\mathcal{H}_0 = \{|\psi\rangle : A_v |\psi\rangle = B_p |\psi\rangle = |\psi\rangle, \forall v \in K_0, p \in K_2\}.$$

The *loop gas* state

$$|\psi_0\rangle = N \prod_{v \in K_0} A_v \bigotimes_{l \in K_1} |e\rangle_l, \tag{2.2.18}$$

where $e \in G$ is the group identity and N is some normalization constant, is an example of a ground-state in $\mathcal{H}_0$. In the general case of the Quantum Double Model for arbitrary gauge group
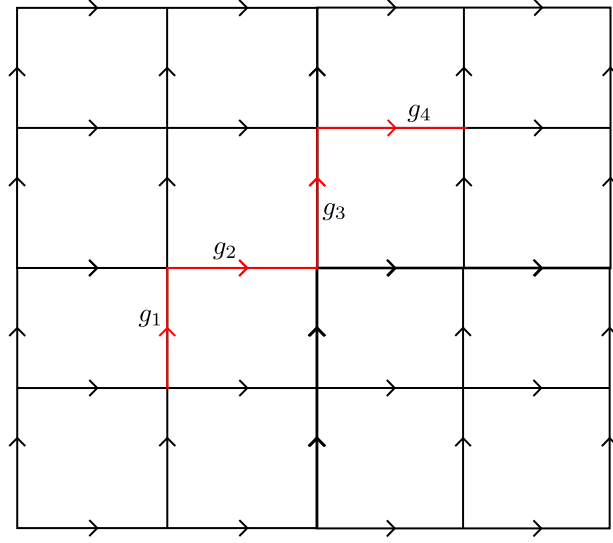
Figure 2.2.4: For the path γ (in red), $g_\gamma = g_1 g_2 g_3 g_4$.

G, it is not as straightforward to construct the basis of ground-states as in the Toric Code case. However, we can use this general setting to prove that the dimension of $\mathcal{H}_0$, i.e., the *ground-state degeneracy* of the Quantum Double Model for any gauge group G, is a topological invariant of the manifold M. To show that, we follow the steps in [40].

From now on, we consider that M is a manifold without a boundary. Consider a basis state $|\psi\rangle = \bigotimes_{l \in K_1} |g\rangle_l \in \mathcal{H}$. This state is constructed by assigning to each link $l \in K_1$ a group element in G. Given an oriented path γ in the lattice given by a sequence of connected links, we define g_γ as the product of the group elements assigned to the links in the path (see figure 2.2.4). If a link is oriented opposite to the path, we multiply the inverse of the group element assigned to that link.

If the state $|\psi\rangle$ is such that $B_p |\psi\rangle = |\psi\rangle$ for some $p \in K_2$, from (2.2.12) and (2.2.15) we have that $g_{\partial p} = e$. The subspace spanned by all eigenstates with eigenvalue $\lambda = 1$ of all plaquette operators is given by

$$V = \{|\psi\rangle = \bigotimes_{l \in K_1} |g\rangle_l : g_{\partial p} = e \ \forall p \in K_2\}.$$

That is, since we are considering the $\lambda = 1$ eigenstates of all plaquette operators and M has no boundary,

$$V = \{|\psi\rangle = \bigotimes_{l \in K_1} |g\rangle_l : g_\gamma = e \text{ for every contractible loop } \gamma\},$$

because every contractible loop can be written as the union of plaquette boundaries.

29

Let $|\psi\rangle, |\phi\rangle \in V$. Given $h \in G$, we state that $|\psi\rangle$ and $|\phi\rangle$ are gauge equivalent, denoted by $|\psi\rangle \sim |\phi\rangle$, if one can be obtained from the other by applications of operators A_v^h, given by (2.2.11), at an arbitrary number of vertices $v \in K_0$. Note that since the operator A_v^h preserves the relation $g_\gamma = e$ for contractible loops γ in the lattice, the subspace V is invariant under gauge transformations. Gauge equivalence is *reflexive*, i.e., $|\psi\rangle \sim |\psi\rangle$, since $|\psi\rangle = A_v^e |\psi\rangle$ for any $v \in K_0$ and any $h \in G$. Gauge equivalence is also *symmetric*, i.e., $|\psi\rangle \sim |\phi\rangle \Leftrightarrow |\phi\rangle \sim |\psi\rangle$, since $|\phi\rangle = A_v^h |\psi\rangle \Rightarrow |\psi\rangle = A_v^{h^{-1}} |\phi\rangle$ for any $v \in K_0$ and any $h \in G$. Finally, gauge equivalence is *transitive*, i.e., given $|\chi\rangle \in V$, $|\psi\rangle \sim |\chi\rangle$ and $|\chi\rangle \sim |\phi\rangle$ implies $|\psi\rangle \sim |\phi\rangle$, since $|\chi\rangle = A_v^h |\psi\rangle$, $|\phi\rangle = A_{v'}^{h'} |\chi\rangle$ and thus $|\phi\rangle = A_{v'}^{h'} A_v^h |\psi\rangle$ for any $v, v' \in K_0$ and any $h, h' \in G$. Therefore, gauge equivalence introduces an equivalence relation on V

Let $[V]$ be the set of equivalence classes and let $[\psi] \in [V]$ be any class. Let

$$|[\psi]\rangle = \sum_{|\psi\rangle \sim |\phi\rangle} |\phi\rangle \,.$$

For any $v \in K_0$, we have that

$$A_v |[\psi]\rangle = \frac{1}{|G|} \sum_{g \in G} A_v^g |[\psi]\rangle \,,$$

where

$$A_v^g |[\psi]\rangle = \sum_{|\psi\rangle \sim |\phi\rangle} A_v^g |\phi\rangle = \sum_{|\psi\rangle \sim |\chi\rangle} |\chi\rangle = |[\psi]\rangle$$

by definition. Thus,

$$A_v |[\psi]\rangle = \frac{1}{|G|} \sum_{g \in G} |[\psi]\rangle = |[\psi]\rangle$$

and the set $[V]$ contains eigenstates of A_v, $\forall v \in K_0$, with eigenvalue $\lambda = 1$. It follows that the states $|[\psi]\rangle \in \mathcal{H}_0$, where $\mathcal{H}_0$ is the ground state subspace of the Quantum Double Model. Note that the way we constructed these ground states generalizes the way we constructed Toric Code ground states by taking flat holonomy configurations and applying all gauge transformations to them. Given any $|\chi\rangle \in \mathcal{H}_0$, we can express it as an element $|[\chi]\rangle \in [V]$. In fact, the state $|\chi\rangle$ has flat holonomy and thus we can define $|[\chi]\rangle$ by summing all states with flat holonomy that are gauge equivalent to $|\chi\rangle$. Therefore, the set $\{|[\psi]\rangle : [\psi] \in [V]\}$ forms a basis of $\mathcal{H}_0$.

Given a vertex $v_0 \in K_0$, let $\pi_1(M, v_0)$ be the *fundamental group* of M at v_0. We define a
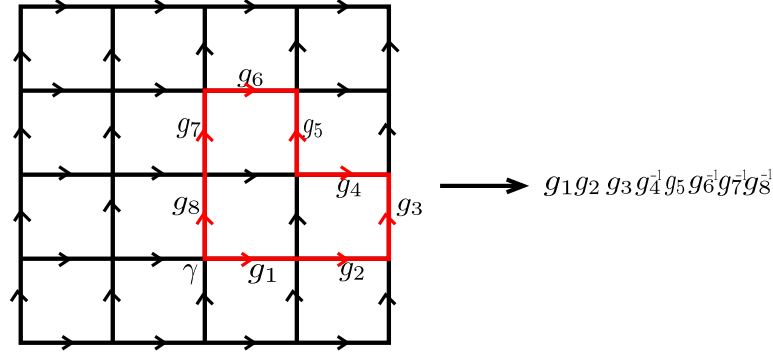
Figure 2.2.5: Given a configuration with flat holonomy, the map f takes any loop and associates it with the product of group elements along that loop.

map

$$f : V \to \mathrm{Hom}(\pi_1(M, v_0), G), \qquad (2.2.19)$$

such that, for any

$$|\psi\rangle = \bigotimes_{l \in K_1} |g\rangle_l \in V$$

and any oriented loop $\gamma \in M$ starting and ending at v_0,

$$f(|\psi\rangle)([\gamma]) = g_\gamma. \qquad (2.2.20)$$

That is, this map takes a configuration with flat local holonomy and associates to it a map $\pi_1(M, v_0) \to G$. This map in its turn associates homotopy classes of loops to the product of group elements along that loop. This is illustrated in figure 2.2.5. For a product of loops $[\gamma\gamma'] \in \pi_1(M, v_0)$, it is clear that $f(|\psi\rangle)([\gamma\gamma']) = g_\gamma g_{\gamma'}$. Thus, $f(|\psi\rangle)$ is indeed a group homomorphism, i.e., $f(|\psi\rangle) \in \mathrm{Hom}(\pi_1(M, v_0), G)$.

Consider a *spanning tree* T starting at v_0. A spanning tree is a connected graph connecting all vertices in the lattice in a way that it does not contains any loops. An example of a spanning tree is given in figure 2.2.6. Given its definition, the number of links in T is given by $m = |K_0| - 1$. We will use this concept to show that f is onto and $|G|^m$-to-1.

Let $\phi \in \mathrm{Hom}(\pi_1(M, v_0), G)$. Thus, given any class of loops $[\gamma] \in \pi_1(M, v_0)$, $\phi([\gamma]) = g$, for some $g \in G$. We will build a configuration $|\psi\rangle \in S$ fixed by ϕ such that $f(|\psi\rangle) = \phi$. Let $l \in K_1$ be a link that is not in T. Let $v_1, v_2 \in K_0$ be the two vertices in the boundary ∂l of l. By definition, there are unique paths γ_1 and γ_2 along T connecting v_0 to v_1 and v_2, respectively.
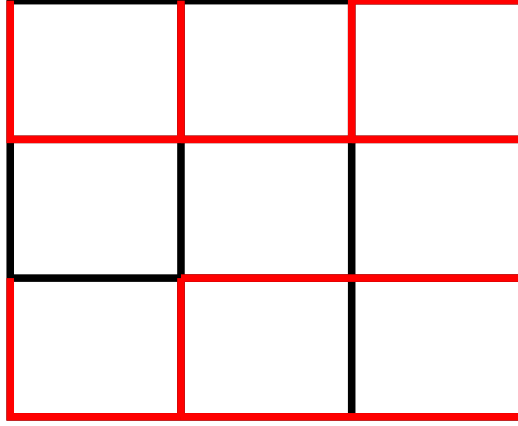
Figure 2.2.6: Example of a spanning tree (in red).

We can then form a loop $\gamma = \gamma_1 l \gamma_2^{-1}$, that is, we go from v_0 to v_1 along γ_1, transverse l and then we go from v_2 back to v_0 following the inverse path of γ_2 (see figure 2.2.7). Given this loop, $\phi([\gamma]) = g$ is fixed. The idea here is that we can choose arbitrarily the group elements associated to the links in T, but the group element of $l \notin T$ is fixed by the ones in T together with $\phi([\gamma]) = g$. That is, there is a unique group element g_l such that

$$g_{\gamma_1} g_l g_{\gamma_2^{-1}} = g = \phi([\gamma]).$$

Thus, given $\phi \in \text{Hom}(\pi_1(M, v_0), G)$, we constructed a configuration $|\psi\rangle = \bigotimes_{l \in K_1} |g\rangle_l \in \mathcal{H}$ by assigning arbitrarily group elements to a spanning tree T. Note that, since ϕ is a group homomorphism, when γ is contractible, i.e., when it is in the class of the identity loop $[\gamma_0] \in \pi_1(M, v_0)$, we have that $\phi([\gamma]) = e \in G$. Thus, in the way we construct the configuration by equating $g_\gamma = \phi([\gamma])$ for γ built from the union of a spanning tree and the link outside the tree, $g_\gamma = e$ when γ is contractible, which means that the configuration $|\psi\rangle \in V$. By definition, $f(|\psi\rangle)([\gamma]) = g_\gamma$ for any loop γ, and thus $f(|\psi\rangle) = \phi$. Therefore, f is onto. Since there are $|G|^m$ choices of configurations to put on the links of T, f is $|G|^m$-to-one.

Note that, if we apply gauge transformations to $|\psi\rangle$ at vertices $v \in K_0$ such that $v \neq v_0$, the image $f(|\psi\rangle)$ doesn't change. This is because the gauge transformations applied along the path γ (excluding its start and end point v_0) doesn't change the holonomy g_γ, as shown in figure 2.2.8. Thus, for two states $|\psi\rangle$ and $|\psi'\rangle$ related by gauge transformations at vertices different from v_0, we have that

$$f(|\psi\rangle)([\gamma]) = g_\gamma = f(|\psi'\rangle)([\gamma]),$$

for any $[\gamma] \in \pi_1(M, v_0)$. Note that there are $|G|^m$ such transformations we can perform. Let
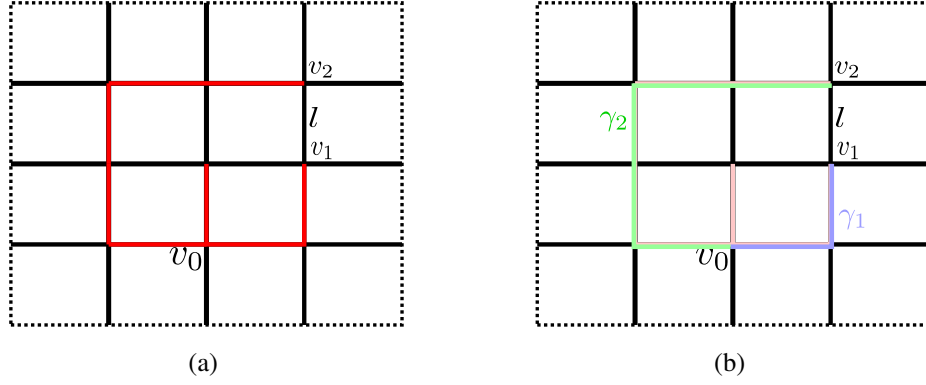
Figure 2.2.7: (a) A spanning tree in a manifold without a boundary. (b) The composition of the paths γ_1, γ_2 and l forms a loop.
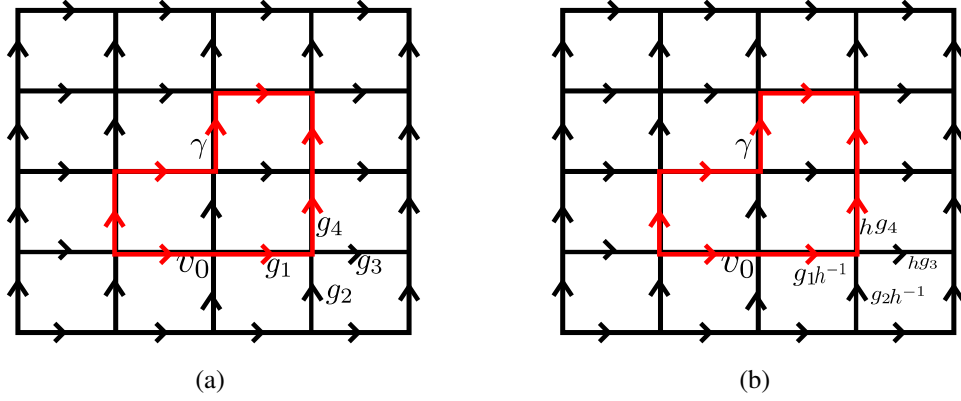
Figure 2.2.8: (a) A loop with base point at v_0 and a arbitrary gauge configuration on links. (b) Applying a gauge transformation at a vertex different from v_0 does not change the product g_γ, because $g_1 h^{-1} h g_4 = g_1 g_4$.

$g \in G$. A gauge transformation $A_{v_0}^g$ applied to the vertex v_0 is such that

$$f(A_{v_0}^g |\psi\rangle)([\gamma]) = g g_{l_1} ... g_{l_{|\gamma|}}^{-1} g^{-1} = g g_\gamma g^{-1} = g f(|\psi\rangle)([\gamma]) g^{-1}.$$

Thus, gauge classes in V are in one-to-one correspondence with orbits in $\mathrm{Hom}(\pi_1(M, v_0), G)$. Therefore, the number of ground states $|[V]|$ must be equal to the number of elements in $\mathrm{Hom}(\pi_1(M, v_0), G)$, i.e.,

$$GSD = |\mathrm{Hom}(\pi_1(M, v_0), G)|. \tag{2.2.21}$$

For example, consider the case in which $G = \mathbb{Z}_2$ and $M = T^2$, the 2-torus. We have that

$\pi_1(T^2, v_0) = \mathbb{Z} \times \mathbb{Z}$ and thus

$$GSD = |\mathrm{Hom}(\mathbb{Z} \times \mathbb{Z}, \mathbb{Z}_2)| = 2^2,$$

which is exactly the GSD of the Toric Code (2.1.28).

Excitations of the Quantum Double Models are, in general, *non-Abelian anyons*. The construction and classification of excited states for a general group G is highly non-trivial and out of the scope of this thesis, since here we only deal with Abelian groups. We refer to [15] for further details.

Chapter 3

Topological phases from abelian higher gauge theories

In 2-dimensions, given a finite group G we can define a system with topological order through the corresponding Quantum Double Model, as shown in chapter 2. However, for $D > 2$ spatial dimensions, there is no general formalism in which, given some mathematical object, we can immediately define a model of topological order. A step in that direction was given in [1], where a generalization of the Abelian Quantum Double Models to any dimension D in terms of *Abelian Higher Gauge Theories* (AHGT) was described. The Abelian higher gauge theory is a generalization to any dimension D of a particular case of the 2-gauge theory in 3-dimensions introduced in [26, 1] (see appendix B). In this chapter, we review that construction.

3.1 Abelian higher gauge theories in D-dimensions

In this section, we give a brief review of the general theory of *Abelian higher gauge theories* introduced in [1]. Our focus here is on giving an overview of the main definitions and developing some intuition on the theory. For a more rigorous approach to the construction of this theory, see [1, 41, 42], where most proofs that are omitted here can be found.

Given a geometrical chain complex that describes the discretization of a D-dimensional manifold M and a chain complex of Abelian finite groups, an Abelian higher gauge theory can be defined. The *ground state degeneracy* of this theory is given by the cohomology groups of the geometrical chain complex, and as such it is a topological invariant of the underlying manifold [43]. Moreover, given a bipartition $M = A \cup B$, the *entanglement entropy S_A* of the theory is

35

given by a sum of two terms. The first one depends on the *area* of the entangling surface ∂A, while the second one depends on cohomology groups of both the boundary ∂A and the bulk A [1]. These characteristics indicate that Abelian higher gauge theories can be used as models of *topological order*. For more details, we refer to [43, 1].

3.1.1 Higher gauge configurations

Let K be a simplicial decomposition of a D-dimensional manifold M. That is,

$$K = K_0 \cup K_1 \cup K_2 \cup \cdots \cup K_D,$$

where K_n is the set of n-dimensional simplices. The simplicial decomposition K is the lattice over which we will define a lattice higher gauge theory. For each $n = 0, ..., D$, let C_n be the *chain group* of K_n, i.e., the Abelian group freely generated by K_n. An element $c \in C_n$ can be written as

$$c = \sum_{x \in K_n} n(x)x,$$

where $n(x) \in \mathbb{Z}$. Given the standard boundary maps $\partial_n^C : C_n \to C_{n-1}$ such that $\partial_n^C \circ \partial_{n+1}^C = 0$, we can associate to K a chain complex [44]

$$0 \to C_D \xrightarrow{\partial_D^C} C_{D-1} \xrightarrow{\partial_{D-1}^C} \ldots \xrightarrow{\partial_2^C} C_1 \xrightarrow{\partial_1^C} C_0 \to 0 \tag{3.1.1}$$

that we will denote $(C(K), \partial^C)$.

To describe the higher gauge symmetry, we take a sequence $\{G_n\}_{n=0}^D$ of finite groups and define the *higher gauge group* as the abstract chain complex of groups

$$0 \to G_D \xrightarrow{\partial_D^G} G_{D-1} \xrightarrow{\partial_{D-1}^G} \ldots \xrightarrow{\partial_2^G} G_1 \xrightarrow{\partial_1^G} G_0 \to 0, \tag{3.1.2}$$

where for each $n = 1, ..., D$, $\partial_n^G : G_n \to G_{n-1}$ is a group homomorphism such that $\partial_n^G \circ \partial_{n+1}^G = 0$.

We define a *higher gauge configuration* as the sequence $f = \{f_n\}_{n=0}^D$ of maps $f_n : K_n \to G_n$. The map f_n assign a group element $g \in G_n$ to a n-simplice $x \in K_n$. Each such map

$$\cdots \xrightarrow{\partial^C_{n+2}} C_{n+1} \xrightarrow{\partial^C_{n+1}} C_n \xrightarrow{\partial^C_n} C_{n-1} \xrightarrow{\partial^C_{n-1}} \cdots$$

$$\cdots \xrightarrow{\partial^G_{n+2}} G_{n+1} \xrightarrow{\partial^G_{n+1}} G_n \xrightarrow{\partial^G_n} G_{n-1} \xrightarrow{\partial^G_{n-1}} \cdots$$

with vertical maps f_{n+1}, f_n, f_{n-1}.

Figure 3.1.1: A higher gauge configuration $f \in \mathrm{hom}(C, G)^0$.

defines a unique group homomorphism $f_n : C_n \to G_n$ as follows: let $c \in C_n$. Then

$$f_n(c) = \sum_{x \in K_n} n(x) f_n(x).$$

Roughly speaking, a higher gauge configuration f is a section of a G-bundle over M.

For each $n = 0, ..., D$, let $\mathrm{Hom}(C_n, G_n)$ be the set of maps $f_n : C_n \to G_n$. It can be given the structure of an Abelian group if we define, for any $f_n, g_n \in \mathrm{Hom}(C_n, G_n)$,

$$(f_n + g_n)(x) = f_n(x) + g_n(x).$$

Then, the direct sum

$$\mathrm{hom}(C, G)^0 = \bigoplus_{n=0}^{D} \mathrm{Hom}(C_n, G_n) \tag{3.1.3}$$

is also an Abelian group. The notation $\mathrm{hom}(C, G)^0$ will be clarified when we discuss other maps between the complexes that can be constructed. The higher gauge configuration $f = \{f_n\}_{n=0}^{D}$ is an element of $\mathrm{hom}(C, G)^0$. Thus, a higher gauge configuration can be pictured as a sequence of maps between chain complexes, as shown in figure 3.1.1. The diagram in figure 3.1.1 is, in general, not commutative.

3.1.2 The Hilbert space

We define the Hilbert space of our theory as the complex vector space $\mathcal{H}$ generated by the orthonormal basis set

$$\left\{ |f\rangle = \bigotimes_{n=0}^{D} \bigotimes_{x \in K_n} |f_n(x)\rangle : f \in \mathrm{hom}(C, G)^0 \right\}. \tag{3.1.4}$$

That is, the basis of $\mathcal{H}$ is given by vectors labelled by higher gauge configurations. Note that since each $f_n(x) \in G_n$, this definition generalizes the basis states of the Quantum Double Model by assigning to each simplex (not only links) a group element. The dimension of the Hilbert space is given by the number of higher gauge configurations, that is, the order of the group $\mathrm{hom}(C, G)^0$:

$$\dim(\mathcal{H}) = |\mathrm{hom}(C, G)^0| = \prod_{n=0}^{D} |G_n|^{|K_n|}. \tag{3.1.5}$$

The orthonormality of the basis means that

$$\langle f | g \rangle = \delta(f, g) = \begin{cases} 1, & \text{if} \quad f = g, \\ 0, & \text{if} \quad f \neq g. \end{cases}$$

for all $f, g \in \mathrm{hom}(C, G)^0$, where we consider that $f = g$ when for every $n = 0, ..., D$, $f_n = g_n$, and $f \neq g$ when there is at least one $n = 0, ..., D$ for which $f_n \neq g_n$.

Since (3.1.4) is a basis of the Hilbert space, any state $|\psi\rangle \in \mathcal{H}$ can be written as the linear combination

$$|\psi\rangle = \sum_{f \in \mathrm{hom}(C,G)^0} \psi(f) |f\rangle,$$

where $\psi(f) = \langle f | \psi \rangle \in \mathbb{C}$. Since $f = \{f_n\}_{n=0}^{D} \in \mathrm{hom}(C, G)^0$ assigns a group element to every simplex in the lattice, the basis state $|f\rangle \in \mathcal{H}$ can be written explicitly as the tensor product over simplexes of the local degrees of freedom living over them. For example, in $D = 3$ dimensions, a higher gauge configuration is given by $f = \{f_0, f_1, f_2, f_3\}$, and a basis state $|f\rangle \in \mathcal{H}$ can be written as

$$|f\rangle = \bigotimes_{v \in K_0} |f_0(v)\rangle \bigotimes_{l \in K_1} |f_1(l)\rangle \bigotimes_{p \in K_2} |f_2(p)\rangle \bigotimes_{c \in K_3} |f_3(c)\rangle.$$

3.1.3 Brown cohomology

Before we define the Hamiltonian of our theory, we need to establish a few concepts. For $p \in \mathbb{Z}$, let's define the Abelian groups

$$\mathrm{hom}(C, G)^p = \bigoplus_{n=0}^{D} \mathrm{Hom}(C_n, G_{n-p}), \tag{3.1.6}$$

where we set $G_{n-p} = 0$ (the trivial group) if $n - p > D$ or $n - p < 0$. An element $g \in$ $\hom(C, G)^p$ is a sequence $g = \{g_n\}_{n=0}^D$ of p-skewed homomorphisms $g_n : C_n \to G_{n-p}$. An example of $g \in \hom(C, G)^1$ is shown in figure 3.1.2. These skewed maps will be useful to define the *higher gauge transformations* and the *higher holonomies* of our theory.

Given a $p \in \mathbb{Z}$, we can define a *co-boundary operator* $\delta^p : \hom(C, G)^p \to \hom(C, G)^{p+1}$. For any $h = \{h_n\}_{n=0}^D \in \hom(C, G)^p$, the operator δ^p acts over h and returns the sequence of maps $\delta^p h = \{(\delta^p h)_n\}_{n=0}^D$ such that

$$(\delta^p h)_n = h_{n-1} \circ \partial_n^C - (-1)^p \partial_{n-p}^G \circ h_n. \tag{3.1.7}$$

It can be shown that the operators δ^p satisfy

$$\delta^{p+1} \circ \delta^p = 0. \tag{3.1.8}$$

Thus, using the sequence of Abelian groups $\hom(C, G)^p$ we can naturally define a *co-chain complex* $(\hom(C, G)^p, \delta^p)$ as

$$\cdots \xrightarrow{\delta^{-2}} \hom(C, G)^{-1} \xrightarrow{\delta^{-1}} \hom(C, G)^0 \xrightarrow{\delta^0} \hom(C, G)^1 \xrightarrow{\delta^1} \cdots \tag{3.1.9}$$

where we exhibit only the part of the co-chain complex that will be useful for our theory. For a more detailed account, please refer to [43]. Associated to the co-chain complex (3.1.9), we can define *Brown cohomology groups* [45]

$$\mathrm{H}^p(C, G) = \ker(\delta^p)/\mathrm{Im}(\delta^{p-1}). \tag{3.1.10}$$

These groups are isomorphic to the direct product of the cohomology groups of the geometric chain complex (C, ∂^C) with coefficients in the homology groups of (G, ∂^G) [45]. That is,

$$\mathrm{H}^p(C, G) \cong \bigoplus_{n=0}^D H^n(C, H_{n-p}(G)). \tag{3.1.11}$$

From (3.1.11), it is clear that Brown cohomology groups are topological invariants of the manifold M. The Brown cohomology plays an important role in proving that the ground state degeneracy of an Abelian higher gauge theory is a topological invariant.

Now, for each $n = 0, ..., D$, let $\hat{G}_n = \mathrm{Hom}(G_n, U(1))$ be the set of group homomorphisms

Figure 3.1.2: An element $g \in \hom(C, G)^1$ as a sequence $\{g_n\}_{n=0}^d$ of skewed maps.

$a_n : G_n \to U(1)$. Since G_n is Abelian, $\hat{G}_n$ is the set of irreducible unitary representations of G_n. We can give $\hat{G}_n$ the structure of an Abelian group by defining

$$(a_n + b_n)(g) = a_n(g)b_n(g), \quad -a_n(g) = (a_n(g))^{-1},$$

for all $a_n, b_n \in \hat{G}_n$ and all $g \in G_n$. We define the Abelian groups

$$\hom(C, G)_p = \bigoplus_{n=0}^{D} \mathrm{Hom}(C_n, \hat{G}_{n-p}). \tag{3.1.12}$$

An element $m \in \hom(C, G)_p$ is a sequence $m = \{m_n\}_{n=0}^{D}$ of group homomorphisms $m_n : C_n \to \hat{G}_n$ which takes a n-simplex x and associates it to a map $G_n \to U(1)$. We also define a pairing $\langle \cdot, \cdot \rangle : \hom(C, G)_p \times \hom(C, G)^p \to U(1)$ such that, for any $m \in \hom(C, G)_p$ and $f \in \hom(C, G)^p$,

$$\langle m, f \rangle = \prod_{n=0}^{D} \prod_{x \in K_n} m_n(x)(f_n(x)). \tag{3.1.13}$$

We now define a boundary map $\delta_p : \hom(C, G)_p \to \hom(C, G)_{p-1}$ such that, for any $m \in \hom(C, G)_p$ and any $f \in \hom(C, G)^{p-1}$,

$$\langle \delta_p m, f \rangle = \langle m, \delta^{p-1} f \rangle. \tag{3.1.14}$$

It can be shown that

$$\delta_{p-1} \circ \delta_p = 0. \tag{3.1.15}$$

Hence, we can use the sequence of Abelian groups $\hom(C, G)_p$ to naturally define a chain

complex $(\mathrm{hom}(C,G)_p, \delta_p)$ as

$$\cdots \xleftarrow{\delta_{-1}} \mathrm{hom}(C,G)_{-1} \xleftarrow{\delta_0} \mathrm{hom}(C,G)_0 \xleftarrow{\delta_1} \mathrm{hom}(C,G)_1 \xleftarrow{\delta_2} \cdots \qquad (3.1.16)$$

3.1.4 Higher gauge transformations, higher holonomy operators and the Hamiltonian

Here we define the operators that compose the Hamiltonian. To gain some intuition, let's ana-lyze the gauge theory aspects of a special case. Let $D = 2$ and suppose that the discretization of the manifold M described by the geometrical chain complex (3.1.1) is a square lattice. Suppose also that the only non-trivial group of the chain complex (3.1.2) is G_1. This defines what we call a *1-gauge theory*. We have group degrees of freedom living over links of the square lattice.

Roughly speaking, we can say that we have a G_1 principal bundle over M. A fixed gauge configuration $f_1 : C_1 \to G_1$ is a section of this principal bundle. Intuitively, the restriction of f_1 to a particular link can be seem as a local section. Local sections defined on two different intersecting links must be related through a *gauge transformation* [46].

Hence, at a vertex of the lattice, we must be able to define a gauge transformation acting over higher gauge configurations. To do so, let $t \in \mathrm{hom}(C,G)^{-1}$ and let $f \in \mathrm{hom}(C,G)^0$ be any higher gauge configuration. We define the *higher gauge transformation* operator $A_t : \mathcal{H} \to \mathcal{H}$ as

$$A_t \, |f\rangle = |f + \delta^{-1} t\rangle \,, \qquad (3.1.17)$$

where $|f\rangle \in \mathcal{H}$ is the basis vector labelled by the higher gauge configuration f. Note that, in the 1-gauge theory case, $t = t_0 : C_0 \to G_1$ and

$$A_t \, |f\rangle = \bigotimes_{x \in K_1} |f_1(x) + (t_0 \circ \partial_1^C)(x)\rangle \,.$$

That is, the operator assigns group elements to the vertices of a link $x \in K_1$ and sums the result to the group element $f_1(x)$, returning the gauge transformed state $|f_1(x) + (t_0 \circ \partial_1)(x)\rangle$, as we would intuitively expect from usual gauge theory.

Now, let $m \in \mathrm{hom}(C,G)_1$ and let $f \in \mathrm{hom}(C,G)^0$ be any higher gauge configuration. We

define the *higher holonomy operator* $B_m : \mathcal{H} \to \mathcal{H}$ as

$$B_m \left| f \right\rangle = \left\langle m, \delta^0 f \right\rangle \left| f \right\rangle , \tag{3.1.18}$$

where $\left| f \right\rangle \in \mathcal{H}$ is the basis state labelled by the higher gauge configuration f. To see the intuition behind this definition, consider again the 1-gauge theory case in the square lattice. We have that $m = m_2 : C_2 \to \hat{G}_1$ and

$$\left\langle m, \delta^0 f \right\rangle = \prod_{x \in K_2} m_2(x)((f_1 \circ \partial_2^C)(x)).$$

Consider a plaquette $p \in K_2$ and links $l_i \in \partial p$, $i = 1, ..., 4$. The operator $f_1 \circ \partial_2^C$ sends $\sum_i (-1)^i l_i \to \sum_i (-1)^i g_i \in G_1$. The map m_2 then takes the sum $\sum_i (-1)^i g_i$ and returns $e^{i \sum_k (-1)^k \theta_k} \in U(1)$. This last form resembles a discrete version of the holonomy of the gauge connection in an usual gauge theory [46].

For any $t \in \mathrm{hom}(C, G)^{-1}$ and any $m \in \mathrm{hom}(C, G)_1$, the operators A_t and B_m commute. In fact, let $f \in \mathrm{hom}(C, G)^0$ be a higher gauge configuration and let $\left| f \right\rangle \in \mathcal{H}$. We have that

$$A_t B_m \left| f \right\rangle = \left\langle m, \delta^0 f \right\rangle \left| f + \delta^{-1} t \right\rangle ,$$

while

$$B_m A_t \left| f \right\rangle = \left\langle m, \delta^0 (f + \delta^{-1} t) \right\rangle \left| f + \delta^{-1} t \right\rangle .$$

From (3.1.8), $\delta^0 \circ \delta^{-1} = 0$ and thus $A_t B_m = B_m A_t$.

Note that for any $t \in \mathrm{hom}(C, G)^{-1}$ and any $m \in \mathrm{hom}(C, G)_1$, the operators A_t and B_m act on the entire lattice. To define local projectors based on A_t and B_m, we fix $n = 0, ..., D$ and choose a n-simplex $x \in K_n$. We also fix a group element $g \in G_{n+1}$ and a representation $r \in \hat{G}_{n-1}$. Let $e[n, x, g] \in \mathrm{hom}(C, G)^{-1}$ be a map such that, for any $y \in K$,

$$e[n, x, g](y) = \begin{cases} g, & \text{if} \quad y = x, \\ 0, & \text{if} \quad y \neq x. \end{cases} \tag{3.1.19}$$

Also, let $\hat{e}[n, x, r] \in \mathrm{hom}(C, G)_1$ be a map such that, for any $f \in \mathrm{hom}(C, G)^1$,

$$\hat{e}[n, x, r](f) = r(f_n(x)). \tag{3.1.20}$$

The operators $A_{e[n,x,g]}$ and $B_{\hat{e}[n,x,r]}$ act locally around a n-simplex $x \in K_n$. Hence, we define the local operators

$$A_{n,x} = \frac{1}{|G_{n+1}|} \sum_{g \in G_{n+1}} A_{e[n,x,g]}, \tag{3.1.21}$$

$$B_{n,x} = \frac{1}{|G_{n-1}|} \sum_{r \in \hat{G}_{n-1}} B_{\hat{e}[n,x,r]}. \tag{3.1.22}$$

It can be shown that the operators (3.1.21) and (3.1.22) are commuting projectors [41]. Using these local projectors, we define the Hamiltonian of an Abelian higher gauge theory in D dimensions as

$$H_{HGT} = -\sum_{n=0}^{D} \sum_{x \in K_n} A_{n,x} - \sum_{n=0}^{D} \sum_{x \in K_n} B_{n,x}. \tag{3.1.23}$$

The Hamiltonian (3.1.23) is Hermitian. In fact, for any $n = 0, ..., D$ and for any $x \in K_n$, we have that, for basis states $|f\rangle, |f'\rangle \in \mathcal{H}$,

$$\langle f'| A_{n,x} |f\rangle = \frac{1}{|G_{n+1}|} \sum_{g \in G_{n+1}} \langle f'| A_{e[n,x,g]} |f\rangle$$

and

$$\langle f'| B_{n,x} |f\rangle = \frac{1}{|G_{n-1}|} \sum_{r \in \hat{G}_{n-1}} \langle f'| B_{\hat{e}[n,x,r]} |f\rangle.$$

From (3.1.17), the matrix element $\langle f'| A_{e[n,x,g]} |f\rangle$ is given by

$$\langle f'| A_{e[n,x,g]} |f\rangle = \langle f'|f + \delta^{-1}e[n,x,g]\rangle = \delta(f', f + \delta^{-1}e[n,x,g]),$$

and thus the operator $A_{n,x}$ is Hermitian. From (3.1.18), the matrix element $\langle f'| B_{\hat{e}[n,x,r]} |f\rangle$ is given by

$$\langle f'| B_{\hat{e}[n,x,r]} |f\rangle = \langle \hat{e}[n,x,r], \delta^0 f\rangle \, \delta(f', f).$$

From (3.1.13) and (3.1.20), we have that

$$\langle \hat{e}[n,x,r], \delta^0 f\rangle = r\left((\delta^0 f)_n(x)\right) = r\left((f_{n-1} \circ \partial_n^C)(x)\right) r^{-1}\left((\partial_n^G \circ f_n)(x)\right),$$

where we used the definition (3.1.7) of the co-boundary operator δ^0. Since $r \in \hat{G}_{n-1}$, $r(g) \in$

$U(1)$ for any $g \in G_{n-1}$. Thus, $r(g) = e^{i\theta(g)}$, for some angle θ depending on g. This means that $r^{-1}(g) = e^{-i\theta(g)}$, which is the same as taking the complex conjugate $(r(g))^*$. Therefore, consider the transpose complex conjugate

$$\langle f | B_{\hat{e}[n,x,r]} | f' \rangle^* = r^{-1}\left((f_{n-1} \circ \partial_n^C)(x)\right) r\left((\partial_n^G \circ f_n)(x)\right) \delta(f, f').$$

Taking the sum over all elements $r \in \hat{G}_{n-1}$, we have that

$$\sum_{r \in \hat{G}_{n-1}} r^{-1}\left((f_{n-1} \circ \partial_n^C)(x)\right) r\left((\partial_n^G \circ f_n)(x)\right) = \sum_{r \in \hat{G}_{n-1}} r\left((f_{n-1} \circ \partial_n^C)(x)\right) r^{-1}\left((\partial_n^G \circ f_n)(x)\right),$$

because in the sum over all group elements it will always appear both r and r^{-1}. Therefore,

$$\sum_{r \in \hat{G}_{n-1}} \langle f' | B_{\hat{e}[n,x,r]} | f \rangle = \sum_{r \in \hat{G}_{n-1}} \langle f | B_{\hat{e}[n,x,r]} | f' \rangle^*,$$

and thus the operator $B_{n,x}$ is also Hermitian. It follows that the Hamiltonian, being a sum of Hermitian operators, is also Hermitian.

The ground states of the Hamiltonian (3.1.23) are states $|\psi\rangle \in \mathcal{H}$ such that

$$A_{n,x} |\psi\rangle = B_{n,x} |\psi\rangle = |\psi\rangle,$$

for all $n = 0, ..., D$ and $x \in K_n$. The subspace of $\mathcal{H}$ spanned by the ground states of H is denoted by $\mathcal{H}_0$, whose dimension is the *ground state degeneracy* $GSD = \dim(\mathcal{H}_0)$. We have that $GSD \geq 1$, i.e., H is *frustration free*. In fact, let $0 \in \hom(C, G)^0$ be the higher gauge configuration that assigns the group identity $0 \in G_n$ to every n-simplex of the lattice. The state

$$|0\rangle_G = \prod_{n=0}^{D} \prod_{x \in K_n} A_{n,x} |0\rangle,$$

is not zero and is such that

$$A_{n,x} |0\rangle_G = B_{n,x} |0\rangle_G = |0\rangle_G,$$

for all $n = 0, ..., D$ and $x \in K_n$. Moreover, it can be shown [43, 42] that the ground state degeneracy is equal to the order of $H^0(C, G)$, the Brown cohomology group of order zero. That

is,

$$GSD = |\mathrm{H}^0(C, G)| = \prod_{n=0}^{D} |\mathrm{H}^n(C, \mathrm{H}_n(G))|. \tag{3.1.24}$$

Hence, the ground state degeneracy GSD can be written explicitly as a topological invariant of the manifold M.

3.2 Examples of topological phases

3.2.1 0-gauge theory in $D = 2$ dimensions

We start with a simple 2-dimensional example. Consider that the chain complex

$$0 \to C_2 \xrightarrow{\partial_2^C} C_1 \xrightarrow{\partial_1^C} C_0 \to 0$$

describes a regular square lattice. The higher gauge group (G, ∂^G) is given by the chain complex

$$0 \to G_2 \xrightarrow{\partial_2^G} G_1 \xrightarrow{\partial_1^G} G_0 \to 0,$$

where we choose $G_2 = G_1 = 0$. The higher gauge configurations are given as in figure 3.2.1. That is, we have degrees of freedom labelled by G_0 living on vertices of the square lattice. The Hilbert space $\mathcal{H}$ of this theory is generated by vectors

$$|f\rangle = \bigotimes_{v \in K_0} |f_0(v)\rangle,$$

for all $f \in \mathrm{hom}(C, G)^0 = \mathrm{Hom}(C_0, G_0)$.

To see how the operators (3.1.21) and (3.1.22) act over the basis states, let's analyse the localization maps (3.1.19) and (3.1.20). First, note that, since $G_2 = G_1 = 0$, the map $e[n, x, g] = 0$ for all $n = 0, 1, 2$ and $x \in K_n$. Thus, the operator $A_{e[n,x,g]}$ acts as the identity for all n, x. Now, $\hat{G}_{n-1} \neq 0$ only when $n = 1$, so $B_{\hat{e}[n,x,r]}$ is the identity operator for $n = 0, 2$. For $n = 1$, we have that

$$B_{\hat{e}[1,x,r]} |f\rangle = r\left((f_0 \circ \partial_1^C)(x)\right) |f\rangle,$$

for any $|f\rangle \in \mathcal{H}$.

$$0 \xrightarrow{} C_2 \xrightarrow{\partial_2^C} C_1 \xrightarrow{\partial_1^C} C_0 \xrightarrow{} 0$$

$$m_1 \qquad \downarrow f_0$$

$$0 \xrightarrow{} G_0 \xrightarrow{} 0$$

Figure 3.2.1: Gauge theory data for an Abelian 0-gauge theory.

We can now write the Hamiltonian of the Abelian 0-gauge theory. Since $A_{n,x}$ is the identity operator for all n, x, it gives only a constant energy term which we drop from the Hamiltonian. For the same reason, we also drop $B_{n,x}$ for $n = 0, 2$. Thus, we have that the Hamiltonian of the 0-gauge theory is given by

$$H_0 = -\sum_{x \in K_1} B_{1,x}, \tag{3.2.1}$$

where

$$B_{1,x} = \frac{1}{|G_0|} \sum_{r \in \hat{G}_0} B_{\hat{e}[1,x,r]}. \tag{3.2.2}$$

We can give a more explicit example by setting $G_0 = \mathbb{Z}_2 = \{0, 1\}$, with the group operation being addition mod 2. We then have *qubits* living on vertices of the square lattice. At each vertex, we have a local Hilbert space spanned by the basis vectors $\{|0\rangle, |1\rangle\}$.

There are only two possible homomorphisms $r : \mathbb{Z}_2 \to U(1)$, the map r_1 such that $r_1(0) = r_1(1) = 1$ and the map r_2 such that $r_2(0) = 1, r_2(1) = -1$. The local operator $B_{\hat{e}[1,x,r]}$ acts over links of the lattice. Given a state $|f\rangle \in \mathcal{H}$, we have clearly that $B_{\hat{e}[1,x,r_1]} |f\rangle = |f\rangle$. Let's write the link x as $x = (v_0 v_1)$, where v_0 and v_1 are its boundary vertices, i.e., we have that $\partial_1^C x = v_0 - v_1$. If the map $f_0 : C_0 \to \mathbb{Z}_2$ assigns elements $a, b \in \mathbb{Z}_2$ to $v_0, v_1 \in \partial_1^C x$, respectively, we have that $B_{\hat{e}[1,x,r_2]} |f\rangle = r(a)r(b)^{-1} |f\rangle$. The result of the product $r(a)r(b)^{-1}$ is either $+1$ or -1, and thus it can be shown that the matrix form of $B_{\hat{e}[1,x,r_2]}$ in the basis $\{|0\rangle, |1\rangle\}$ is given by

$$B_{\hat{e}[1,x,r_2]} = \sigma_{v_0}^z \otimes \sigma_{v_1}^z,$$

where σ_v^z are the usual Pauli z matrices acting over the local Hilbert space at the vertex v.

Therefore, we have that

$$B_l = B_{1,l} = \frac{1}{2} \left(\mathbb{1} + \sigma_{v_0}^z \otimes \sigma_{v_1}^z \right),$$

where $l = (v_0 v_1)$ and then the Hamiltonian of the 0-gauge theory is

$$H_0 = -\sum_{l \in K_1} B_l = -\frac{1}{2} \sum_{l \in K_1} \left(\mathbb{1} + \sigma_{v_0}^z \otimes \sigma_{v_1}^z \right). \tag{3.2.3}$$

Thus, 2-dimensional 0-gauge theory with gauge group $\mathbb{Z}_2$ is nothing but the $2D$ *Ising model* on a square lattice.

3.2.2   1-gauge theory in $D = 2$ dimensions

We again consider that the chain complex

$$0 \to C_2 \xrightarrow{\partial_2^C} C_1 \xrightarrow{\partial_1^C} C_0 \to 0$$

describes a regular square lattice. The higher gauge group is given by

$$0 \to G_2 \xrightarrow{\partial_2^G} G_1 \xrightarrow{\partial_1^G} G_0 \to 0,$$

but now we choose $G_2 = G_0 = 0$ and $G_1 \neq 0$. The higher gauge configurations are given as in figure 3.2.2. We have degrees of freedom at links of the square lattice, labelled by elements of the group G_1. The Hilbert space $\mathcal{H}$ of the theory is generated by the basis vectors

$$|f\rangle = \bigotimes_{l \in K_1} |f_1(l)\rangle,$$

for all $f \in \mathrm{hom}(C, G)^0 = \mathrm{Hom}(C_1, G_1)$.

Since $\mathrm{hom}(C, G)^{-1} = \mathrm{Hom}(C_0, G_1)$, higher gauge transformations A_t are parametrized by maps $t_0 \in \mathrm{Hom}(C_0, G_1)$. The localization map (3.1.19) is non-zero only for $n = 0$, $x \in K_0$. Let $v \in K_0$ be any vertex and $g \in G_1$ be any group element. For any link $l = (v_0 v_1) \in K_1$, we

have that

$$(\delta^{-1}e[0,v,g])_1(l) = e[0,v,g](\partial_1^C l)$$

$$= e[0,v,g](v_0 - v_1)$$

$$= (\delta(v,v_0) - \delta(v,v_1)) g,$$

where $\delta(v,v') = 1$ if $v = v'$ and zero otherwise. Then, for any basis vector $|f\rangle \in \mathcal{H}$, we have that

$$A_{e[0,v,g]} |f\rangle = \bigotimes_{l \in K_1} |f_1(l) + (\delta(v,v_0) - \delta(v,v_1)) g\rangle.$$

In a square lattice, we have four links sharing the vertex v. Let them be given by $l_i = (v_i v)$, $l_j = (vv_j)$, $l_k = (vv_k)$ and $l_m = (v_m v)$. We thus have that

$$A_{e[0,v,g]} |f\rangle = |f_1(x_1)\rangle \otimes ... \otimes |f_1(l_i) - g\rangle \otimes |f_1(l_j) + g\rangle \otimes |f_1(l_k) + g\rangle \otimes |f_1(l_m) - g\rangle \otimes ... \otimes |f_1(l_{|K_1|})\rangle.$$

Hence, the action of the local operator $A_v^g = A_{e[0,v,g]}$ is to enforce a gauge transformation by a group element g on links around the vertex v. If we let $f_1(l_i) = a_i$, $f_1(l_j) = a_j$, $f_1(l_k) = a_k$ and $f_1(l_m) = a_m$, with $a_i, a_j, a_k, a_m \in G_1$, we can represent this action as

$$A_v^g \left| \begin{array}{c} a_k \\ a_m \xrightarrow{} v \xrightarrow{} a_j \\ a_i \end{array} \right\rangle = \left| \begin{array}{c} a_k+g \\ a_m-g \xrightarrow{} v \xrightarrow{} a_j+g \\ a_i-g \end{array} \right\rangle. \tag{3.2.4}$$

The group $\hom(C,G)_1 = \text{Hom}(C_2, \hat{G}_1)$, which means that higher holonomy operators B_m are parametrized by maps $m_2 \in \text{Hom}(C_2, \hat{G}_1)$. The only non-zero localization map (3.1.20) is $\hat{e}[2,x,r]$, with $x \in K_2$ and $r \in \hat{G}_1$. Given $x \in K_2$ and $r \in \hat{G}_1$, the operator $B_{\hat{e}[2,x,r]}$ acts over a basis state $|f\rangle \in \mathcal{H}$ as

$$B_{\hat{e}[2,x,r]} |f\rangle = r\left((f_1 \circ \partial_2^C)(x) \right) |f\rangle. \tag{3.2.5}$$

To explain this action, let $x = (v_0 v_1 v_2 v_3) \in K_2$ be a plaquette whose boundary is given by

$$\partial_2^C x = l_0 + l_1 - l_2 - l_3,$$

48

$$0 \longrightarrow C_2 \xrightarrow{\partial_2^C} C_1 \xrightarrow{\partial_1^C} C_0 \longrightarrow 0$$
$$\qquad\qquad \overset{m_2}{\searrow} \quad \downarrow f_1 \quad \overset{t_0}{\swarrow}$$
$$0 \longrightarrow G_1 \longrightarrow 0$$

Figure 3.2.2: Gauge theory data for an Abelian 1-gauge theory.

where $l_0 = (v_0 v_1)$, $l_1 = (v_1 v_2)$, $l_2 = (v_3 v_2)$ and $l_3 = (v_0 v_3)$ are links in K_1. A gauge configuration $f_1 : C_1 \to G_1$ assigns group elements to all links in the lattice. In particular, it assigns $g_i \in G_1$ to the links l_i, $i = 0, 1, 2, 3$, that is,

$$f_1(\partial_2^C x) = g_0 + g_1 - g_2 - g_3.$$

An irreducible unitary representation $r \in \hat{G}_1$ relates a group element $g_k \in G_1$ to a phase factor $e^{i\theta_k} \in U(1)$ through a homomorphism. Hence, the local operator $B_{\hat{e}[2,x,r]}$ acts over the plaquette x and returns a phase factor

$$r(g_0 + g_1 - g_2 - g_3) = e^{i(\theta_0 + \theta_1 - \theta_2 - \theta_3)}$$

which is a measure of the holonomy along the boundary of x.

Using (3.1.23), we can write the Hamiltonian of the 1-gauge theory as

$$H_1 = -\sum_{v \in K_0} A_{0,v} - \sum_{p \in K_2} B_{2,p}, \qquad (3.2.6)$$

where we dropped terms proportional to the identity operator,

$$A_{0,v} = \frac{1}{|G_1|} \sum_{g \in G_1} A_v^g,$$

with A_v^g given by (3.2.4) and

$$B_{2,p} = \frac{1}{|G_1|} \sum_{r \in \hat{G}_1} B_{\hat{e}[2,p,r]},$$

with $B_{\hat{e}[2,p,r]}$ given by (3.2.5).

A more familiar example can be given by considering the case in which $G_1 = \mathbb{Z}_2 = \{0, 1\}$, with the group operation being addition mod 2. In this case, we have qubits living on links of the square lattice. At each link $l \in K_1$, we have a local Hilbert $\mathcal{H}_l$ space generated by the basis

vectors $\{|0\rangle_l, |1\rangle_l\}$.

From (3.2.4), it is straightforward to see that the local operator A_v^g acts as the identity operator when $g = 0$. When $g = 1$, A_v^1 flips the qubits living on links around the vertex v. Hence,

$$A_{0,v} = \frac{1}{2}\left(\mathbb{1} + A_v^1\right).$$

Expressing $A_{0,v}$ as a matrix in the basis $\{|0\rangle, |1\rangle\}$, we have that

$$A_v = A_{0,v} = \frac{1}{2}\left(\mathbb{1} + \bigotimes_{l \in \text{star}(v)} \sigma_l^x\right), \tag{3.2.7}$$

where σ_l^x are the usual Pauli x matrices acting over the local Hilbert space at the link l.

As in the 0-gauge example, there are only two possible homomorphisms $r : \mathbb{Z}_2 \to U(1)$, the map r_1 such that $r_1(0) = r_1(1) = 1$ and the map r_2 such that $r_2(0) = 1$ and $r_2(1) = -1$. Then, for $p \in K_2$, the operator $B_{\hat{e}[2,p,r_1]}$ acts as the identity. Let's write the plaquette $p = (v_0 v_1 v_2 v_3)$. Its boundary is given by $\partial_2^C p = l_0 + l_1 - l_2 - l_3$, where $l_0 = (v_0 v_1)$, $l_1 = (v_1 v_2)$, $l_2 = (v_3 v_2)$ and $l_3 = (v_0 v_3)$ are links in K_1. If $f_1 : C_1 \to \mathbb{Z}_2$ assigns the elements $a, b, c, d \in \mathbb{Z}_2$ to $l_0, l_1, l_2, l_3 \in \partial_2^C p$, respectively, we have that for $|f\rangle \in \mathcal{H}$,

$$B_{\hat{e}[2,p,r_2]} |f\rangle = r(a)r(b)r(c)^{-1}r(d)^{-1} |f\rangle,$$

with $r(a)r(b)r(c)^{-1}r(d)^{-1} = \pm 1$. The matrix form of $B_{2,p}$ in the basis $\{|0\rangle, |1\rangle\}$ is given by

$$B_p = B_{2,p} = \frac{1}{2}\left(\mathbb{1} + \bigotimes_{l \in \partial p} \sigma_l^z\right), \tag{3.2.8}$$

where σ_l^z are the usual Pauli z matrices acting over qubits in $\mathcal{H}_l$.

Thus, the Hamiltonian of $\mathbb{Z}_2$ 1-gauge theory is given by

$$H_1 = -\sum_{v \in K_0} A_v - \sum_{p \in K_2} B_p, \tag{3.2.9}$$

where A_v is given by equation (3.2.7) and B_p is given by equation (3.2.8). Therefore, $\mathbb{Z}_2$ 1-gauge theory is Kitaev's *Toric Code* in $D = 2$ dimensions of section 2.1. For arbitrary G_1, 1-gauge theory is equivalent to the *Quantum Double Model* of section 2.2 with Abelian gauge group G_1.

3.2.3 $1,2$-gauge theory in $D = 3$ dimensions

Let's define a $1,2$-gauge theory in $3D$ defined on a regular cubic lattice, given by the chain complex

$$0 \to C_3 \xrightarrow{\partial_3^C} C_2 \xrightarrow{\partial_2^C} C_1 \xrightarrow{\partial_1^C} C_0 \to 0.$$

The higher gauge group is given by

$$0 \to G_3 \xrightarrow{\partial_3^G} G_2 \xrightarrow{\partial_2^G} G_1 \xrightarrow{\partial_1^G} G_0 \to 0,$$

with $G_3 = G_0 = 0$ and $G_2, G_1 \neq 0$. The higher gauge configurations are given as in figure 3.2.3. There are degrees of freedom on links and faces of the cubic lattice, labelled by elements of G_1 and G_2, respectively. For all $f = \{f_1, f_2\} \in \text{hom}(C, G)^0 = \text{Hom}(C_1, G_1) \oplus \text{Hom}(C_2, G_2)$, the Hilbert space $\mathcal{H}$ of the theory is generated by the basis vectors

$$|f\rangle = \bigotimes_{l \in K_1} |f_1(l)\rangle \bigotimes_{p \in K_2} |f_2(p)\rangle.$$

We have that

$$\text{hom}(C, G)^{-1} = \text{Hom}(C_0, G_1) \oplus \text{Hom}(C_1, G_2).$$

Thus, higher gauge transformations are parametrized by maps $t = \{t_0, t_1\}$, where $t_0 \in \text{Hom}(C_0.G_1)$ and $t_1 \in \text{Hom}(C_1, G_2)$. Since the only non-trivial groups are G_2 and G_1, the only non-trivial higher gauge transformations that enter the sum in the Hamiltonian (3.1.23) are $A_v = A_{0,v}$, with $v \in K_0$, and $A_l = A_{1,l}$, with $l \in K_1$. From (3.1.21), the operator A_v is given by

$$A_v = \frac{1}{|G_1|} \sum_{g \in G_1} A_v^g,$$

where $A_v^g = A_{e[0,v,g]}$. Given a basis vector $|f\rangle \in \mathcal{H}$, we have that

$$
\begin{aligned}
A_v^g |f\rangle = A_{e[0,v,g]} |f\rangle &= |f + \delta^{-1} e[0, v, g]\rangle \\
&= \bigotimes_{l \in K_1} |f_1(l) + (\delta^{-1} e[0, v, g])_1(l)\rangle \\
&\quad \bigotimes_{p \in K_2} |f_2(p) + (\delta^{-1} e[0, v, g])_2(p)\rangle.
\end{aligned}
$$

$$
\begin{array}{ccccccccc}
0 & \longrightarrow & C_3 & \xrightarrow{\partial_3^C} & C_2 & \xrightarrow{\partial_2^C} & C_1 & \xrightarrow{\partial_1^C} & C_0 & \longrightarrow & 0 \\
& & & m_3 \quad f_2 & & m_2 \quad t_1 & & f_1 \quad t_0 & & & \\
& & & 0 & \longrightarrow & G_2 & \xrightarrow{\partial_2^G} & G_1 & \longrightarrow & 0
\end{array}
$$

Figure 3.2.3: Higher gauge theory data for an Abelian $1, 2$-gauge theory.

Since, for any $l \in K_1$ and any $p \in K_2$, $e[0, v, g](l) = 0$ and $e[0, v, g](\partial_2^C p) = 0$,

$$
(\delta^{-1} e[0, v, g])_1(l) = e[0, v, g](\partial_1^C l),
$$

and

$$
(\delta^{-1} e[0, v, g])_2(p) = 0.
$$

Thus, the local operator A_v^g acts over basis vector just like in the 1-gauge theory case, applying a gauge transformation by a group element $g \in G_1$ on links around the vertex v. Then, we can represent the action of A_v^g as

$$
A_v^g \left| \begin{array}{c} a_k \quad a_m \\ a_l \quad v \quad a_j \\ a_n \quad a_i \end{array} \right\rangle = \left| \begin{array}{c} a_{k+g} \quad a_{m-g} \\ a_{l-g} \quad v \quad a_{j+g} \\ a_{n+g} \quad a_{i-g} \end{array} \right\rangle . \tag{3.2.10}
$$

From (3.1.21), the operator A_l is given by

$$
A_l = \frac{1}{|G_2|} \sum_{\gamma \in G_2} A_l^\gamma,
$$

where $A_l^\gamma = A_{e[1, l, \gamma]}$. Given a basis state $|f\rangle \in \mathcal{H}$, we have that

$$
\begin{aligned}
A_l^\gamma |f\rangle = A_{e[1, l, \gamma]} |f\rangle &= |f + \delta^{-1} e[1, l, \gamma]\rangle \\
&= \bigotimes_{l' \in K_1} |f_1(l') + (\delta^{-1} e[1, l, \gamma])_1(l')\rangle \\
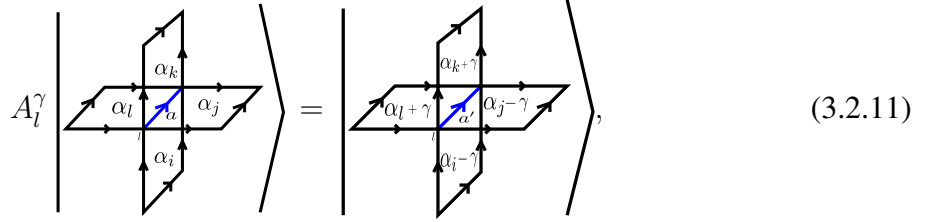&\quad \bigotimes_{p \in K_2} |f_2(p) + (\delta^{-1} e[1, l, \gamma])_2(p)\rangle .
\end{aligned}
$$

It is straightforward to check that

$$(\delta^{-1}e[1,l,\gamma])_1(l') = \delta(l,l')\partial_2^G\gamma,$$

for any $l, l' \in K_1$ and any $\gamma \in G_2$, and that, given a plaquette $p \in K_2$ such that $\partial_2^C p = l_0 + l_1 - l_2 - l_3$,

$$(\delta^{-1}e[1,l,\gamma])_2(p) = \gamma(\delta(l,l_0) + \delta(l,l_1)$$
$$-\delta(l,l_2) - \delta(l,l_3)).$$

Hence, the local operator A_l^γ applies a gauge transformation on plaquettes sharing the link l, while transforming the state of the link l as well. We can represent the action of A_l^γ over any basis state as

$$(3.2.11)$$

where the link l is shown in blue and $a' = a + \partial_2^G\gamma$.

Since

$$\mathrm{hom}(C,G)_1 = \mathrm{Hom}(C_2,\hat{G}_1) \oplus \mathrm{Hom}(C_3,\hat{G}_2),$$

higher holonomy operators are parametrized by maps $m = \{m_2, m_3\}$, where $m_2 \in \mathrm{Hom}(C_2, \hat{G}_1)$ and $m_3 \in \mathrm{Hom}(C_3, \hat{G}_2)$. The only non-trivial higher holonomy operators that enter the sum in the Hamiltonian (3.1.23) are $B_p = B_{2,p}$, where $p \in K_2$, and $B_c = B_{3,c}$, where $c \in K_3$. From (3.1.22), the operator B_p is given by

$$B_p = \frac{1}{|G_1|}\sum_{r\in\hat{G}_1} B_{\hat{e}[2,p,r]}.$$

The operator $B_{\hat{e}[2,p,r]}$, for any $r \in \hat{G}_1$, acts over a basis state $|f\rangle \in \mathcal{H}$ as follows:

$$B_{\hat{e}[2,p,r]}|f\rangle = r\left((f_1 \circ \partial_2^C)(p)\right) r\left((\partial_2^G \circ f_2)(p)\right)^{-1}|f\rangle.$$

We can interpret this action as measuring the holonomy along the boundary of the plaquette p and comparing the result with the image in G_1 of the value $f_2(p) \in G_2$. If both are equal, the

state $|f\rangle$ is invariant under $B_{\hat{e}[2,p,r]}$. If they are different, $|f\rangle$ acquires a phase.

From (3.1.22), the operator B_c is given by

$$B_c = \frac{1}{|G_2|} \sum_{r \in \hat{G}_2} B_{\hat{e}[3,c,r]}.$$

Given $r \in \hat{G}_2$ and a basis state $|f\rangle \in \mathcal{H}$, we have that

$$B_{\hat{e}[3,c,r]} |f\rangle = r \left((f_2 \circ \partial_3^C)(c) \right) |f\rangle .$$

Then, $B_{\hat{e}[3,c,r]}$ measures a higher holonomy value along the boundary of the cube c.

Using (3.1.23), we can write the Hamiltonian of the $1, 2$-gauge theory as

$$H_{1,2} = -\sum_{v \in K_0} A_v - \sum_{l \in K_1} A_l - \sum_{p \in K_2} B_p - \sum_{c \in K_3} B_c. \tag{3.2.12}$$

The group chain complex

$$0 \to G_2 \xrightarrow{\partial_2^G} G_1 \to 0$$

can be recast into the language of *strict 2-groups* or equivalently, *crossed modules*. A crossed module is a quadruple $(G_1, G_2, \partial_2^G, \rhd)$, where G_1 and G_2 are groups, $\partial_2^G : G_2 \to G_2$ is a group homomorphism and $\rhd : G_1 \times G_2 \to G_2$ is an action of G_1 on G_2, which satisfies

$$\partial_2^G(g \rhd \alpha) = g(\partial_2^G \alpha)g^{-1}, \tag{3.2.13}$$

$$(\partial_2^G \beta) \rhd \alpha = \beta \alpha \beta^{-1}, \tag{3.2.14}$$

where $g \in G_1$ and $\alpha, \beta \in G_2$. If G_1 and G_2 are Abelian, as we are assuming here, the group chain complex (G, ∂^G) defines a crossed module with trivial action. Crossed modules were used to define Hamiltonian models of topological phases of matter in $(3 + 1)d$ in [26]. In fact, $1, 2$-gauge theory in $3D$ is an Abelian version of the Hamiltonian model defined in [26] (see appendix B).

Chapter 4

Quantum phases from abelian higher gauge theories

In chapter 3, we saw that given a geometrical chain complex (C, ∂^C) in any dimension D and an Abelian higher gauge group (G, ∂^G), exactly solvable models of topological order can be immediately constructed. To go beyond topological order, i.e., to find novel phases of matter that are neither symmetry breaking phases nor topological phases, we can either modify some assumptions made when constructing the general formalism of chapter 3 or introduce new objects and new degrees of freedom to the theory.

In this chapter, we pursue both lines of investigation. First, we modify the geometrical chain complex and build AHGT models inspired by the steps shown in chapter 3. The results are models of what we call *subsystem symmetry enriched topological phases* [2]. These are quantum phases of matter with the property that they reduce to regular topological phase when subsystem symmetry is broken. By subsystem symmetry we mean an extended symmetry that acts only over a sub-manifold of the space.

Next, we take AHGT models and place them in the presence of external *classical static fields* that resemble higher gauge configurations. This results in models with ground-state degeneracy depending on geometrical properties of the manifold, like shortest paths (geodesics) between two points. Such Hamiltonians can be used to find shortest paths between pairs of points in a graph.

4.1 Subsystem symmetry enriched topological phases

The Hamiltonian (3.1.23) is exactly solvable because the operators (3.1.21) and (3.1.22) commute for all $n = 0, ..., D$ and all $x \in K_n$. These commutation relations, in turn, correspond to the statement that the boundary of any n-simplex $x \in K_n$ has no boundary, that is,

$$\partial_{n-1}^C \circ \partial_n^C = 0$$

as an operator identity.

This suggests a path to construct novel exactly solvable Hamiltonian models by modifying the chain complex (C, ∂^C) in such a way that there exists $n = 0, ..., D$ such that

$$\partial_{n-1}^C \circ \partial_n^C \neq 0,$$

but, because $\partial_{n-2}^C \circ \partial_{n-1}^C = 0$,

$$\partial_{n-2}^C \circ \partial_{n-1}^C \circ \partial_n^C = 0.$$

Models constructed from these *modified geometrical chain complexes* exhibit *subsystem symmetry enriched topological phases*. These are phases that reduce to regular topological phase when subsystem symmetries are explicitly broken by perturbations. In this section, we discuss how to construct these models and their physical properties.

4.1.1 AHGT in a modified geometric chain complex

For simplicity, from here on we will only consider two kinds of lattices: the regular square lattice in $2D$ and the regular cubic lattice in $3D$. However, the modifications we will perform can be adapted to other kinds of lattices in any dimensions in a straightforward fashion.

In 2-dimensions

Consider an oriented regular square lattice in $2D$ given by the *augmented chain complex* [44]

$$0 \to C_2 \xrightarrow{\partial_2^C} C_1 \xrightarrow{\partial_1^C} C_0 \xrightarrow{\partial_0^C} \mathbb{Z} \to 0,$$
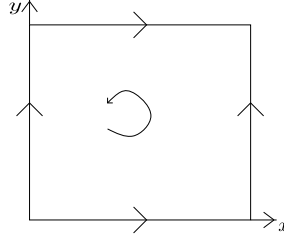
Figure 4.1.1: Lattice orientation and axis directions conventions.

where ∂_0^C sends vertices $v \in K_0$ to the generator $1 \in \mathbb{Z}$. We will modify this chain complex as follows: fix two orthogonal directions in the lattice defined by the unit vectors x and y, as in figure 4.1.1. For $\mu = x, y$, define the operators

$$\partial_{2,\mu}^C : C_2 \to C_1, \tag{4.1.1}$$

such that

$$\partial_{2,x}^C \left(\begin{array}{c} \vphantom{X} \end{array} \right) = + \longrightarrow - \longrightarrow, \tag{4.1.2}$$

and

$$\partial_{2,y}^C \left(\begin{array}{c} \vphantom{X} \end{array} \right) = + \uparrow - \uparrow. \tag{4.1.3}$$

We then replace the operator ∂_2^C by the operators $\partial_{2,\mu}^C$ and consider

$$0 \to C_2 \xrightarrow{\partial_{2,\mu}^C} C_1 \xrightarrow{\partial_1^C} C_0 \xrightarrow{\partial_0^C} \mathbb{Z} \to 0.$$

Strictly speaking, this sequence is not a chain complex anymore, because $\partial_1^C \circ \partial_{2,\mu}^C \neq 0$. We will call it a *modified chain complex* (C, ∂_μ^C). Note that $\partial_2^C = \partial_{2,x}^C + \partial_{2,y}^C$, and we can interpret the operators $\partial_{2,\mu}^C$ as a kind of partition of the operator ∂_2^C.

Using the formalism of chapter 3, we can use (C, ∂_μ^C) to construct a Hamiltonian model of

$$0 \xrightarrow{\quad} C_2 \xrightarrow{\partial^C_{2,\mu}} C_1 \xrightarrow{\partial^C_1} C_0 \xrightarrow{\partial^C_0} \mathbb{Z} \xrightarrow{\quad} 0$$

$$\downarrow^{f_0} \qquad \qquad 0 \xrightarrow{\quad} G_0 \xrightarrow{\quad} 0$$

with labels m_2, f_0, t_{-1}

Figure 4.1.2: Gauge theory data for an Abelian 0-gauge theory over the modified chain complex (C, ∂^C_μ).

Abelian higher gauge theory. The higher gauge group (G, ∂^G) is given by the chain complex

$$0 \to G_2 \xrightarrow{\partial^G_2} G_1 \xrightarrow{\partial^G_1} G_0 \to 0,$$

where we choose $G_2 = G_1 = 0$. The higher gauge configurations are given as in figure 4.1.2. That is, we have degrees of freedom labelled by G_0 living on vertices of the square lattice. The Hilbert space $\mathcal{H}$ of this theory is generated by vectors

$$|f\rangle = \bigotimes_{v \in K_0} |f_0(v)\rangle,$$

for all $f \in \hom(C, G)^0 = \mathrm{Hom}(C_0, G_0)$.

Note that in the 0-gauge theory example of section 3.2.1, we did not use an augmented chain complex. The result was that we could not define a gauge transformation operator, and the resulting Hamiltonian was already diagonal, composed of operators that trivially commute. Here, with an augmented chain complex, we can define a *global* gauge transformation.

As we saw in section 3.1.4, higher gauge transformations are parameterized by maps $t \in \hom(C, G)^{-1}$. With the chain complexes defined as in figure 4.1.2, we have that $\hom(C, G)^{-1} = \mathrm{Hom}(\mathbb{Z}, G_0)$. So, there is no geometrical information in the maps that parameterize higher gauge transformations. Thus, there is no need to make them local, as we did in section 3.1.4, and we can use definition (3.1.17) to build a *global* higher gauge transformation operator.

Given a map $t_{-1} : \mathbb{Z} \to G_0$, we have that the higher gauge transformation parameterized by t_{-1} acts over a basis state $|f\rangle \in \mathcal{H}$ as

$$A_{t_{-1}} |f\rangle = |f + \delta^{-1} t_{-1}\rangle = |f_0 + t_{-1} \circ \partial^C_0\rangle. \tag{4.1.4}$$

The map t_{-1} takes the generator of $\mathbb{Z}$ to an element of G_0. That is, we have $|G_0|$ possible maps

t_{-1}. Since, for any $v \in K_0$,

$$(t_{-1} \circ \partial_0^C)(v) = t_{-1}(\partial_0^C(v)) = t_{-1}(1) = g \in G_0,$$

we can consider $A_{t_{-1}} = A_g$. The action of A_g is *global*, in the sense that it acts over every lattice site at once, and it is given by

$$A_g |f\rangle = \bigotimes_{v \in K_0} |f_0(v) + g\rangle, \qquad (4.1.5)$$

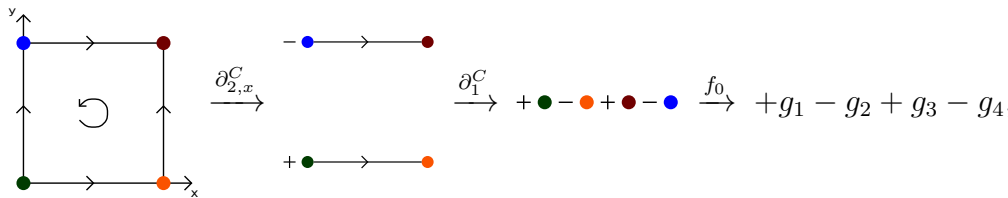for all $g \in G_0$. Inspired by (3.1.21), we then write the *global gauge transformation* as

$$A = \frac{1}{|G_0|} \sum_{g \in G_0} A_g. \qquad (4.1.6)$$

Note that we could still define a regular 0-gauge theory over the modified chain complex (C, ∂_μ^C). The resulting theory would be the same as the one in section 3.2.1. However, making use of the modifications in the chain complex, we can also define a theory that differs significantly from 0-gauge theory.

Since we have two boundary operators $\partial_{2,\mu}^C$, $\mu = x, y$, we can define two *modified holonomy operators* based on the definition (3.1.18). Let $m_2 : C_2 \to \hat{G}_0$ be a map, $m_2 \in \hom(C, G)_1 = \mathrm{Hom}(C_2, \hat{G}_0)$. We define the *modified holonomy operator* as follows:

$$B_{m_2}^{(\mu)} |f\rangle = \langle m_2, f_0 \circ \partial_1^C \circ \partial_{2,\mu}^C \rangle |f\rangle, \qquad (4.1.7)$$

for any $|f\rangle \in \mathcal{H}$, where $\mu = x, y$. The action of (4.1.7) is best seen as the sequence of operations

$$\qquad (4.1.8)$$

59

for $\mu = x$, while for $\mu = y$ the sequence is given by

$$\xrightarrow{\partial^C_{2,y}} \qquad \xrightarrow{\partial^C_1} \qquad \xrightarrow{f_0} -g_1 + g_2 - g_3 + g_4, \qquad (4.1.9)$$

Localizing the operators at the plaquettes of the lattice we have finally that

$$B_p^{(x)} \left| \begin{array}{c} d \quad\quad c \\ \circlearrowright \\ a \quad\quad b \end{array} \right\rangle = \delta(a - b - c + d, 0) \left| \begin{array}{c} d \quad\quad c \\ \circlearrowright \\ a \quad\quad b \end{array} \right\rangle, \qquad (4.1.10)$$

$$B_p^{(y)} \left| \begin{array}{c} d \quad\quad c \\ \circlearrowright \\ a \quad\quad b \end{array} \right\rangle = \delta(a + b - c - d, 0) \left| \begin{array}{c} d \quad\quad c \\ \circlearrowright \\ a \quad\quad b \end{array} \right\rangle. \qquad (4.1.11)$$

Therefore, the action of $B_p^{(\mu)}$ for $\mu = x, y$ can be seen as comparing the 0-holonomies of the links parallel to the μ axis. If a plaquette has links in the μ direction with equal 0-holonomies, $B_p^{(\mu)}$ acts as the identity. Plaquettes with links in the μ direction with different 0-holonomies are annihilated by $B_p^{(\mu)}$.

Note that, as defined, the operators (4.1.4) and (4.1.7) commute for every $\mu = x, y$ and every $t_{-1} \in \mathrm{Hom}(\mathbb{Z}, G_0)$ and $m_2 \in \mathrm{Hom}(C_2, \hat{G}_0)$. In fact, we have that

$$A_{t_{-1}} B_{m_2}^{(\mu)} |f\rangle = \langle m_2, f_0 \circ \partial_1^C \circ \partial_{2,\mu}^C \rangle \, |f_0 + t_{-1} \circ \partial_0^C \rangle \,,$$

$$B_{m_2}^{(\mu)} A_{t_{-1}} |f\rangle = \langle m_2, (f_0 + t_{-1} \circ \partial_0^C) \circ \partial_1^C \circ \partial_{2,\mu}^C \rangle \, |f_0 + t_{-1} \circ \partial_0^C \rangle$$

$$= \langle m_2, f_0 \circ \partial_1^C \circ \partial_{2,\mu}^C \rangle \, |f_0 + t_{-1} \circ \partial_0^C \rangle \,,$$

$\forall \, |f\rangle \in \mathcal{H}$ and $\mu = x, y$, because $\partial_0^C \circ \partial_1^C \circ \partial_{2,\mu}^C = 0$. Thus, we can define the Hamiltonian of this theory as

$$H_{2D} = -A - \sum_{p \in K_2} (B_p^{(x)} + B_p^{(y)}), \qquad (4.1.12)$$

and this Hamiltonian is exactly solvable, composed by commuting projectors. In section 4.1.2, we will study the physics of this model for a particular choice of gauge group. As shown in [2],

this model exhibits fractonlike order with subsystem-symmetry protected ground-states.
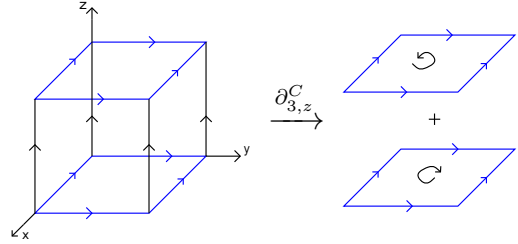
In 3-dimensions

Consider an oriented regular cubic lattice in $3D$ given by the chain complex

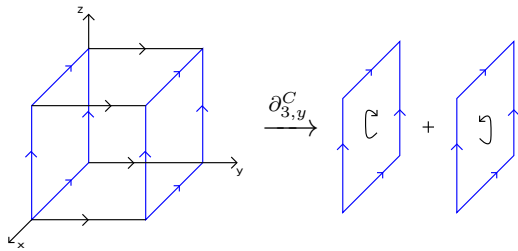$$0 \to C_3 \xrightarrow{\partial_3^C} C_2 \xrightarrow{\partial_2^C} C_1 \xrightarrow{\partial_1^C} C_0 \to 0.$$

Following the ideas in 4.1.1, we modify this chain complex by fixing three orthogonal directions in the lattice defined by unit vectors x, y and z, as in figure 4.1.3. For $\mu = x, y, z$, define the operators
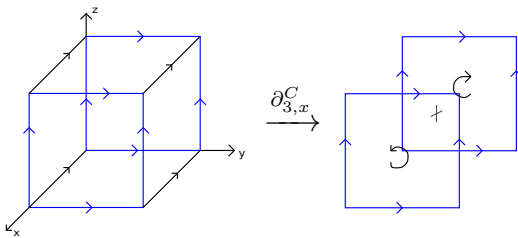
$$\partial_{3,\mu}^C : C_3 \to C_2, \tag{4.1.13}$$

such that

$$\tag{4.1.14}$$

$$\tag{4.1.15}$$

$$\tag{4.1.16}$$
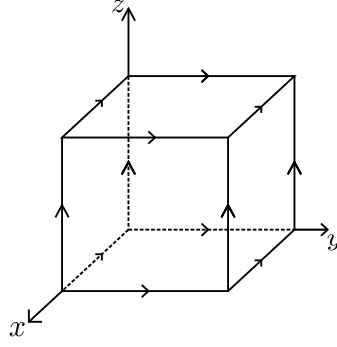
Figure 4.1.3: Lattice orientation and axis directions conventions.

$$0 \longrightarrow C_3 \xrightarrow{\partial^C_{3,\mu}} C_2 \xrightarrow{\partial^C_2} C_1 \xrightarrow{\partial^C_1} C_0 \longrightarrow 0$$
$$\quad\quad\quad\quad\quad m_3 \searrow \quad\quad f_1 \downarrow \quad t_0$$
$$0 \longrightarrow G_1 \longrightarrow 0$$

Figure 4.1.4: Gauge theory data for an Abelian 1-gauge theory over the modified chain complex (C, ∂^C_μ).

We then replace the operator ∂^C_3 by the operators $\partial^C_{3,\mu}$ and consider

$$0 \to C_3 \xrightarrow{\partial^C_{3,\mu}} C_2 \xrightarrow{\partial^C_2} C_1 \xrightarrow{\partial^C_1} C_0 \to 0.$$

Just as in 4.1.1, this *modified chain complex* (C, ∂^C_μ) is not a chain complex in the usual sense, because $\partial^C_2 \circ \partial^C_{3,\mu} \neq 0$. Note that $\partial^C_3 = \partial^C_{3,x} + \partial^C_{3,y} + \partial^C_{3,z}$, and we can interpret the operators $\partial^C_{3,\mu}$ as a kind of partition of the operator ∂^C_3.

Now we employ the formalism of chapter 3 to construct a Hamiltonian model of Abelian higher gauge theory over the modified chain complex (C, ∂^C_μ). We choose the higher gauge group (G, ∂^G) as

$$0 \to G_3 \xrightarrow{\partial^G_3} G_2 \xrightarrow{\partial^G_2} G_1 \xrightarrow{\partial^G_1} G_0 \to 0,$$

where $G_3 = G_2 = G_0 = 0$. Higher gauge configurations are given as in figure 4.1.4. We have degrees of freedom labelled by G_1 living on links in the cubic lattice. The Hilbert space $\mathcal{H}$ is generated by vectors

$$|f\rangle = \bigotimes_{l \in K_1} |f_1(l)\rangle,$$

$\forall f \in \text{hom}(C, G)^0 = \text{Hom}(C_1, G_1)$.

Note that the rightmost part of the complex 4.1.4 is exactly the same as the one in regular 1-gauge theory. This means that we can define gauge transformations in the usual way. From

the definition (3.1.21), we have that the only non-trivial gauge transformations are $A_v = A_{0,v}$, for any $v \in K_0$. The operator A_v is given by

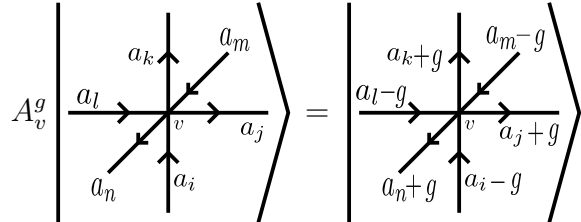$$A_v = \frac{1}{|G_1|} \sum_{g \in G_1} A_v^g, \qquad (4.1.17)$$

where $A_v^g = A_{e[0,v,g]}$. Given a basis vector $|f\rangle \in \mathcal{H}$, we have that

$$A_v^g |f\rangle = A_{e[0,v,g]} |f\rangle = |f + \delta^{-1} e[0,v,g]\rangle$$

$$= \bigotimes_{l \in K_1} |f_1(l) + (\delta^{-1} e[0,v,g])_1(l)\rangle.$$

Since, for any $l \in K_1$, $e[0,v,g](l) = 0$,

$$(\delta^{-1} e[0,v,g])_1(l) = e[0,v,g](\partial_1^C l).$$

Thus, the local operator A_v^g acts over basis vectors in a similar way as in the $2D$ 1-gauge theory case of section 3.2.2. It performs a gauge transformation by a group element $g \in G_1$ on every link around the vertex v. We can represent the action of A_v^g as

$$A_v^g \left| \begin{array}{c} a_k \quad a_m \\ a_l \quad \overrightarrow{v} \quad a_j \\ a_n \quad a_i \end{array} \right\rangle = \left| \begin{array}{c} a_k+g \quad a_m-g \\ a_l-g \quad \overrightarrow{v} \quad a_j+g \\ a_n+g \quad a_i-g \end{array} \right\rangle. \qquad (4.1.18)$$

Note that we can still define a regular 1-gauge theory over the modified chain complex (C, ∂_μ^C), resulting in a theory which is the $3D$ version of the one in section 3.2.2. However, we can use the modified chain complex to define a theory with different physics than 1-gauge theory.

From the three boundary operators ∂_μ^C, $\mu = x, y, z$, we can define three *modified holonomy operators* based on the definition (3.1.18). Let $m_3 \in \mathrm{Hom}(C_3, \hat{G}_1) = \mathrm{hom}(C, G)_1$ be a map. The modified holonomy operators $B_{m_2}^{(\mu)} : \mathcal{H} \to \mathcal{H}$ are such that

$$B_{m_3}^{(\mu)} |f\rangle = \langle m_3, f_1 \circ \partial_2^C \circ \partial_{3,\mu}^C \rangle |f\rangle, \qquad (4.1.19)$$

$\forall \, |f\rangle \in \mathcal{H}$. This action is best seem as a sequence of operations. For example, for $\mu = z$,

$$\xrightarrow{\partial_{3,z}^C} \qquad \xrightarrow{\partial_2^C} \qquad \xrightarrow{f_1} \; +g_1 + g_2 - g_3 - g_4 - g_5 + g_6 + g_7 - g_8.$$

(4.1.20)

Localizing the operators at cubes, we get the holonomies

$$B_c^{(x)} \left| \quad \right\rangle = \delta(a_1 + c_1 - b_1 - c_4 + a_3 + c_2 - b_3 - c_3, 0) \left| \quad \right\rangle,$$

(4.1.21)

$$B_c^{(y)} \left| \quad \right\rangle = \delta(a_2 + c_2 - b_2 - c_1 + a_4 + c_4 - b_4 - c_4, 0) \left| \quad \right\rangle,$$

(4.1.22)

$$B_c^{(z)} \left| \quad \right\rangle = \delta(a_1 + a_2 - a_3 - a_4 + b_1 + b_2 - b_3 - b_4, 0) \left| \quad \right\rangle.$$

(4.1.23)

Thus, the action of $B_c^{(\mu)}$ for $\mu = x, y, z$ can be interpreted as comparing the 1-holonomies of the plaquettes in a cube that are perpendicular to the μ direction. If a cube has plaquettes perpendicular to the μ direction with equal 1-holonomies, $B_c^{(\mu)}$ acts as the identity operator. Cubes with plaquettes perpendicular to the μ direction with different 1-holonomies are annihilated by $B_c^{(\mu)}$.

The operators (4.1.17) and (4.1.19) commute for all $v \in K_0$, all $c \in K_3$ and all $\mu = x, y, z$.

For example, for $\mu = z$, we have that, for $g \in G_1$,

$$A_v^g B_c^{(z)} \quad \vcenter{\hbox{}} \quad = \delta(a_1 + a_2 - a_3 - a_4 + b_1 + b_2 - b_3 - b_4, 0) \quad \vcenter{\hbox{}},$$

$$B_c^{(z)} A_v^g \quad \vcenter{\hbox{}} \quad = \delta(a_1 + g + a_2 - a_3 - a_4 - g + b_1 + b_2 - b_3 - b_4, 0) \quad \vcenter{\hbox{}},$$

and, since G_1 is Abelian, we have that $B_c^{(z)} A_v^g = A_v^g B_c^{(z)}$. These commutation relations are simply the statement that $\partial_1^C \circ \partial_2^C \circ \partial_{3,\mu}^C = 0$ for all $\mu = x, y, z$. Therefore, we can define the Hamiltonian of this theory as

$$H_{3D} = -\sum_{v \in K_0} A_v - \sum_{c \in K_3} \left(B_c^{(x)} + B_c^{(y)} + B_c^{(z)} \right). \tag{4.1.24}$$

This is an exactly solvable Hamiltonian made of commuting projectors. In section 4.1.3, we will study the physics of this model for a particular choice of gauge group. As detailed in [2], this model gives an example of subsystem-symmetry enriched topological phase.

4.1.2 The plaquette Ising model

In section 4.1.1, we developed a theory of 0-gauge theory over a modified chain complex in $2D$ for any finite Abelian gauge group G. Here, we give a detailed example of a Hamiltonian model derived from such a theory for $G = \mathbb{Z}_2$.

It turns out that the $\mathbb{Z}_2$ 0-gauge theory over the modified complex of 4.1.1 in $2D$ results in the well-known *plaquette Ising model* [47, 48]. This model is considered as a model for *fracton-like* order in [49, 50]. Its classical version is known as the *gonihedric Ising model*, a particular case of the eight-vertex model [50, 51], studied in the context of string theory and spin-glass physics in [52, 53, 54] and references therein. To construct this example we follow [2], where more details are available.

The model

For $G_0 = \mathbb{Z}_2 = \{0, 1\}$ with the group operation being addition mod 2, we have *qubits* living on vertices of the square lattice. At each vertex $v \in K_0$, there is a local Hilbert space $\mathcal{H}_v$ spanned

by the basis vectors $\{|0\rangle, |1\rangle\}$. The total Hilbert space is given by the tensor product

$$\mathcal{H} = \bigotimes_{v \in K_0} \mathcal{H}_v.$$

From (4.1.6), we have that the global gauge transformation is given by

$$A = \frac{1}{2}(A_0 + A_1),$$

where

$$A_0 |f\rangle = \bigotimes_{v \in K_0} |f_0(v) + 0\rangle = \bigotimes_{v \in K_0} |f_0(v)\rangle = |f\rangle$$

and

$$A_1 |f\rangle = \bigotimes_{v \in K_0} |f_0(v) + 1\rangle,$$

$\forall f = f_0 \in \mathrm{Hom}(C_0, \mathbb{Z}_2)$. Thus, since $A_0 |f\rangle = |f\rangle$ for any $f_0 \in \mathrm{Hom}(C_0, \mathbb{Z}_2)$, we have that $A_0 = \bigotimes_{v \in K_0} \mathbb{1}_v$, the identity operator over $\mathcal{H}$. Moreover, note that, for any $v \in K_0$, if $f_0(v) = 0$, $f_0(v) + 1 = 1$ and if $f_0(v) = 1$, $f_0(v) + 1 = 0$. Thus, the action of A_1 over some configuration $|f\rangle \in \mathcal{H}$ is to flip every qubit. In the σ^z basis, we can then write that $A_1 = \bigotimes_{v \in K_0} \sigma^x_v$. Therefore, the global gauge transformation is given by

$$A = \frac{1}{2}\left(\bigotimes_{v \in K_0} \mathbb{1}_v + \bigotimes_{v \in K_0} \sigma^x_v\right), \tag{4.1.25}$$

Now, from (4.1.10) and (4.1.11), since for $g \in \mathbb{Z}_2$, $-g = g$, we have that $B_p^{(x)} = B_p^{(y)} = B_p$. Following the reasoning in 3.2.1, we have that the matrix form of the modified holonomy operator is given by

$$B_p = \frac{1}{2}\left(\bigotimes_{v \in p} \mathbb{1}_v + \bigotimes_{v \in p} \sigma^z_v\right), \tag{4.1.26}$$

This operator collects the values of spins at the vertices of p, such that it favors configurations with even number of $|1\rangle$ around plaquettes.

The Hamiltonian defined by

$$H = -A - \sum_p B_p \tag{4.1.27}$$

is an example of *fractonlike model with subsystem symmetries*. Systems with fracton phases are characterized by a subextensive behavior of the ground-state degeneracy, quasiparticles with mobility restrictions and topologically protected ground-states. The quasiparticles usually called fractons are completely immobile. The model defined by the Hamiltonian (4.1.27) indeed hosts fractons and a subextensive ground-state degeneracy, but it lacks topologically protected ground-states. Its ground-states are subsystem-symmetry protected. The global $\mathbb{Z}_2$ operator X given by

$$X = \bigotimes_{v \in K_0} \sigma_v^x \tag{4.1.28}$$

commutes with H.

Next we show that the model defined in section 4.1.2 indeed supports quasi-particles with restricted mobility and a ground state degeneracy that grows exponentially with the system's size. However, as we will demonstrate, this degeneracy can be lifted by local stabilizer operators and thus its ground states are not topologically protected. Hence, when perturbations to the system do not break the subsystem symmetry, we consider this model as an example of fractonlike order.

Ground State Degeneracy

The operators A and B_p are commuting projectors for every plaquette p, and thus we can solve this Hamiltonian exactly and find its spectrum. The ground-state subspace of the model is the subspace

$$\mathcal{H}_0 = \{|\psi\rangle \in \mathcal{H} \mid A|\psi\rangle = |\psi\rangle \text{ and } B_p|\psi\rangle = |\psi\rangle\},$$

for every plaquette $p \in K_2$. To find such states, let $|+\rangle \in \mathcal{H}$ be the state where every vertex spin in the lattice is in the $|0\rangle_v$ configuration, namely

$$|+\rangle = \bigotimes_v |0\rangle_v.$$

Similarly, the state where all local degrees of freedom are in the $|1\rangle_v$ state is written

$$|-\rangle = \bigotimes_v |1\rangle_v.$$

The two states above satisfy the condition $B_p |\psi\rangle = |\psi\rangle$ for all plaquettes $p \in K_2$. Then, the state $|\psi_0\rangle = A |+\rangle = A |-\rangle = \frac{1}{2} (|+\rangle + |-\rangle)$ is a ground state.
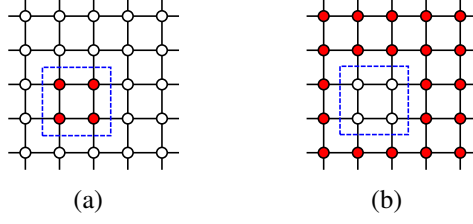

(a)   (b)

Figure 4.1.5: The domain wall (in blue) of (a) separates two regions with different spin configurations. The same domain wall also determines the separation between configurations of (b). The configuration in (a) is gauge equivalent to that of (b).

Now, in order to construct other ground states, we will introduce a graphical notation to represent the basis states of $\mathcal{H}$ as follows; we color (red) any vertex that holds a $|1\rangle_v$ local degree of freedom, see figure 4.1.5. We also draw domain walls separating two regions with different spin configuration. In general, a single domain wall is associated with two basis states of $\mathcal{H}$, as shown in figure 4.1.5. However, because of the global gauge transformation the two basis states associated to one domain wall diagram are gauge equivalent. Thus, domain walls are enough to represent gauge equivalence classes of basis states, or *physical states*. For example, in figure 4.1.6 we show two domain wall diagrams and the respective states they represent.

(a)

(b)

Figure 4.1.6: In (a) the domain wall diagram at the left represents the linear combinations of states at the right, in this case the ground state $|\psi_0\rangle = A |+\rangle$. In (b) the diagram at the left represents the state $|\phi\rangle$, which in fact is an excited state of the model.

The trivial ground state, $|\psi_0\rangle$ is represented by a diagram with no domain walls, as shown in figure 4.6(a). The diagram at the left of figure 4.6(b) stands for an elementary excited state of the model as we will see in section 4.1.2.

Other ground states are given by gauge-equivalence classes of states in $\mathcal{H}$ on which B_p acts trivially for every $p \in K_2$. In order to be invariant under B_p, a state must have either
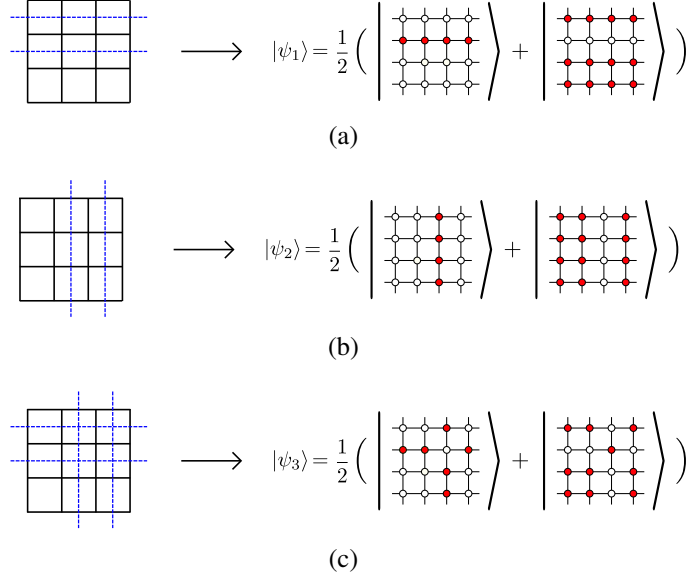
Figure 4.1.7: Some possible ground states of the model. The domain wall lines must begin and end at the boundary of the lattice.

an even number of vertices with $|1\rangle_v$ spins at each plaquette of the lattice, or no $|1\rangle_v$ spins at all. The latter case is taken care of by the state $|\psi_0\rangle$. Examples of the former case are illustrated in figure 4.1.7. Domain wall lines must begin and end at the boundary of M. In case M has no boundary, the starting points of the blue domain wall lines must be identified with its ending points. Essentially, domain wall lines cannot have corners, i.e., every domain wall line that enters a plaquette must exit it in the diametrically opposite side, as opposed to figure 4.6(b), which clearly represents an excited state because it has plaquettes with an odd number of vertices with spin $|1\rangle$. Since the global gauge transformation A does not change domain wall diagrams, any domain wall configuration that represents a (gauge equivalent) linear combination of trivial eigenstates of B_p, for every p, is a ground state.

We can have ground states with an arbitrary number of domain wall lines in both directions. If M is a manifold with boundary and has dimension $L_x \times L_y$, this means that we can construct 2^{L_x} states with domain wall lines in the $x-$direction and 2^{L_y} states with domain wall lines in the $y-$direction, giving a total of

$$GSD = 2^{L_x + L_y} \tag{4.1.29}$$

possible ground states. This subextensive behavior of the ground-state degeneracy is characteristic of fracton phases.

Nevertheless, there are local operators that commute with A and B_p, for every $p \in K_2$, that can be added to the Hamiltonian (4.1.27) which may destroy this degeneracy. We can define,

for every link $l \in K_1$ in the lattice, the 0-holonomy operator [1, 43]

$$B_l = \frac{1}{2} \left(\bigotimes_{v \in \partial l} \mathbb{1}_v + \bigotimes_{v \in \partial l} \sigma_v^z \right).$$ (4.1.30)

For each plaquette $p \in K_2$, B_p can be regarded as an operator that compares the 0-holonomy of parallel links that belong to the boundary ∂p of p. By this we mean that B_p gives an eigenvalue equal to one whenever parallel links in p have the same value of 0-holonomy, and zero otherwise. Fix a plaquette $p' \in K_2$ and subtract of the Hamiltonian (4.1.27) a 0-holonomy operator $B_{l'}$, where l' is any link in the boundary $\partial p'$ of p'. The new Hamiltonian is given by

$$H' = -A - \sum_{p \neq p'} B_p - B_{p'} - B_{l'}.$$ (4.1.31)

The ground states of H' must have a 0-holonomy value of one for the link l', which means that the spins at the vertices in the boundary of l' must be aligned. This introduces an additional constraint to the number of possible ground state configurations of the plaquette p', and thus it reduces the ground state degeneracy. Now, if we subtract two 0-holonomy operators, B_{l_1} and B_{l_2}, for two arbitrary links l_1 and l_2 in the boundary $\partial p'$ of p', this gives the following new Hamiltonian

$$H'' = -A - \sum_{p \neq p'} B_p - B_{p'} - B_{l_1} - B_{l_2},$$ (4.1.32)

for $l_1, l_2 \in \partial p'$. The ground state of the system now must have a 0-holonomy value equal to one for both links l_1 and l_2 in $\partial p'$. This means that the spins at the vertices of each link in question must be aligned. If l_1 and l_2 are parallel to each other, this implies that the configuration of the plaquette p' is fixed; it either has all spins up or all spins down, and both are related by the global gauge transformation A, i.e., they represent the same physical state. An identical situation happens if l_1 and l_2 are perpendicular to each other. Therefore, adding 0-holonomy operators for the plaquette p' fixes its state, reducing the number of possible ground states. One can immediately see that, if we were to do the same process for every plaquette in the lattice, the degeneracy would be destroyed. Thus, we can decrease the ground state degeneracy shown in equation (4.1.29) by adding local 0-holonomy operators, and therefore the ground states are not topologically protected. We can move from one state in the ground state subspace to another by applying combinations of 0-holonomy operators. Perturbations in the form of Ising-like
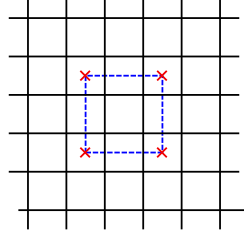
Figure 4.1.8: The configuration of figure 4.6(b) has four fractons, represented here as four red crosses.

interactions can drive the system out of its fractonlike phase, into a more regular Ising phase.

This discussion can be summarized by noting that the model has subsystem symmetries given by operators that flip all spins along a straight line in the lattice. The ground state degeneracy (4.1.29) can be calculated by counting the number of such operators, and the 0-holonomy operators explicitly break this subsystem symmetry, thus drastically reducing the number of ground states. It follows that, when the subsystem symmetry is respected, i.e., when perturbations don't break this symmetry, the model presents fracton-like order.

Fracton excitations

The excited states of the model $|\phi\rangle \in \mathcal{H}$ are states for which either $A|\phi\rangle = 0$ or, for some plaquette $p \in K_2$, $B_p|\phi\rangle = 0$. The excited state coming from the condition on the A operator is usually called *charge*. It is created by acting locally with σ^z on a single (arbitrary) vertex over a ground state of the model. The global nature of the gauge transformation makes it impossible to localize the charge, since we can only know whether a charge is present or not. For this reason, the charge is said to be global.

Plaquette excitations live at plaquettes that have a spin configuration with an odd number of vertices with spin $|1\rangle_v$. Therefore, they live at the corners of domain walls. For example, the configuration in figure 4.6(b) has four excitations living at the four corners of the domain wall, as explicitly shown in figure 4.1.8. We can move pairs of excitations along straight lines, but individual excitations cannot be moved without costing energy to the system, and so they are essentially immobile. Therefore, plaquette excitations in this model are completely immobile fractons, and indeed the system described by the Hamiltonian in equation (4.1.27) exhibits fractonlike order in two dimensions.

4.1.3 Subsystem symmetry-enriched topological phase in 3-dimensions

In section 4.1.1, we constructed an Abelian 1-gauge theory in $3D$ over a modified chain complex for a general Abelian finite gauge group G_1. Here we present an example of such theory for a particular choice of gauge group, namely $G_1 = \mathbb{Z}_2$. As we will see, this model presents fractonlike order in three spatial dimensions and reduces to the $3D$ Toric Code when subsystem symmetry is broken, being thus an example of *subsystem symmetry-enriched topological phase* [2].

The model

For $G_1 = \mathbb{Z}_2 = \{+1, -1\}$ with the group operation being multiplication, we have *qubits* living on links of the cubic lattice. At each link $l \in K_1$, there is a local Hilbert space $\mathcal{H}_l$ spanned by the basis vectors $\{|+1\rangle, |-1\rangle\}$. The total Hilbert space is given by the tensor product

$$\mathcal{H} = \bigotimes_{l \in K_1} \mathcal{H}_l.$$

For each vertex v, the local gauge transformation is given by equation (4.1.17), namely
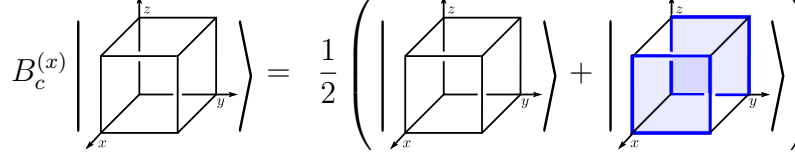
$$A_v = \frac{1}{2}\left(A_{+1} + A_{-1}\right), \tag{4.1.33}$$

where, from (4.1.18), we can see that $A_{+1} = \mathbb{1}$, the identity operator over $\mathcal{H}$, and $A_{-1} = \bigotimes_{l \in \text{star}(v)} \sigma_l^x$, where $\text{star}(v)$ is the set of links that touch v. Thus, we can represent the gauge transformation as
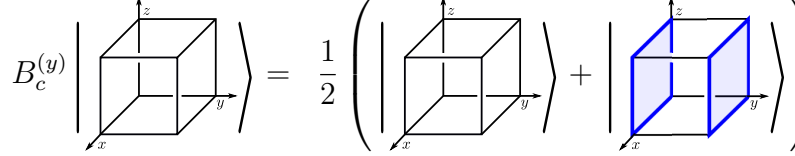
$$A_v \left| \begin{array}{c} \overset{e}{\underset{a}{\searrow}} \overset{d}{\underset{b}{\nearrow}} \overset{c}{f} \end{array} \right\rangle = \frac{1}{2}\left(\left| \begin{array}{c} \overset{e}{\underset{a}{\searrow}} \overset{d}{\underset{b}{\nearrow}} \overset{c}{f} \end{array} \right\rangle + \left| \begin{array}{c} \overset{-e}{\underset{-a}{\searrow}} \overset{-d}{\underset{-b}{\nearrow}} \overset{-c}{-f} \end{array} \right\rangle \right), \tag{4.1.34}$$
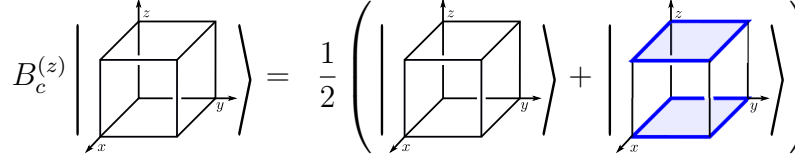
where $a, b, c, d, e, f \in \{1, -1\}$.

From (4.1.21), (4.1.22) and (4.1.23), for each elementary cube $c \in K_3$, we have three holonomy operators, $B_c^{(x)}, B_c^{(y)}$ and $B_c^{(z)}$. We can follow the reasoning in 3.2.2 to write these operators in matrix form in the basis $\{|+1\rangle, |-1\rangle\}$. To write them in a neat way, we represent the action of σ^z operators by coloring links. That is, links in blue are the ones over which a σ^z

operator act.

$$B_c^{(x)} \left| \vcenter{\hbox{\includegraphics{cube}}} \right\rangle = \frac{1}{2} \left(\left| \vcenter{\hbox{\includegraphics{cube}}} \right\rangle + \left| \vcenter{\hbox{\includegraphics{cube}}} \right\rangle \right), \qquad (4.1.35)$$

$$B_c^{(y)} \left| \vcenter{\hbox{\includegraphics{cube}}} \right\rangle = \frac{1}{2} \left(\left| \vcenter{\hbox{\includegraphics{cube}}} \right\rangle + \left| \vcenter{\hbox{\includegraphics{cube}}} \right\rangle \right), \qquad (4.1.36)$$

$$B_c^{(z)} \left| \vcenter{\hbox{\includegraphics{cube}}} \right\rangle = \frac{1}{2} \left(\left| \vcenter{\hbox{\includegraphics{cube}}} \right\rangle + \left| \vcenter{\hbox{\includegraphics{cube}}} \right\rangle \right). \qquad (4.1.37)$$

The operator $B_c^{(\mu)}$, for each direction $\mu = x, y, z$, projects states into the subspace of states in which the holonomies of two opposite plaquettes in ∂c in the direction μ are equal. This is obtained by taking the product of holonomies of the two plaquettes in the boundary of c whose surfaces are orthogonal to μ. If both plaquettes have the same holonomy, this product is equal to $+1$, which gives an eigenstate of $B_c^{(\mu)}$ with eigenvalue $+1$. Likewise, if the two opposing plaquettes have different holonomies, the product is equal to -1 and we have an eigenstate of $B_c^{(\mu)}$ with zero eigenvalue. We will say that a state has trivial holonomy in the direction μ if it is invariant under $B_c^{(\mu)}$, for every cube c in the lattice.

The Hamiltonian is given by

$$H = -\sum_v A_v - \sum_c \left(B_c^{(x)} + B_c^{(y)} + B_c^{(z)} \right). \qquad (4.1.38)$$

As we will see next, this Hamiltonian models a system in a *subsystem symmetry-enriched topological phase* [2]. That is, the ground-states in this model are protected by symmetries that act only over a sub-manifold of the manifold. When these subsystem symmetries are broken, the ground-states become topological, equal to the ground-states of the $3D$ Toric Code.

Ground State Degeneracy

The operators A_v and $B_c^{(\mu)}$ are commuting projectors for all vertices v, cubes c and directions μ in the lattice. Thus, the Hamiltonian (4.1.38) can be exactly solved. The ground-state of the model is given by all gauge-equivalence classes of states with trivial holonomy in all directions. Therefore, we must search for states such that, at each cube of the lattice, opposite plaquettes at each direction have the same holonomy. A natural ground state is $|\psi_0\rangle = \prod_v A_v |+\rangle$, where $|+\rangle \in \mathcal{H}$ is the state of the system where every link is in the $|+1\rangle_l$ state.

To visualize these states, we introduce a graphical notation as follows: whenever a link has spin $|-1\rangle_l$, we draw a blue dual plaquette, as shown in figure 4.1.9, while links with spin $|+1\rangle_l$ have no additional drawings.
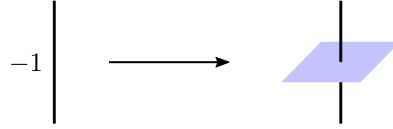

Figure 4.1.9: Links holding a $|-1\rangle_l$ spin are represented by being crossed by a blue dual surface.

In this graphical notation, the action of A_v, for some vertex v, over the state $|+\rangle$ is understood as introducing a blue closed surface around the vertex v. That is,

$$
A_v \left| \vcenter{\hbox{\includegraphics{}}} \right\rangle = \frac{1}{2} \left(\left| \vcenter{\hbox{\includegraphics{}}} \right\rangle + \left| \vcenter{\hbox{\includegraphics{}}} \right\rangle \right), \tag{4.1.39}
$$

where the vertex v is the one at the center of the cubic lattice. Therefore, the state $|\psi_0\rangle$ is the superposition of all closed surfaces one can draw around vertices in the lattice. This ground state, as shown in equation (4.1.40), can be interpreted as a membrane gas much like the loop gas ground state of the Toric Code.

When the manifold M has the topology of a 3-torus, non-contractible closed surfaces give different equivalence classes of ground states. This increases the GSD with topological terms coming from the $3D$ Toric Code. The ground states of the $3D$ Toric Code are also ground states of (4.1.38), and there is a purely topological contribution to the ground state of the Hamiltonian (4.1.38).

Consider M as having the topology of a 3-dimensional ball with dimensions $L_x \times L_y \times L_z$. States represented by membranes beginning at one of the boundaries of M and ending at the

diametrically opposite boundary are also ground states of the model. For instance, the state represented by figure 4.1.10(a). Membranes can have arbitrary shapes in every one of the three directions as long as they end at the boundaries of M, as in figure 4.1.10(b). If the membranes do not end at the boundaries of M, we have an excited state, as in figure 4.13(a), where we have a link with spin $|-1\rangle$ shared by four cubes, which yields an excited state of cube operators in the z and y directions. In the interior of M, membranes cannot bend to perpendicular directions, for if they do we get excitations of cube operators at the folding regions of the bent membranes, as in figure 4.13(b) where the membrane of figure 4.13(a) is folded into the x direction, giving rise to excitations of $B_c^{(x)}$ operators at the folding line. The gauge transformation acts at vertices and can be pictured as adding a closed (dual) surface around the vertex it acts, see eq. (4.1.39). Thus, gauge transformations can only deform membranes without changing their boundary.

$$|\psi_0\rangle = N \left(\left| \vcenter{\hbox{}} \right\rangle + \left| \vcenter{\hbox{}} \right\rangle + \left| \vcenter{\hbox{}} \right\rangle + \left| \vcenter{\hbox{}} \right\rangle + \ldots \right), \quad (4.1.40)$$

(a)   (b)
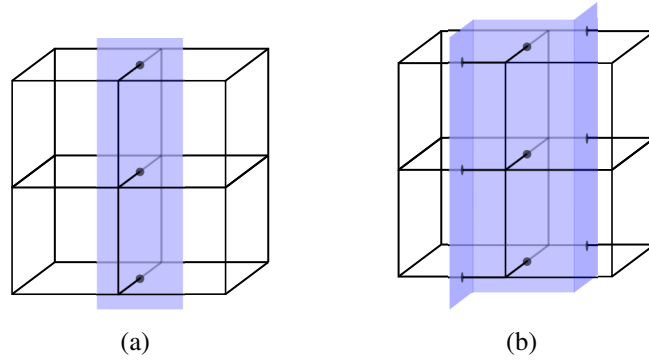
Figure 4.1.10: Two possible ground state configurations of the Hamiltonian (4.1.38). The membrane must begin at the boundary of M and end at the diametrically opposite region. Inside M, the membrane cannot curve to perpendicular directions.

Since the boundary lines of the membranes are gauge-invariant, we use them to count how many possible ground state configurations we can construct in this model. Therefore, the problem of counting ground states reduces to the problem of counting how many straight lines, beginning at one side of the boundary of M and ending at the diametrically opposite side, can be drawn on the manifold. We represent as a dot in the boundary of the manifold the beginning of a line that extends, in a straight fashion, through the interior of M to the diametrically opposite boundary point, as in figure 4.1.11. Each plaquette in the boundary of M either has

Figure 4.1.11: To count the number of ground states of the Hamiltonian (4.1.38), we draw straight lines in the interior of M ending at dots on its boundary ∂M. These straigh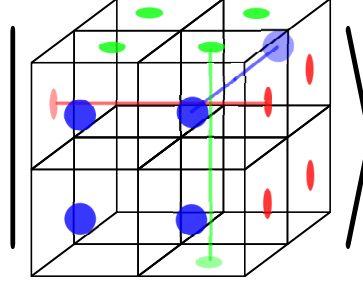t lines are boundary lines of the membranes representing ground states (see figure 4.1.10). The problem then reduces to counting how many dots we can draw on the boundary of M.

a dot on it or it doesn't. For each boundary plane of M, there can be 2^{N_p} configurations of plaquettes with dots, where N_p is the number of plaquettes on the plane in question. Since M has dimensions $L_x \times L_y \times L_z$, the number of plaquettes in the boundary plane with dimensions $L_i \times L_j$ is $L_i L_j$, where $i, j = x, y, z$ and $i \neq j$. Thus, there are

$$GSD = 2^{L_x L_y + L_x L_z + L_y L_z} \tag{4.1.41}$$

possible ground states. It is useful to think of the ground states of this model as condensations of the the $3D$ Toric Code model. Note that every ground state of the $3D$ Toric Code is a ground state of (4.1.38). Moreover, some excited states of the $3D$ Toric Code are ground states of (4.1.38). In particular, the flux excitations of the TC that lie on a single plane are ground states of (4.1.38).

There are local operators that commute with the Hamiltonian (4.1.38), i.e., local symmetry operators, which can lift the degeneracy given by equation (4.1.41) to that of the $3D$ Toric Code. To see this, fix a cube c' in the lattice and subtract from the Hamiltonian (4.1.38) a $3D$ Toric Code's plaquette operator $B_{p'}$, where p' is some arbitrary plaquette in the boundary $\partial c'$. We have the new Hamiltonian

$$H' = -\sum_v A_v - \sum_{c,\mu} B_c^{(\mu)} - B_{p'}, \tag{4.1.42}$$

where $\mu = x, y, z$. Ground states of H' must have a 1-holonomy value of one for the plaquette p'. Since the cube operators $B_c^{(\mu)}$ constrain parallel plaquettes to have the same 1-holonomy in the ground state, the plaquette which is parallel to p' will also have a 1-holonomy value of one. This reduces the number of ground state configurations the cube c' can have, thus reducing the

ground state degeneracy.

Now, if we subtract from the Hamiltonian (4.1.38) $3D$ Toric Code's plaquette operators $B_{p'}$ for four of the six plaquettes in the boundary $\partial c'$, the new Hamiltonian is then given by

$$H'' = -\sum_v A_v - \sum_{c,\mu} B_c^{(\mu)} - \sum_{p' \in \partial c'} B_{p'}, \qquad (4.1.43)$$

where $\mu = x, y, z$ and $B_{p'}$ are the 1-holonomy operators of the $3D$ Toric Code for four specific plaquettes $p' \in \partial c'$. The ground state of the model must have the four chosen plaquettes with holonomy equal to one. This fixes the allowed ground state configurations of the whole cube c', reducing further the number of allowed ground states. Subtracting $3D$ Toric Code's plaquette operators for every plaquette in the lattice, the ground state degeneracy would end up being that of the $3D$ Toric Code, because the contribution given by equation (4.1.41) would be destroyed and only the topological terms would survive.

Thus, this model is not stable under local perturbations, reducing to the $3D$ Toric Code when local operators are added. Therefore it gives an example of a subsystem symmetry enriched topological phase, showing that not only topological phases enriched by global symmetries hosts fractonic behavior [55], but also subsystem symmetry-enriched ones. The question of whether the model presented here can be protected by a global symmetry is an open one.

We saw that we can go from the fractonlike model defined by equation (4.1.38) to the Toric Code by adding plaquette operators that break the subsystem symmetry. A reasonable question is then whether there is a way to go from the $3D$ Toric Code to the fractonlike model. To answer it, suppose we start with the $3D$ Toric Code defined on the 3-torus, whose Hamiltonian is

$$H_{TC} = -\sum_v A_v - \sum_p B_p.$$

In the graphical notation introduced in this section, ground states of the Toric Code are represented by closed dual surfaces. Dual surfaces with boundary correspond to plaquette excitations. Consider an excited state of the Toric Code represented by a non-contractible dual ribbon, as in figure 4.12(a). In this figure, there are flux quasi-particles at all plaquettes along the $\hat{z}$ direction. The boundary of this ribbon is composed by two non-contractible curves. The energy of this state is two times the length L_z of the torus in the $\hat{z}$ direction.

We will now replace plaquette operators of the Toric Code with the cube operators defined in equations (4.1.35), (4.1.36) and (4.1.37). To better visualize what is happening, we assign

the following graphical notation to the process of replacing plaquette with cube operators: we draw a straight red line connecting two parallel plaquettes whose operators are removed from the TC Hamiltonian. Then, to any cube hosting such a red line we associate a cube operator $B_c^{(\mu)}$, where μ is the direction parallel to the red line. As an example, in figure 4.12(b), we perform this procedure to the cube c', associating to it an $B_{c'}^{(\hat{z})}$ operator. In this example, the resulting Hamiltonian is

$$H'_{TC} = -\sum_v A_v - \sum_{p \neq q, q'} B_p - B_{c'}^{(z)}.$$

Then, consider again the Toric Code excited state of figure 4.12(a), but now with a red line linking two parallel plaquettes in the $\hat{z}$ direction, as in figure 4.12(c). Now, the Hamiltonian of the model has an $B_c^{(\hat{z})}$ operator corresponding to the cube hosting the red line. Since the plaquettes connected by the red line in the $\hat{z}$ direction share the same holonomy, the cube is not excited. Hence, the energy of the state is reduced by two unities. However, it is still an excited state of the Toric Code. The ground state degeneracy of the Toric Code does not change under this modification of the Hamiltonian.
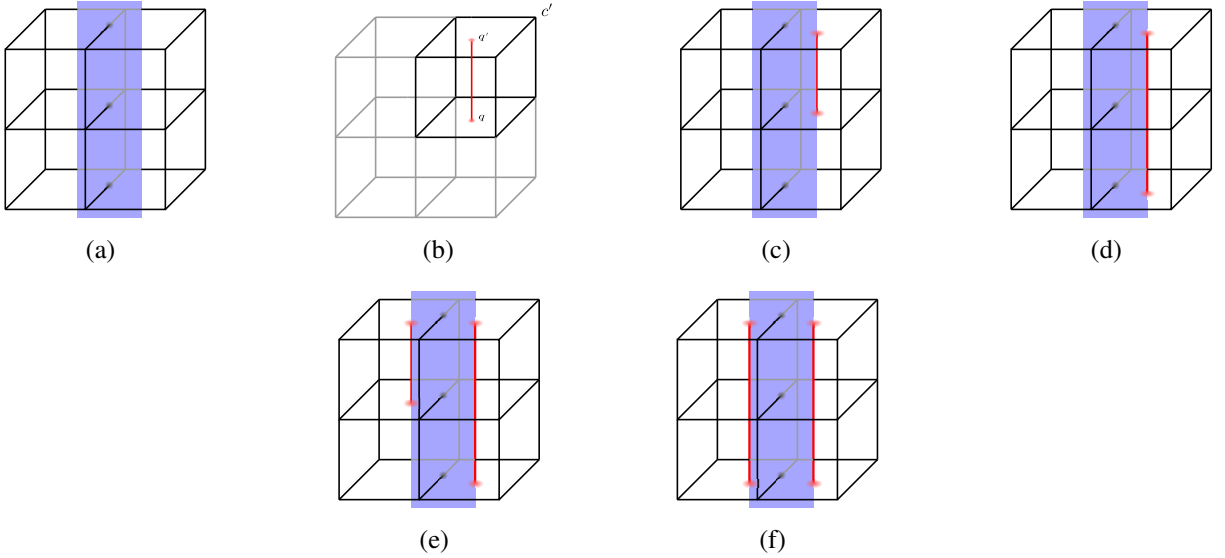
Figure 4.1.12: In (a), we show an excited state of the Toric Code. In (b), we illustrate the graphical notation corresponding to add a cube operator $B_{c'}^{(\hat{z})}$ and remove the plaquette operators B_q and $B_{q'}$ of the Toric Code Hamiltonian. In (c), we take the model defined by the Hamiltonian obtained in figure (b) and consider the TC excited state of figure (a) in this new context. It is still an excited state, but its energy is reduced by two unities. In (d), by continuously extending the red line of figure (c), we obtain a state with an even more reduced energy. In (e) and (f), the same procedure is done for all cubes hosting a half of the ribbon, resulting in a ground state.

By continuously extending the red line of figure 4.12(c) to the boundary, we obtain figure 4.12(d). The red line closes into a non-contractible curve. The energy of the state is reduced to be equal to the length of the torus in the z direction. The resulting state of figure 4.12(d) is still an excited state of the Toric Code, and the corresponding modified Hamiltonian remains equivalent to H_{TC}.

The same procedure can be performed to the neighbouring cubes that host the other half of the dual ribbon, as shown in figures 4.12(e) and 4.12(f). However, the resulting state in figure 4.12(f) is a ground state. Thus, the Hamiltonian obtained at the end of the process shown in figures 4.12(c)–4.12(f) defines a new model, in which ground states are given by closed dual surfaces and surfaces bounded by the red non-contractible curves. Its ground state degeneracy is $GSD_{TC} + 2$, where GSD_{TC} is the ground state degeneracy of the Toric Code.

The procedure of connecting parallel plaquettes by red lines can be extended to the whole lattice at every direction. The resulting Hamiltonian is the one given by equation (4.1.38), and it describes the fractonlike model. In this way, there is a continuous process in which we can go from the Toric Code Hamiltonian to equation (4.1.38). In this process, TC excitations condense into ground states of the fractonlike model. However, note that only TC excitations given by non-contractible ribbons condense into fractonlike ground states. For instance, an TC excitation given by a contractible surface, as in figure 4.13(a), is a fracton excitation in the fractonlike model.

Fracton excitations

The elementary excited states $|\phi\rangle \in \mathcal{H}$ are such that either $A_v |\phi\rangle = 0$, for some vertex v, or $B_c^{(\mu)} |\phi\rangle = 0$, for some cube c and direction μ. A string of σ^z operators, beginning at a vertex v and ending at a vertex v', creates excitations of A_v and $A_{v'}$, also called charge excitations. Since A_v is essentially the gauge transformation of the $3D$ Toric Code, the charge excitations of the model (4.1.38) are the same charge excitations of the $3D$ Toric Code, and they can move freely in the lattice without an energy cost.

Now, excited states of the cube operators $B_c^{(\mu)}$ are called μ-flux excitations and can be pictured as lying at the corners of membranes. This can be better understood using the graphical representation of states as in figure 4.1.13. The simplest μ-flux excited state is created by the action of a σ^x operator on a single site over a ground state of the model. Note that whether this operator acts on a link along the $\hat{x}, \hat{y}$ or $\hat{z}$-axis will result on certain combinations of $\hat{x}, \hat{y}$ and
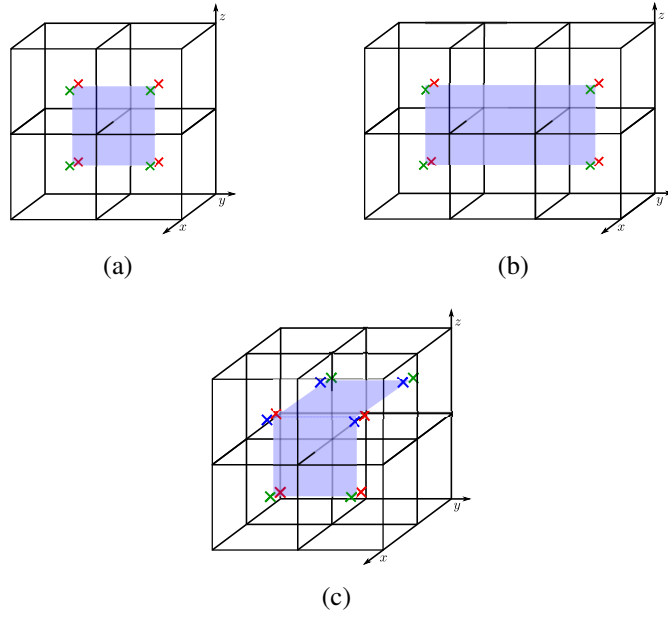
Figure 4.1.13: (a) An state represented by the membrane diagram inside M has flux excitations and the four cubes at its corners. The red crosses represent what we call $\hat{z}$-fluxes, excitations of $B_c^{(\hat{z})}$. Whereas the green ones are $\hat{y}$-fluxes, excitations of $B_c^{(\hat{y})}$. Blue crosses stand for $\hat{x}$-fluxes, excitations of $B_c^{(\hat{x})}$ (b) Excitations can freely move as long as the number of corners remains invariant. (c) If a membrane bends into a orthogonal direction, flux excitations are created at every corner it has.

$\hat{z}$-fluxes. For instance, acting with σ_l^x on a ground state:

$$|\phi\rangle = \sigma_l^x |\psi_0\rangle, \tag{4.1.44}$$

where l is a $\hat{x}$-like link, results on a state with pairs of $\hat{y}$ and $\hat{z}$-fluxes at the boundaries of the membrane as depicted in figure 4.13(a).

These excitations have restricted mobility since their localization is associated to the corners of the membrane. For example, the state represented by figure 4.13(b) shows that extending the membrane along the $\hat{y}$-direction move pairs of μ-fluxes. In general, moving these excitations correspond to extending the membrane without changing the number of corners. On the contrary, if the membrane is bent towards its orthogonal direction more excited states are created increasing the energy of the state, as shown in figure 4.13(c). Again, this is interpreted as an energy penalization to deformations of membranes that change their number of corners.

4.2 Quantum phases with geometry-dependent ground state degeneracy

In the previous sections, we built models of quantum phases based on AHGT by constructing Hamiltonians that define the interactions among the higher gauge degrees of freedom. Since the interactions defined are among the quantum dynamical degrees of freedom of the theory, there is not much external control on the behavior of the system.

This suggests another modification one can perform to a Hamiltonian model of an AHGT. Namely, we can introduce an *external non-dynamical classical field* to the quantum system. To build intuition, we can think of this construction as equivalent to studying quantum particles in the presence of a classical external electromagnetic field. Here however, we will consider a very particular kind of external field, which is one which resembles a higher gauge configuration. Thus, the external field can be seen as a *decoration* of the lattice that controls the interactions between the quantum degrees of freedom. Models with this modification have ground states that depend on the *geometry* of the manifold. More specifically, they depend on the shortest paths between two points one can draw on the manifold. These models can thus be used to compute the shortest path between two points in a graph.

4.2.1 AHGT in the presence of a decoration of the lattice

As in section 4.1, here we will focus on $2D$ and $3D$ models that are more intuitive. We also restrict ourselves to regular square (in $2D$) and cubic (in $3D$) lattices. Nevertheless, the constructions described here can be extended to any lattice in any dimension.

In 2-dimensions

Let M be a 2-manifold discretized by a regular square lattice $K = K_0 \cup K_1 \cup K_2$, which we use to build the chain complex

$$0 \to C_2 \xrightarrow{\partial_2^C} C_1 \xrightarrow{\partial_1^C} C_0 \to 0.$$

We can define a 0-gauge theory over this lattice as in section 3.2.1. That is, we choose the higher gauge group

$$0 \to G_2 \xrightarrow{\partial_2^G} G_1 \xrightarrow{\partial_1^G} G_0 \to 0$$

with $G_2 = G_1 = 0$, the trivial group. The higher gauge configurations $f = \{f_0\} \in \hom(C, G)^0$, where $f_0 \in \mathrm{Hom}(C_0, G_0)$, are given as in figure 3.2.1. These configurations label the basis states

$$|f\rangle = \bigotimes_{v \in K_0} |f_0(v)\rangle$$

of the Hilbert space

$$\mathcal{H} = \bigotimes_{v \in K_0} \mathcal{H}_v$$

of the theory.

The Hamiltonian of a 0-gauge theory is given by (3.2.1). That is,

$$H = -\sum_{l \in K_1} B_l, \tag{4.2.1}$$

where

$$B_l \left| \begin{array}{c} \underset{l}{\overset{g_1 \longrightarrow g_2}{}} \end{array} \right\rangle = \delta(g_1 g_2^{-1}, e) \left| \begin{array}{c} \underset{l}{\overset{g_1 \longrightarrow g_2}{}} \end{array} \right\rangle. \tag{4.2.2}$$

We introduce a *decoration of the lattice* ξ to this system by placing group degrees of freedom at the links of the lattice. That is, at every link $l \in K_1$, we fix a group element $\xi(l) = \alpha \in G_1$. The decoration is thus similar to a *classical 1-gauge field* configuration. We also fix the decoration configuration in such a way that its flux around any plaquette is zero. That is, we fix a classical static 1-gauge field configuration with flat local holonomy to the system.

With this fixed decoration, we define a Hamiltonian model of a 0-gauge theory by defining the Hamiltonian

$$H(\xi) = -\sum_{l \in K_1} B_l(\xi), \tag{4.2.3}$$

where

$$B_l(\xi) \left| \begin{array}{c} \underset{v_0}{\overset{g_1}{}} \underset{l}{\overset{\longrightarrow}{}} \underset{v_1}{\overset{g_2}{}} \end{array} \right\rangle = \delta(g_1 g_2^{-1}, \partial_1^G \xi(l)) \left| \begin{array}{c} \underset{v_0}{\overset{g_1}{}} \underset{l}{\overset{\longrightarrow}{}} \underset{v_1}{\overset{g_2}{}} \end{array} \right\rangle. \tag{4.2.4}$$

We can think of ξ as a coupling strength of the interaction between sites. For instance, when $\xi(l)$ is constant for all $l \in K_1$, it acts as a usual coupling constant, setting the energy scale of the system.

The Hamiltonian (4.2.3) depends on the choice of a fixed decoration of the links of the

lattice. Since we have $|G_1|^{|K_1|}$ possible configurations, the number of Hamiltonian models we can build scales exponentially with the system size. However, not all such models exhibit different physics. As we will show, some of them are unitarily equivalent to others, which means that they share the same spectra. Thus, we can divide models into equivalence classes of spectra.

Let $v \in K_0$ be any vertex and let $\alpha \in G_1$. We define the local gauge transformation of a decoration configuration as

$$(4.2.5)$$

Decorations configurations that differ by a local gauge transformation yield Hamiltonians with the same spectra. To see this, let ξ, ξ' be two decorations such that they differ by a local gauge transformation around a vertex $v_0 \in K_0$, as in (4.2.5). We define a local unitary transformation $U_v(\alpha) : \mathcal{H} \to \mathcal{H}$ given by

$$(4.2.6)$$

We have that

$$B_l(\xi') = U_{v_0}^{-1}(\alpha) B_l(\xi) U_{v_0}(\alpha). \tag{4.2.7}$$

In fact,

$$U_{v_0}^{-1}(\alpha)B_l(\xi)U_{v_0}(\alpha)\left|\begin{matrix}g_1 & \xrightarrow{\quad l \quad} & g_2 \\ v_0 & & v_1\end{matrix}\right\rangle = U_{v_0}^{-1}(\alpha)B_l(\xi)\left|\begin{matrix}\partial_1^G\alpha g_1 & \xrightarrow{\quad l \quad} & g_2 \\ v_0 & & v_1\end{matrix}\right\rangle$$

$$= U_{v_0}^{-1}(\alpha)\delta\left(\partial_1^G\alpha g_1 g_2^{-1}, \partial_1^G\xi(l)\right)\left|\begin{matrix}\partial_1^G\alpha g_1 & \xrightarrow{\quad l \quad} & g_2 \\ v_0 & & v_1\end{matrix}\right\rangle$$

$$= \delta\left(g_1 g_2^{-1}, \partial_1^G(\alpha^{-1})\partial_1^G\xi(l)\right)\left|\begin{matrix}g_1 & \xrightarrow{\quad l \quad} & g_2 \\ v_0 & & v_1\end{matrix}\right\rangle$$

$$= \delta\left(g_1 g_2^{-1}, \partial_1^G(\alpha^{-1}\xi(l))\right)\left|\begin{matrix}g_1 & \xrightarrow{\quad l \quad} & g_2 \\ v_0 & & v_1\end{matrix}\right\rangle$$

$$= B_l(\xi') \qquad (4.2.8)$$

Therefore, not all decorations yield different Hamiltonians. The ones which are related by a local gauge transformation parameterize Hamiltonians with the same spectra. This means that we have to consider only gauge equivalence classes decorations when analysing the physical properties of the Hamiltonians (4.2.3).

Note that, strictly speaking, if we were analysing a usual $0, 1$-gauge theory, the flat gauge equivalence classes of 1-gauge configurations we are considering would correspond to ground state configurations. From our discussion on the Quantum Double Models in chapter 2, we know that gauge equivalence classes of 1-gauge field configurations in the ground state are determined by the topology of the underlying $2D$ manifold. So, the number of Hamiltonians of the type (4.2.3) with non-equivalent spectra one can construct depends on the homology classes of the surface.

To summarize, the model defined by the Hamiltonian (4.2.3) can be thought of as a 0-gauge theory in 2-dimensions in the presence of a classical external 1-gauge field that resembles the dynamical 1-gauge fields we constructed from usual AHGT. In section 4.2.2, we will analyse an example of such model for the case in which the gauge fields are $\mathbb{Z}_2$ gauge fields. As we will see, the resulting model is intuitively simple and, as we will soon demonstrate, has as its main property the fact that its ground-state depends on the *shortest paths* of the underlying 2-manifold.

In 3-dimensions

As in the 2-dimensional case, here we start by defining a particular Abelian higher gauge theory in 3-dimensions. Let M be a 3-manifold discretized by a regular square lattice $K = K_0 \cup K_1 \cup K_2 \cup K_3$, over which we have the chain complex

$$0 \to C_3 \xrightarrow{\partial_3^C} C_2 \xrightarrow{\partial_2^C} C_1 \xrightarrow{\partial_1^C} C_0 \to 0.$$

We define a 1-gauge theory over this lattice much like we did in section 3.2.2. We set the higher gauge group

$$0 \to G_3 \xrightarrow{\partial_3^G} G_2 \xrightarrow{\partial_2^G} G_1 \xrightarrow{\partial_1^G} G_0 \to 0$$

in such a way that $G_3 = G_2 = G_0 = 0$, while G_1 is any Abelian finite group. Higher gauge configurations $f = \{f_1\} \in \mathrm{hom}(C, G)^0$, where $f_1 \in \mathrm{Hom}(C_1, G_1)$, are given as in figure 4.2.1. The basis states

$$|f\rangle = \bigotimes_{l \in K_1} |f_1(l)\rangle$$

of the Hilbert space

$$\mathcal{H} = \bigotimes_{l \in K_1} \mathcal{H}_l$$

are labelled by these configurations.

From chapter 3, we have that the Hamiltonian model of a 1-gauge theory in 3-dimensions is given by

$$H = -\sum_{v \in K_0} A_v - \sum_{p \in K_2} B_p, \tag{4.2.9}$$

where

$$A_v = \frac{1}{|G_1|} \sum_{g \in G_1} A_v^g, \tag{4.2.10}$$

with A_v^g acting over basis states as in equations (3.2.10), and

$$B_p \left| \begin{array}{c} g_3 \\ g_4 \boxed{} g_2 \\ g_1 \end{array} \right\rangle = \delta(g_1 g_2 g_3^{-1} g_4^{-1}, e) \left| \begin{array}{c} g_3 \\ g_4 \boxed{} g_2 \\ g_1 \end{array} \right\rangle. \tag{4.2.11}$$

$$0 \xrightarrow{\quad} C_3 \xrightarrow{\partial_3^C} C_2 \xrightarrow{\partial_2^C} C_1 \xrightarrow{\partial_1^C} C_0 \xrightarrow{\quad} 0$$

Figure 4.2.1: Gauge theory data for an Abelian 1-gauge theory in 3-dimensions.

We introduce an *decoration of the lattice* ξ to this system whose configurations are given by placing group degrees of freedom at the *plaquettes* of the lattice. That is, at every plaquette $p \in K_2$, there is a fixed group element $\alpha = \xi(p) \in G_2$. This decoration can thus be considered as a *classical 2-gauge field*. We also choose only decorations with flat local holonomy. That is, we only consider classical 2-gauge fields whose flux around a cube is zero.

Given a decoration ξ, we construct a Hamiltonian model of a 1-gauge theory by defining the Hamiltonian

$$H(\xi) = -\sum_{v \in K_0} A_v - \sum_{p \in K_2} B_p(\xi), \tag{4.2.12}$$

where A_v is given by (4.2.10) and (3.2.10) and

$$B_p(\xi) \left| \begin{array}{c} \end{array} \right\rangle = \delta(g_1 g_2 g_3^{-1} g_4^{-1}, \partial_2^G \xi(p)) \left| \begin{array}{c} \end{array} \right\rangle. \tag{4.2.13}$$

As in the $2D$ case, ξ can be thought of as a coupling in the four body interaction between degrees of freedom located at links in the boundary of plaquettes.

Much like in the $2D$ case, here we also have a very large number of possible choices of Hamiltonians (4.2.12) (in the order of $|G_2|^{|K_2|}$) of which only a few doesn't share the same spectra and thus yield truly different physics. To see this, let $l \in K_1$ and $\alpha \in G_2$. We define the

local gauge transformation of a decoration as follows:

$$\text{(4.2.14)}$$

Note that this is just the same action as A_l^α in (3.2.11). Decorations that differ only by a local gauge transformation yield unitarily equivalent Hamiltonians. In fact, let $\xi, \xi' \in \text{Hom}(C_2, G_2)$ be two decorations differing only by a local gauge transformation around the link $l \in K_1$ as in figure 4.2.14. Let $U_l(\alpha) : \mathcal{H} \to \mathcal{H}$ be an operator given by

$$U_l(\alpha) \left| g \right\rangle_l = \left| \partial_2^G \alpha g \right\rangle_l, \qquad (4.2.15)$$

where $\left| g \right\rangle_l$ is some state at l labelled by $g \in G_1$. We have that

$$B_p(\xi') = U_l^{-1}(\alpha) B_p(\xi) U_l(\alpha), \qquad (4.2.16)$$

and the proof follows the exact same logic as the one in (4.2.8) of the $2D$ case.

Thus, we have to consider only gauge equivalence classes of decorations when studying the physical properties of the Hamiltonian (4.2.12). Note that the decorations we consider here, if they were quantum 2-gauge fields in a 1,2-gauge theory, they would correspond to ground states. Gauge equivalence classes of 2-gauge fields in the ground-state are determined by the topology of the underlying manifold. Thus, the decorations one can consider to construct Hamiltonians (4.2.12) with different spectra depend on the homology of the manifold M.

To summarize, the Hamiltonian model (4.2.12) can be seen as a 1-gauge theory in 3-dimensions in the presence of a decoration of the lattice that resembles the dynamical 2-gauge field of a 1,2-gauge theory constructed from usual AHGT. In section 4.2.3, we will analyse an example of such model with $\mathbb{Z}_2$ gauge fields. We will see that the resulting model is very similar to the Toric Code in $3D$, except that some of its ground-states depend on the *geodesics* of the underlying manifold M.

4.2.2 The Ising model mixing ferromagnetic and antiferromagnetic interactions

Here we give an example in 2-dimensions of the Abelian Higher Gauge theory defined in 4.2.1 for the case in which we choose both the gauge group and the group over which the decoration assumes its values to be $\mathbb{Z}_2$. This model exhibits *frustration*, meaning that a true zero energy ground state cannot be achieved. It turns out that this frustration leads to a ground-state that *localizes paths of minimum length*, as we will see next.

The model

To give a concrete example of the model given by the Hamiltonian (4.2.3), let's choose the groups $G_1 = G_0 = \mathbb{Z}_2 = \{+1, -1\}$, with multiplication as the group operation. We also choose the map $\partial_1^G : G_1 \to G_0$ such that $\partial_1^G = \mathrm{id}_{\mathbb{Z}_2}$, the identity map on $\mathbb{Z}_2$. The 0-gauge configurations assign a spin-1/2 degree of freedom to each vertex of the lattice, while the fixed decoration assigns a constant equal to ± 1 to links in the lattice. The local Hilbert space $\mathcal{H}_v$ is generated by the basis vectors $\{|+1\rangle_v, |-1\rangle_v\}$. The total Hilbert space is the product

$$\mathcal{H} = \bigotimes_{v \in K_0} \mathcal{H}_v.$$

Given these choices of groups, we have that the matrix form of the operator (4.2.4) is given by

$$B_l(\xi) = \frac{1}{2}\left(\bigotimes_{v \in K_0} \mathbb{1}_v + \xi(l)\sigma_v^z \otimes \sigma_{v'}^z\right), \tag{4.2.17}$$

for any $\xi \in \mathrm{Hom}(C_1, \mathbb{Z}_2)$, where $v, v' \in \partial l$. Given $\xi \in \mathrm{Hom}(C_1, \mathbb{Z}_2)$, the Hamiltonian (4.2.3) is then

$$H(\xi) = -\sum_{l \in K_1} B_l(\xi) = -\frac{1}{2}\sum_{l \in K_1}\left(\bigotimes_{v \in K_0} \mathbb{1}_v + \xi(l)\sigma_v^z \otimes \sigma_{v'}^z\right). \tag{4.2.18}$$

Since the first term is a constant, we can also write

$$H(\xi) = E_0 - \frac{1}{2}\sum_{\langle v, v'\rangle} \xi(v, v')\sigma_v^z \otimes \sigma_{v'}^z, \tag{4.2.19}$$
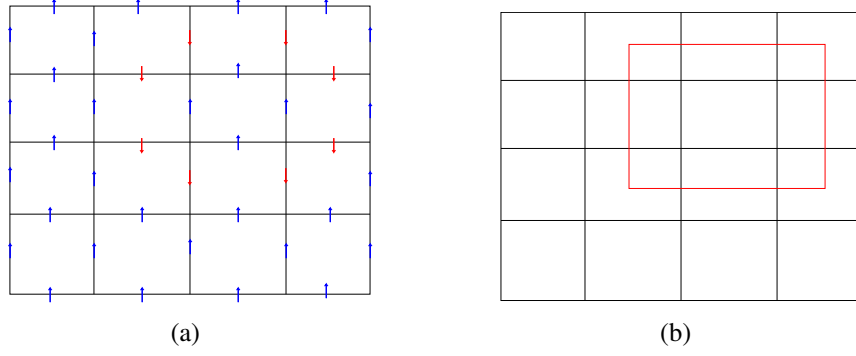
88

Figure 4.2.2: (a) Some classical 1-gauge configuration. (b) The same configuration in graphical notation.

where $E_0 = -\frac{1}{2}|K_1| \bigotimes_{v \in K_0} \mathbb{1}_v$ and we write $l = \langle v, v' \rangle$, because in a regular square lattice a link connects vertices that are nearest neighbours. This Hamiltonian resembles the Edwards-Anderson model [56], but here we have an example of realized disorder. Since $\xi(v, v') \in \mathbb{Z}_2$, we call the Hamiltonian the *F-AF Ising model*, mixing ferromagnetic and antiferromagnetic interactions depending on the choice of classical external field configuration $\xi \in \text{Hom}(C_1, \mathbb{Z}_2)$.

As we explained in section 4.2.1, not all decorations with flat local holonomy yield different physics. We can separate models into gauge equivalence classes of decorations. Each model in a class gives rise to the same spectra. These gauge equivalence classes are determined by the topology of the underlying surface M.

We introduce a graphical notation to represent decorations in a lattice. To each link $l \in K_1$ where $\xi(l) = -1$, we assign a dual red link, while links l for which $\xi(l) = +1$ are kept empty. This notation is illustrated in figure 4.2.2. With this notation, we define a Hamiltonian model (4.2.18) by drawing red dual links in a lattice, while remembering that interactions between spins placed at vertices are Ising-like. In this notation, the gauge transformation defined in 4.2.5 is represented by the addition of a dual red loop around a vertex. Note that since the decoration belong to $\mathbb{Z}_2$, dual red links annihilate each other.

We also introduce a graphical notation to represent the spin states of the system. A vertex with a spin up degree of freedom is colored blue, while a vertex with a spin down degree of freedom is not colored. We will use this notation to analyse the physics of the ground state of this model.
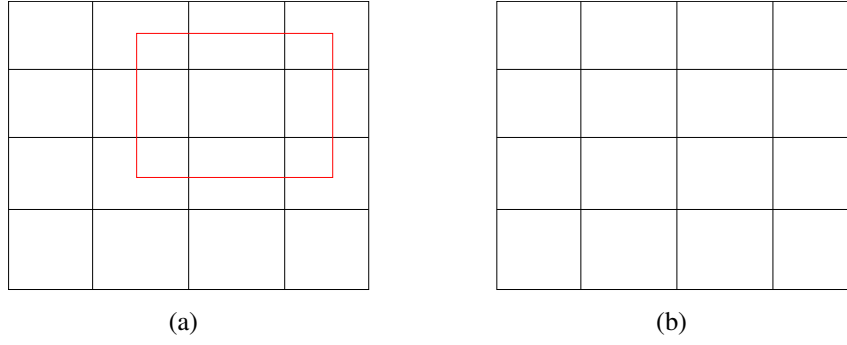
Figure 4.2.3: The model in (a) is equivalent to the model in (b) because they differ from each other only by a sequence of local gauge transformations.

Ground State Degeneracy

Since gauge equivalence classes of decorations depend on the topology of the underlying manifold M, we have to first fix a manifold and then choose a decoration which is representative of the corresponding class to start analysing the physics of the Hamiltonian (4.2.18).

Thus, let's consider the case where M is a plane or a sphere, discretized by a lattice with open or closed boundary. This is a manifold with trivial topology and thus there is only one class of decorations, the trivial one. This can be seen in figure 4.2.3. Any non-trivial decoration with flat local holonomy parameterize a model which has the same spectra as the model parameterized by the decoration $\xi(l) = 1 \ \forall l \in K_1$. This is so because any non-trivial decoration with flat local holonomy in a manifold with trivial topology differs from the trivial decoration only by local gauge transformations of the type (4.2.5). Thus, any model (4.2.18) defined over such manifold has the same physics as the model

$$H(\xi) = H(\xi = 1) = E_0 - \frac{1}{2} \sum_{\langle v,v' \rangle} \sigma_v^z \otimes \sigma_{v'}^z, \tag{4.2.20}$$

which is nothing but the ferromagnetic Ising model in $2D$. The ground states of this model are well-known, given by configurations will all spins aligned in the same direction. The ground state degeneracy of this model is $GSD = 2$.

The next cases we will consider are the ones in which M has non-trivial topology. First, let's take M as the 2-dimensional torus, discretized by a square lattice with periodic boundary conditions. As we pointed out in section 4.2.1, the allowed classes of decorations that yield models with different spectra are equivalent to the classes of ground state 1-gauge configurations of a Quantum Double Model defined over the same surface. In this example, the 1-gauge
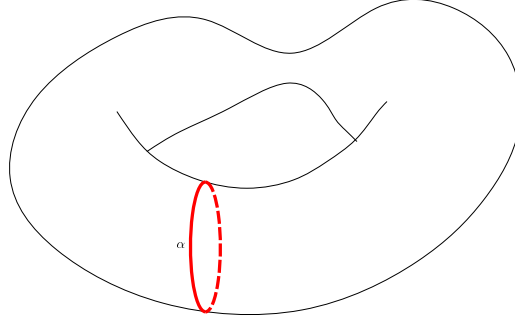
90

Figure 4.2.4: Non-trivial F-AF Ising model.

configurations take values on $\mathbb{Z}_2$ and are defined over a torus. Thus, the classes of decorations that yield models with different physics are equivalent to the classes of ground states of the Toric Code. Since we have four classes of Toric Code ground states, we can construct four different Hamiltonian models of the type (4.2.18).

As we saw in section 2.1, the classes of Toric Code ground states are determined by the non-contractible loops in the torus. If we choose decorations that form contractible loops, the resulting model is in the class of the model with trivial decorations, just as in the case where we considered a manifold with trivial topology. The model is then equivalent to the $2D$ ferromagnetic Ising model, and its physics is known.

Now, let α be a non-contractible dual loop in the lattice, as in figure 2.1.5. Let's choose a decoration ξ such that

$$\xi(l) = \begin{cases} +1, & \text{if} \quad l^* \notin \alpha \\ -1, & \text{if} \quad l^* \in \alpha \end{cases}, \tag{4.2.21}$$

for $l \in K_1$, where l^* is the link dual to l. This configuration is illustrated in figure 4.2.4. Then, we have a model mixing antiferromagnetic interactions in the links crossed by the non-contractible red line and ferromagnetic interactions in all the other links. In a ground state, the spins connected by links which are crossed by red lines must be antiparalell, while all other spins must be paralell due to the ferromagnetic interaction. Since the manifold is closed, we see that we cannot minimize all $B_l(\xi)$ terms in the Hamiltonian at the same time (see figure 4.2.5). Starting from one side of the non-contractible red line and making all spins up, we end-up on the opposite side of the red line, where we have to make the spins down to minimize the $B_l(\xi)$ terms corresponding to links crossed by red lines. This model is thus *frustrated*, meaning that the ground-state is attained by a configuration with energy greater than zero.
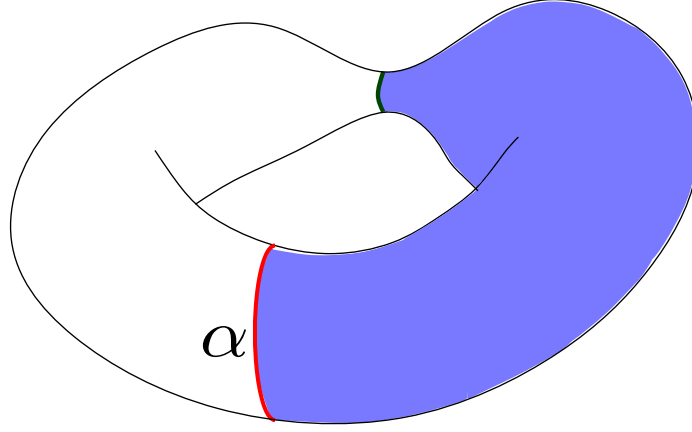
Figure 4.2.5: Ground state of a non-trivial mixed Ising model. We represent spin-down states by coloring blue their location. The green loop is a non-contractible curve where the $B_l(\xi)$ terms are excited.

The minimum energy state in this model is the one in which the *least* number of $B_l(\xi)$ terms is excited. Since the manifold is path connected, it is not possible to have a ground state with a single excited link. In fact, we can only have a whole non-contractible curve excited (see figure 4.2.5). Thus, the ground state is the one in which the links that are crossed by a *non-contractible curve with least length* γ have excited $B_l(\xi)$ terms. The energy of this state is

$$E_{GS} = -(|K_1| - |\gamma|), \tag{4.2.22}$$

where $|K_1|$ is the total number of links in the lattice and $|\gamma|$ is the length of the minimum curve (number of links crossed by it). The ground state is degenerated since there can be more than one non-contractible curve with least length in the lattice. The ground state degeneracy thus counts the number of non-contractible curves with least length:

$$GSD = n_\gamma, \tag{4.2.23}$$

where n_γ is the number of non-contractible curves with length $|\gamma|$. This length is such that, for any other curve γ' in the lattice, $|\gamma| \leq |\gamma'|$.

We illustrate a ground-state in figure 4.2.5. The ground-state localizes the non-contractible curves with least length in the lattice. Their localization can be made by realizing measurements of the $B_l(\xi)$ operator.

Now we take the surface as the discretization of an annulus, like in figure 4.2.6. In a similar way as explained before, the only models we can define over this surface which don't have
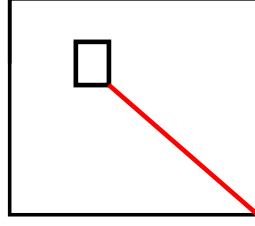
92

Figure 4.2.6: Annulus with a path α^* in red connecting the inner and outer boundaries.

equivalent spectra as the usual ferromagnetic Ising model in $2D$ are the ones in which the decorations form non-contractible paths in the lattice. That is, they are such that

$$\xi(l) = \begin{cases} +1, & \text{if} \quad l^* \notin \alpha^* \\ -1, & \text{if} \quad l^* \in \alpha^* \end{cases}, \tag{4.2.24}$$

where α^* is a dual path connecting the inner and outer boundaries of the annulus, as in figure 4.2.6. Then, as in the case of the torus, we have a model mixing antiferromagnetic spin interactions (in the links crossed by the red line) and ferromagnetic interactions. The ground-state of this model is thus *frustrated*, since it cannot attain zero energy by minimizing all $B_l(\xi)$ terms in the Hamiltonian (4.2.18) at the same time. Starting from one side of the red line and making all spins up, we end-up on the opposite side of the line, where the spins should be down to minimize those link operators.

As in the torus case, the minimum energy state of this model is the one with the smallest number of excited link operators $B_l(\xi)$. The ground state spin configuration must then have as excited links the ones that are crossed by the *least path* γ between the inner and the outer boundary (see figure 4.2.7). The energy of such a spin configuration is

$$E_{GS} = -(|K_1| - |\gamma^*|), \tag{4.2.25}$$

where $|K_1|$ is the total number of links in the lattice and $|\gamma^*|$ is the length of the least path that connects the inner and the outer boundary. Since there can be more than one path with least length, the ground state is degenerated, with the ground state degeneracy counting the number of paths with least length that connect the two boundaries:

$$GSD = \# \text{ of paths with least length that connect the two boundaries.} \tag{4.2.26}$$
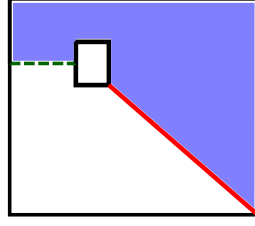
Figure 4.2.7: Ground state of a non-trivial mixed Ising model over an annulus. Spin-down states are represented by coloring blue their location. The green path is the minimum path connecting the inner and outer boundaries.

Thus, the ground-state localizes *geodesics* between the inner and the outer boundary (see figure 4.2.7). Their localization is realized by making measurements of the $B_l(\xi)$ operator.

4.2.3 The $3D$ toric code in an non-uniform external field

We now give an example in 3-dimensions of the Abelian Higher Gauge Theory defined in 4.2.1 for the case in which the gauge groups are $\mathbb{Z}_2$. Just like in the 2-dimensional case, the model we will shortly present exhibits frustration that can be controlled through the lattice decoration. Also as in the 2-dimensional case, the ground state of such a frustrated system depends on *minimal submanifolds* of the underlying space M.

The model

We choose as gauge groups $G_1 = G_2 = \mathbb{Z}_2$, with $\partial_2^G : G_2 \to G_1$ such that $\partial_2^G = \mathrm{id}_{\mathbb{Z}_2}$, the identity on $\mathbb{Z}_2$. That is, there are qubits living on the links of the lattice, and the fixed lattice decoration assigns a constant equal to ± 1 to plaquettes of the lattice. At each link $l \in K_1$ the local Hilbert space $\mathcal{H}_l$ is generated by the basis $\{|+1\rangle_l, |-1\rangle_l\}$. The total Hilbert space $\mathcal{H}$ is given by the tensor product

$$\mathcal{H} = \bigotimes_{l \in K_1} \mathcal{H}_l.$$

The Hamiltonian (4.2.12) that defines the 3-dimensional model is composed by a 1-gauge transformation in $3D$, which is given by equation (3.2.10), and by the holonomy operator (4.2.13), which is parameterized by the lattice decoration. Since the gauge groups are all $\mathbb{Z}_2$, the matrix form of these operators can be immediately written. The matrix form of the 1-gauge
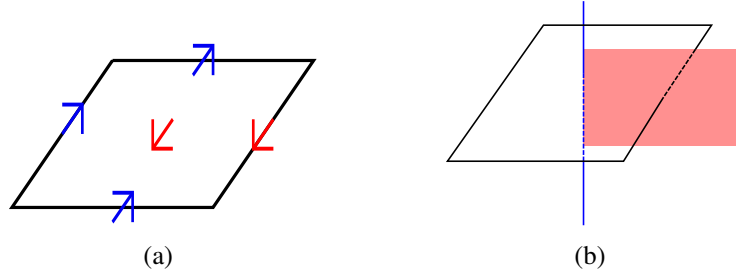
Figure 4.2.8: (a) Higher gauge configuration and (b) corresponding graphical notation.

transformation is given by

$$A_v = \frac{1}{2} \left(\bigotimes_{l \in K_1} \mathbb{1}_l + \bigotimes_{l \in \text{star}(v)} \sigma_l^x \right), \qquad (4.2.27)$$

for any $v \in K_0$, where $\text{star}(v)$ is the set of links that touch the vertex v. The matrix form of the holonomy operator is given by

$$B_p(\xi) = \frac{1}{2} \left(\bigotimes_{l \in K_1} \mathbb{1}_l + \xi(p) \bigotimes_{l \in \partial p} \sigma_l^z \right), \qquad (4.2.28)$$

for any $p \in K_2$. For each plaquette p, the decoration $\xi(p)$ acts as a coupling constant for the four body interaction among the qubits at the boundary of p. The Hamiltonian is thus

$$H(\xi) = -\sum_{v \in K_0} A_v - \sum_{p \in K_2} B_p(\xi). \qquad (4.2.29)$$

This $\mathbb{Z}_2$ model resembles the $3D$ Toric Code, with the difference that depending on the chosen lattice decoration, some plaquettes that would be in the Toric Code ground state are now excited and vice-versa. We consider this model as a decorated $3D$ *Toric Code*.

Ground state degeneracy

Here we introduce a graphical notation to analyze the ground states of this model. We associate dual red plaquettes to links with spin -1, while links with spin $+1$ remain empty. Plaquettes p where the decoration $\xi(p) = -1$ are associated to dual blue links, while plaquettes p for which the decoration $\xi(p) = +1$ remain empty. An example of this notation is shown in figure 4.2.8.

Suppose we define the model over a cubic lattice with open boundary conditions, as in figure 4.2.9. As noted in section 4.2.1, since we have a manifold with trivial topology, we have
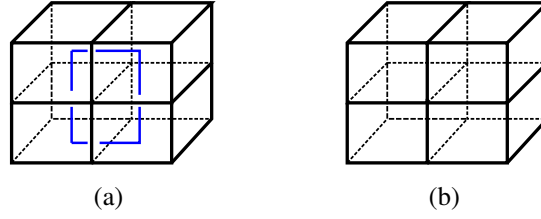
Figure 4.2.9: The model in (a) is equivalent to the model in (b) because they differ from each other only by a local gauge transformation.
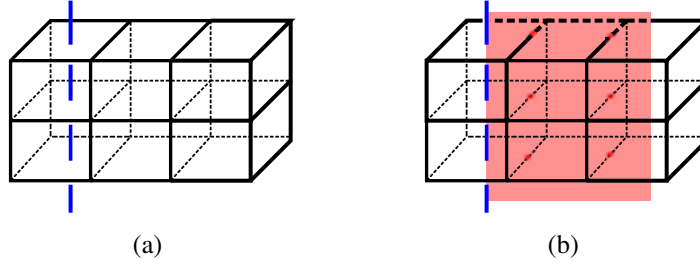

Figure 4.2.10: Non-trivial decorated Toric Code. In a ground state, the red membrane must begin at the blue loop and end at a non-contractible loop with least length.

only one gauge equivalence class of decorations. This can be seen in figure 4.2.9. Any non-trivial decoration with flat local holonomy parameterizes a model which has the same spectra as the model parameterized by the trivial decoration. The model parameterized by the trivial decoration is nothing but the $3D$ Toric Code. Thus, in a lattice with trivial topology, the model (4.2.29) reduces to the Toric Code. There is only one ground state of the Toric Code in $3D$ in a space with trivial topology, which is the *membrane gas state*. Only closed dual red surfaces are allowed in the lattice.

Now suppose we define the model in a cubic lattice with periodic boundary conditions, forming a discretization of a 3-torus (see figure 4.2.10). There are four non-equivalent decorations we can define on the manifold, yielding four different Hamiltonians of the type (4.2.29). Suppose we choose a decoration that forms a non-contractible dual blue loop, as in figure 4.10(a). To be in the ground state, the plaquettes that are crossed by this loop must also have some link crossed by dual red plaquettes, as in figure 4.10(b). The red surface must extend itself to keep plaquettes in the ground state, but if it reaches the other side of the blue dual loop, it will create a line of excited plaquettes there. The model is then *frustrated*, and the minimum energy is attained when the dual red surface ends in a *non-contractible curve with least length*. Thus, in the same way as the F-AF Ising model finds minimal non-contractible curves in a torus in $2D$, the decorated Toric Code in $3D$ finds minimal non-contractible curves in the 3-torus.
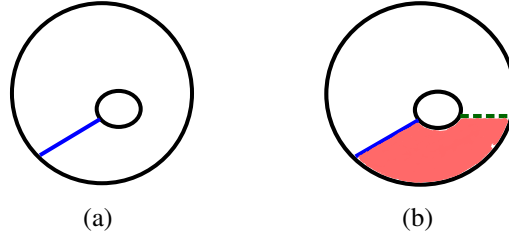
Figure 4.2.11: Schematic drawing of a non-trivial Toric Code in an external field defined over $S^2 \times I$. In a ground state, the red membrane must begin at the blue loop and end at a minimum path between the inner and outer boundaries.

Let's now take the surface as the product $S^2 \times I$, i.e., a 2-sphere inside a 2-sphere. As before, the only model we can define that is not equivalent to the $3D$ Toric Code is the one in which the decoration forms a non-contractible path in the lattice. The only non contractible paths in the lattice are the ones joining the inner and the outer boundary, as in figure 4.11(a). To be in the ground state, the plaquettes that are crossed by the dual blue link must have a dual red plaquette crossing an odd number of its boundary links, as in figure 4.11(b). Again, if the dual red surface reaches the other side of the dual blue path, we have an excited state. The minimum energy is attained when the (red) boundary of the dual red surface ends at a *path of least length* between the inner and outer boundary. Thus, the ground state of this model localizes the path of least length between the two surfaces. The localization is done by measurements of plaquette operators.

Although the model (4.2.29) is very similar to the Toric Code, there are some essential differences. When the model is defined in the 3-torus with a non-trivial classical 2-gauge configuration, it doesn't exhibits a topological ground state degeneracy. The ground state depends on the geometry of the lattice, while still exhibiting long-range entanglement.

4.2.4 Finding the shortest path between two points with AHGT

In sections 4.2.2 and 4.2.3, we defined Hamiltonian models inspired on Abelian higher gauge theories whose ground state depends on specific geometrical characteristics of the lattice. In particular, the ground states of those models localize minimum non-contractible loops when defined on the torus and minimum paths between boundaries when defined on an annulus in $2D$ or on $S^2 \times I$ in $3D$.

Inspired by these models, here we construct a Hamiltonian model based on an Abelian higher gauge theory in D-dimensions which, given two points in the lattice, finds the *shortest*

path between those points. To construct such a model, we first need to define a $(D-2), (D-1)$-gauge theory in the *dual D-dimensional lattice*.

The model

Consider a D-dimensional lattice $K = K_0 \cup K_1 \cup ... \cup K_D$. Let

$$0 \to C_D \xrightarrow{\partial_D^C} C_{D-1} \xrightarrow{\partial_{D-1}^C} ... \xrightarrow{\partial_2^C} C_1 \xrightarrow{\partial_1^C} C_0 \to 0$$

be the D-dimensional chain complex associated to it. We define a $(D-2), (D-1)$-gauge theory on this lattice by defining the higher gauge group

$$0 \to G_D \xrightarrow{\partial_D^G} G_{D-1} \xrightarrow{\partial_{D-1}^G} ... \xrightarrow{\partial_2^G} G_1 \xrightarrow{\partial_1^G} G_0 \to 0$$

such that $G_{D-1}, G_{D-2} \neq 0$, while $G_D = G_{D-3} = ... = G_0 = 0$. The non-trivial higher gauge configurations are given in figure 4.2.12. The higher gauge configurations $f = \{f_{D-1}, f_{D-2}\}$ label the states

$$|f\rangle = \bigotimes_{x \in K_{D-2}} |f_{D-2}(x)\rangle \bigotimes_{y \in K_{D-1}} |f_{D-1}(y)\rangle$$

that form the basis of the Hilbert space

$$\mathcal{H} = \bigotimes_{x \in K_{D-2}} \mathcal{H}_x \bigotimes_{y \in K_{D-1}} \mathcal{H}_y$$

of the system.

Note that the $(D-2), (D-1)$-gauge theory in D-dimensions generalizes the 1,2-gauge theory in 3-dimensions defined in 3.2.3. Thus, we can borrow the intuition developed there to immediately write the operators that compose the Hamiltonian of the theory. For every $x \in K_{D-3}$ and $y \in K_{D-2}$, we have higher gauge operators $A_x : \mathcal{H} \to \mathcal{H}$ and $A_y : \mathcal{H} \to \mathcal{H}$ such that

$$A_x = \frac{1}{|G_{D-2}|} \sum_{g \in G_{D-2}} A_x^g, \tag{4.2.30}$$

$$A_y = \frac{1}{|G_{D-1}|} \sum_{g' \in G_{D-1}} A_y^{g'}, \tag{4.2.31}$$

where $A_x^g = A_{e[D-3,x,g]}$ and $A_y^{g'} = A_{e[D-2,y,g']}$, for any $g \in G_{D-2}, g' \in G_{D-1}, x \in K_{D-3}, y \in$

$$0 \xrightarrow{} C_D \xrightarrow{\partial^C_D} C_{D-1} \xrightarrow{\partial^C_{D-1}} C_{D-2} \xrightarrow{\partial^C_{D-2}} C_{D-3} \xrightarrow{\partial^C_{D-3}} \cdots \xrightarrow{\partial^C_1} C_0 \xrightarrow{} 0$$

$$\begin{array}{ccc} & m_D \; f_{D-1} \Big\downarrow m_{D-1} \; t_{D-2} \; \Big| \; f_{D-2} \; t_{D-3} \\ 0 \xrightarrow{} G_{D-1} \xrightarrow[\partial^G_{D-1}]{} G_{D-2} \xrightarrow{} 0 \end{array}$$

Figure 4.2.12: Higher gauge theory data for an Abelian $(D-2), (D-1)$-gauge theory.

K_{D-2}, with the localization maps e defined as in (3.1.19) and the operator A defined as in (3.1.17).

For every $u \in K_D$ and $w \in K_{D-1}$, we have higher holonomy operators $B_u : \mathcal{H} \to \mathcal{H}$ and $B_w : \mathcal{H} \to \mathcal{H}$ such that

$$B_u = \frac{1}{|G_{D-1}|} \sum_{r \in \hat{G}_{D-1}} B_{\hat{e}[D,u,r]} \tag{4.2.32}$$

and

$$B_w = \frac{1}{|G_{D-2}|} \sum_{r' \in \hat{G}_{D-2}} B_{\hat{e}[D-1,w,r']}, \tag{4.2.33}$$

where the localization maps $\hat{e}$ are given by (3.1.20).

The Hamiltonian model for the $(D-2), (D-1)$-gauge theory is thus

$$H = - \sum_{x \in K_{D-3}} A_x - \sum_{y \in K_{D-2}} A_y - \sum_{w \in K_{D-1}} B_w - \sum_{u \in K_D} B_u. \tag{4.2.34}$$

Since this is a Hamiltonian model based on an Abelian higher gauge theory that follows the theory described in 3.1, it exhibits topological order and thus the ground states of the system depends on the topology of the underlying manifold.

We now *dualize* the model, i.e., we define the model on the dual lattice and make the corresponding changes to the operators in order to be consistent. The operators in Hamiltonian (4.2.34) are parameterized by n-simplexes, where $n = D-3, ..., D$. Thus in our dualization procedure, we are going to describe how to dualize only those simplexes. The other ones will not be of importance to our theory. The dual D-simplex is a 0-simplex, which is a vertex. The dual $(D-1)$-simplex is a 1-simplex, which is a link. The dual $(D-2)$-simplex is a 2-simplex, which is a plaquette or face. Finally, the dual $(D-3)$-simplex is a 3-simplex, which is some polyhedron like a tetrahedron or a cube, depending on the characteristics of the lattice. This is
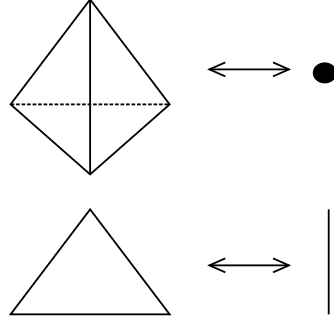
Figure 4.2.13: Dualization of a 3-dimensional lattice made of tetrahedrons.

all illustrated in figure 4.2.13 for the 3-dimensional case of a lattice made of tetrahedrons. We can readily see that our dual theory is effectively at most 3-dimensional.

Now we define the operators that enter the Hamiltonian in this dual lattice. The constructions here are summarized in the dual complex shown in figure 4.2.14. First, we consider the holonomies. Since D-simplexes are equivalent to 0-simplexes in the dual lattice, the D-holonomy operator defined in (4.2.32) must now be changed to be parameterized by 0-simplexes. Thus, for every $v \in K_0$ we define the 0-holonomy operator $B_v : \mathcal{H} \to \mathcal{H}$ as

$$
B_v \left| \begin{array}{c} \includegraphics \end{array} \right\rangle = \delta(x_1 x_2 x_3 x_4 x_5 x_6^{-1} x_7^{-1} x_8^{-1}..., e) \left| \begin{array}{c} \includegraphics \end{array} \right\rangle. \tag{4.2.35}
$$

Likewise, since $(D-1)$-simplexes are equivalent to 1-simplexes in the dual lattice, the $(D-1)$-holonomy operator defined in (4.2.33) must now be changed to be parameterized by 1-simplexes. For every $l \in K_1$, we define the 1-holonomy operator $B_l : \mathcal{H} \to \mathcal{H}$ as

$$
B_l \left| \begin{array}{c} \includegraphics \end{array} \right\rangle = \delta(abc..., \partial_{D-1}^G x) \left| \begin{array}{c} \includegraphics \end{array} \right\rangle. \tag{4.2.36}
$$

Considering now the gauge transformations. For the $(D-2)$-gauge transformation defined in (4.2.30), we define a dual 2-gauge transformation $A_p^g : \mathcal{H} \to \mathcal{H}$ for every $p \in K_2$ and every

Figure 4.2.14: Higher gauge theory data for an Abelian $(D-2), (D-1)$-gauge theory in the dual lattice.

$g \in G_{D-1}$ as

$$A_p^g \left| \begin{array}{c} \includegraphics \end{array} \right\rangle = \left| \begin{array}{c} \includegraphics \end{array} \right\rangle. \tag{4.2.37}$$

Likewise, for the $(D-3)$-gauge transformation defined in (4.2.31), we define a dual 3-gauge transformation $A_x^g : \mathcal{H} \to \mathcal{H}$ for every $x \in K_3$ and every $g \in G_{D-2}$ as

$$A_x^g \left| \begin{array}{c} \includegraphics \end{array} \right\rangle = \left| \begin{array}{c} \includegraphics \end{array} \right\rangle. \tag{4.2.38}$$

Therefore, the Hamiltonian of the *dual* $(D-2), (D-1)$-gauge theory is given by

$$H = -\sum_{x \in K_3} A_x - \sum_{p \in K_2} A_p - \sum_{l \in K_1} B_l - \sum_{v \in K_0} B_v, \tag{4.2.39}$$

where

$$A_x = \frac{1}{|G_{D-2}|} \sum_{g \in G_{D-2}} A_x^g, \tag{4.2.40}$$

and

$$A_p = \frac{1}{|G_{D-1}|} \sum_{g \in G_{D-1}} A_p^g. \tag{4.2.41}$$

Ground state degeneracy

In what follows, we will analyse the ground states of the model (4.2.39) for the particular case where $G_{D-2} = G_{D-1} = \mathbb{Z}_2$, with $\partial_{D-1}^G = \mathrm{id}_{\mathbb{Z}_2}$. In this way, the higher gauge configurations $f = \{f_1, f_2\}$ assign spin-1/2 degrees of freedom to plaquettes and links in the dual lattice. The local Hilbert spaces are given by

$$\mathcal{H}_l = \mathrm{Span}_{\mathbb{C}}\{|+1\rangle_l, |-1\rangle_l\},$$

and

$$\mathcal{H}_p = \mathrm{Span}_{\mathbb{C}}\{|+1\rangle_p, |-1\rangle_p\},$$

for every $l \in K_1$ and $p \in K_2$. The total Hilbert space is given by

$$\mathcal{H} = \bigotimes_{l \in K_1} \mathcal{H}_l \bigotimes_{p \in K_2} \mathcal{H}_p$$

In this particular case, the higher gauge transformation operators are given by

$$A_p \left| \begin{array}{c} z \overset{a}{\triangle} y \\ x \end{array} \right\rangle = \frac{1}{2} \left(\left| \begin{array}{c} z \overset{a}{\triangle} y \\ x \end{array} \right\rangle + \left| \begin{array}{c} {}^{-z}\overset{-a}{\triangle}{}^{-y} \\ {}_{-x} \end{array} \right\rangle \right), \tag{4.2.42}$$

$$A_x \left| \begin{array}{c} a \uparrow b \\ c \end{array} \right\rangle = \frac{1}{2} \left(\left| \begin{array}{c} a \uparrow b \\ c \end{array} \right\rangle + \left| \begin{array}{c} {}_{-a}\uparrow{}_{-b} \\ {}_{-c} \end{array} \right\rangle \right). \tag{4.2.43}$$

That is, the 3-gauge transformation A_x flips the spins at the faces of the 3-simplex x, while the 2-gauge transformation A_p flips both the spin at the plaquette p and the spins at its boundary links $l \in \partial p$. The matrix form of these operators can be written in terms of Pauli operators:

$$A_x = \frac{1}{2} \left(\bigotimes_{l \in K_1} \mathbb{1}_l \bigotimes_{p \in K_2} \mathbb{1}_p + \bigotimes_{p \in \partial x} \tau_p^x \right), \tag{4.2.44}$$

$$A_p = \frac{1}{2} \left(\bigotimes_{l \in K_1} \mathbb{1}_l \bigotimes_{p \in K_2} \mathbb{1}_p + \tau_p^x \bigotimes_{l \in \partial p} \sigma_l^x \right), \tag{4.2.45}$$

$\forall x \in K_3, p \in K_2$, where we use τ to denote the Pauli operators that act over plaquette spins

102

and σ to denote Pauli operators that act over link spins.

As for the higher holonomy operators, the 0-holonomy B_v given by (4.2.35) projects states into states in which the product of the spins at links that touch v is equal to $+1$, while the 1-holonomy B_l given by (4.2.36) projects states into states in which the product of the plaquettes spins that touch l is equal to the spin at the link l. The matrix form of these operators can be written in terms of Pauli operators as

$$B_v = \frac{1}{2} \left(\bigotimes_{l \in K_1} \mathbb{1}_l \bigotimes_{p \in K_2} \mathbb{1}_p + \bigotimes_{l \in \text{star}(v)} \sigma_l^z \right), \tag{4.2.46}$$

$$B_l = \frac{1}{2} \left(\bigotimes_{l \in K_1} \mathbb{1}_l \bigotimes_{p \in K_2} \mathbb{1}_p + \sigma_l^z \bigotimes_{p \in \text{star}(l)} \tau_p^z \right), \tag{4.2.47}$$

$\forall v \in K_0, l \in K_1$.

Let's also define another operator $\tilde{B}_v : \mathcal{H} \to \mathcal{H}$ which is similar to the 0-holonomy, the only difference being that it projects to states in which the product of the link spins that touch the vertex v is equal to -1:

$$\tilde{B}_v \left| \begin{array}{c} \vcenter{\hbox{\includegraphics}} \end{array} \right\rangle = \delta(x_1 x_2 x_3 x_4 x_5 x_6 x_7 x_8 ..., -1) \left| \begin{array}{c} \vcenter{\hbox{\includegraphics}} \end{array} \right\rangle. \tag{4.2.48}$$

Its matrix form is given by

$$\tilde{B}_v = \frac{1}{2} \left(\bigotimes_{l \in K_1} \mathbb{1}_l \bigotimes_{p \in K_2} \mathbb{1}_p - \bigotimes_{l \in \text{star}(v)} \sigma_l^z \right). \tag{4.2.49}$$

This operator will be of importance when we consider the problem of finding the shortest path between two vertices in the dual lattice.

Let's introduce a graphical notation to represent the states of this system. We color red a dual link l that hosts a $|-1\rangle_l$ state and blue a dual plaquette p that hosts a $|-1\rangle_p$ state. Links and plaquettes in the $|+1\rangle$ state are not colored. This is all illustrated in figure 4.2.15.

In this graphical notation, since a 3-gauge transformation flips the states of plaquettes in the boundary of a 3-simplex, it colors blue the boundary of the 3-simplex. The action of the
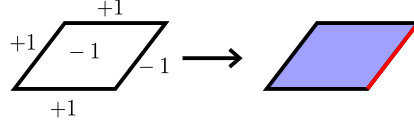
Figure 4.2.15: Graphical notation for the states of the dual $(D-2),(D-1)$-gauge theory.

operator (4.2.44) is thus represented as

$$A_x \left| \text{⟨figure⟩} \right\rangle = \frac{1}{2} \left(\left| \text{⟨figure⟩} \right\rangle + \left| \text{⟨figure⟩} \right\rangle \right) \tag{4.2.50}$$

Given a plaquette in the lattice, the 2-gauge transformation applied to it flips its spin while also flipping the spins of the links that form its boundary. This transformation is represented in graphical notation by coloring the plaquette blue and its boundary red. Thus, the action of the operator (4.2.45) is represented by

$$A_p \left| \text{⟨figure⟩} \right\rangle = \frac{1}{2} \left(\left| \text{⟨figure⟩} \right\rangle + \left| \text{⟨figure⟩} \right\rangle \right) \tag{4.2.51}$$

Note that a 3-gauge transformation of a 3-simplex can be constructed by applying 2-gauge transformations to the plaquettes that form its boundary. Thus, the only independent gauge transformation in this system is the 2-gauge transformation.

The 0-holonomy operator B_v projects states into states with trivial 0-holonomy, which is characterized by the property that the product of spins that touch the vertex v equals unity. In graphical notation, this means that trivial 0-holonomy is represented by either zero or an even

number of red dual links touching the vertex v. Thus,

$$B_v \left| \quad \right\rangle = \left| \quad \right\rangle, \tag{4.2.52}$$

$$B_v \left| \quad \right\rangle = 0, \tag{4.2.53}$$

for example.

The 1-holonomy operator B_l projects states into states in which the product of spins of the plaquettes that touch the link l equals the spin at l. In graphical notation, this means that trivial 1-holonomy states are the ones in which either there are no blue plaquettes and red links or blue dual plaquettes are bounded by red dual links. For example,

$$B_l \left| \quad \right\rangle = \left| \quad \right\rangle, \tag{4.2.54}$$

$$B_l \left| \quad \right\rangle = 0. \tag{4.2.55}$$

With this graphical notation, we can now analyze the ground states of the Hamiltonian (4.2.39). As in the case of all Hamiltonian models of Abelian higher gauge theories analysed in this thesis, the Hamiltonian (4.2.39) is given by a sum of commuting projectors. In fact, it is straightforward to show that the operators (4.2.44), (4.2.45), (4.2.46) and (4.2.47) are projectors by using the property that Pauli matrices square to the identity. The gauge transformation operators commute with each other, because they are composed only by sums and products of identity operators and σ^x, τ^x Pauli matrices. Likewise, the holonomy operators also commute with each other. The 3-gauge transformation commutes with the 0-holonomy operator, because the former acts non-trivially only over plaquettes while the later acts non-trivially only over links. Since higher gauge transformations don't change the higher holonomies of the states, the
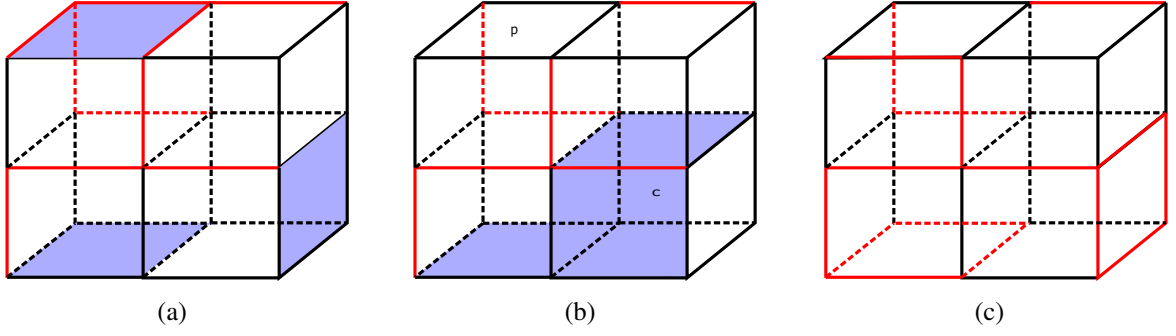
Figure 4.2.16: (a) Graphical representation of an arbitrary state of the dual $(D-2),(D-1)$-gauge theory. (b) Gauge equivalent state obtained from (a) by performing a 2-gauge transformation on p and a 3-gauge transformation on c. (c) State obtained from (a) by gauging away plaquette degrees of freedom by applying 2-gauge transformations.

gauge transformation operators commute with the holonomy operators. For example,

Therefore, since we have a Hamiltonian made of commuting projectors, we can solve this model exactly. The ground state subspace is given by

$$\mathcal{H}_0 = \{|\psi\rangle \in \mathcal{H} : A_x |\psi\rangle = A_p |\psi\rangle = B_v |\psi\rangle = B_l |\psi\rangle = |\psi\rangle, \forall x, p, v, l \in K\}.$$

We focus on finding states with trivial higher holonomy, i.e., we want to find

$$|\phi\rangle \in \mathcal{H}, B_v |\phi\rangle = B_l |\phi\rangle = |\phi\rangle, \forall v, l \in K_0 \cup K_1.$$

The true ground states of (4.2.39) can then be constructed by applying all higher gauge transformations to states with trivial higher holonomy:

$$|\psi\rangle = N \prod_{x \in K_3} A_x \prod_{p \in K_2} A_p |\phi\rangle \in \mathcal{H}_0,$$

where N is some normalization factor.

106

States with non-trivial higher holonomy are shown in figure 4.2.16. Since we will study only ground states of the system, all states from now on are to be considered as representatives of a class of locally gauge equivalent states. That is, we consider the states in figure 4.2.16 to be the same, since they are gauge equivalent. Since we can always make local 2-gauge transformations, we can gauge away the plaquette degrees of freedom of the state in 4.16(a), yielding the state in figure 4.16(c). Therefore, the degrees of freedom that give a non-zero contribution to the energy of the system here are link degrees of freedom. Note that the red links form a graph λ over the lattice. All these links have non-trivial 1-holonomy and thus the size (number of links) of this graph contributes to the energy of the state. Also, vertices that contribute with a non-trivial 0-holonomy touch an odd number of links. Thus, the energy of a state with non-trivial higher holonomy is given by

$$E = E_0 + |\lambda| + N_{I_o}, \tag{4.2.56}$$

where E_0 is the ground state energy, $|\lambda|$ is the size of the graph (number of red links) and N_{I_o} is the number of vertices with odd incidence number.

The ground state is thus attained if there are no red links at all. Therefore, there is only one ground state in this system, which is the trivial one:

$$|\phi_0\rangle = \bigotimes_{l \in K_1} |+1\rangle_l \bigotimes_{p \in K_2} |+1\rangle . \tag{4.2.57}$$

Equation (4.2.56) states that the energy of the system depends on the number of vertices with odd incidence number of red links. If we introduce a coupling constant $\alpha \in \mathbb{R}$ to the 0-holonomy operators and define the parameterized Hamiltonian

$$H(\alpha) = -\sum_{x \in K_3} A_x - \sum_{p \in K_2} A_p - \sum_{l \in K_1} B_l - \alpha \sum_{v \in K_0} B_v, \tag{4.2.58}$$

we can tune the importance of this interaction to the energy of the system, which is given now by
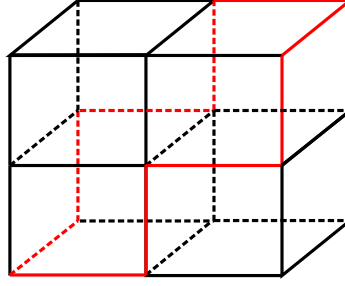
$$E = E_0 + |\lambda| + \alpha N_{I_o}. \tag{4.2.59}$$

Figure 4.2.17: When $\alpha >> |K_1|$, the ground state of the system is formed by closed loops of red links.

The term $|\lambda|$ can be at most proportional to the number of links $|K_1|$ in the lattice. Thus, if

$$\alpha >> |K_1|,$$

we have that the 0-holonomy dominates the contribution to the energy of the system. To minimize this energy and force the system into a ground state, we must then minimize the number of vertices that touch an odd number of red links. Any red link arriving at a vertex must not end there, it must be joined to another red link. Thus, the ground state of the system is formed by *closed loops* of red links, as in figure 4.2.17.

Now, let $v_1, v_2 \in K_0$ be two vertices in the lattice, as in figure 4.18(a). At these vertices, we can define two operators $\tilde{B}_{v_1}, \tilde{B}_{v_2}$ of the kind defined in (4.2.49). We replace the usual 0-holonomies at v_1 and v_2 by the operators $\tilde{B}_{v_1}$ and $\tilde{B}_{v_2}$ in the Hamiltonian (4.2.58). As a result, we have the following parameterized Hamiltonian

$$H(v_1, v_2; \alpha) = -\sum_{x \in K_3} A_x - \sum_{p \in K_2} A_p - \sum_{l \in K_1} B_l - \alpha \sum_{\substack{v \in K_0 \\ v \neq v_1, v_2}} B_v - (\tilde{B}_{v_1} + \tilde{B}_{v_2}). \qquad (4.2.60)$$

From here on we take $\alpha >> |K_1|$. The new added terms $\tilde{B}_{v_1}$ and $\tilde{B}_{v_2}$ project states into states with vertex with an odd incidence number of red links. Therefore, in the ground state, there must be at least one red link that ends at vertices v_1 and v_2, just as in figure 4.18(b). Now, since $\alpha >> |K_1|$, to minimize energy, all other vertices must have an even incidence number of red links. So, red links must end at no other vertices besides v_1 and v_2. The red links must thus be connected, as in figure 4.18(c). Finally, to minimize the 1-holonomy terms is to minimize the number of red links. Thus, the ground state must minimize the number of red links that goes from v_1 to v_2. That is, it must minimize the *path colored by red links* between the two vertices. Therefore, the ground state of this system finds the *shortest path* between the two vertices.
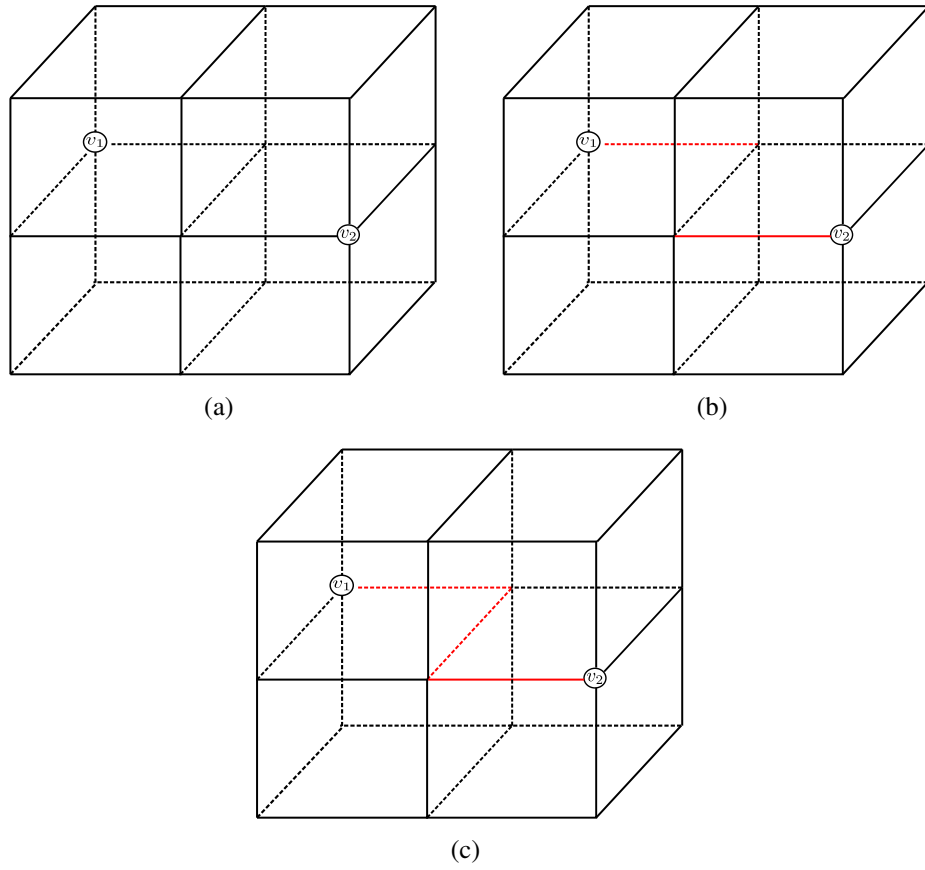
Figure 4.2.18: Given two vertices v_1 and v_2 as in (a), the ground states of the Hamiltonian (4.2.60) are found by coloring red the shortest paths between v_1 and v_2, as in (c). Here we represent this in a regular square lattice for simplicity, but it is true for any lattice.

Thus, given two vertices in the lattice, we can construct the parameterized Hamiltonian (4.2.60) whose ground state finds the shortest path between these two points. The shortest path can be accessed by performing measurements of 1-holonomy operators. This system can thus be considered as a code for quantum computation of the shortest path between points in a graph. The true computation can be done by means of the adiabatic algorithm. The question of whether this algorithm is faster than the classical ones is still an open one.

Chapter 5

Conclusions and outlook

Topological phases of matter are quantum long-range entangled phases that cannot be classified by Landau's theory of symmetry breaking. In $(2+1)d$, all topological phases are known to be classified by *modular unitary tensor categories* (MTCs) [23, 57, 58, 59]. This classification, which is a highly non-trivial subject, is given in the following sense: given a MTC, we can use it to describe the physics of an anyonic system. From this system of anyons, we can figure out the topologically ordered system whose excited states are given by this exact system of anyons. Moreover, given a system with topological order, we can figure out the MTC that describes the physics of its anyonic excitations. This procedure only works in 2-dimensions, and no general classification is known in $(D+1)d$ for $D > 2$.

To provide some insights into how to classify topological order in $(D+1)d$, some examples of exactly solvable Hamiltonian models of topological order in $(3+1)d$ were constructed in the literature [26, 27]. In [43, 1], a general formalism to construct Hamiltonian models of topological order based on Abelian lattice higher gauge theories in any dimension D was introduced. Using this formalism, it is possible to construct many examples of models with topological order in any dimension D. Moreover, this formalism allows us to find explicit formulas for the ground state degeneracy and the topological entanglement entropy in terms of topological invariants of the underlying manifold.

However, it was recently found that, in $(3+1)d$, other phases of matter with long-range entanglement can exist that have different characteristics than those of topological phases of matter. These so-called fracton phases of matter are long-range entangled states [60] whose ground state degeneracy is not topological, and in fact depends on the size of the system. Quasiparticles in fracton phases have mobility restrictions.

In this thesis, we used the general formalism of Abelian higher gauge theories introduced in [1] and reviewed in chapter 3 as an inspiration to construct Hamiltonian models whose ground states are quantum phases of matter exhibiting different behavior than topological phases. Our approach, explained in chapter 4, was to modify some aspects of Abelian higher gauge theories and construct exactly solvable Hamiltonian models based on the modified formalism.

In section 4.1.3, we modified the geometrical input of Abelian higher gauge theories to construct an example of a *subsystem symmetry-enriched topological phase* [2]. This model has subsystem symmetry and reduces to the $3D$ Toric Code when the symmetry is broken. Its physical properties resemble that of fracton phases. Namely, the ground state degeneracy of this model is not topological and grows subextensively with the system size, and some of the quasiparticles in this model are completely immobile.

In section 4.2, we modified the dynamics of the degrees of freedom of Abelian higher gauge theories to construct Hamiltonian models whose ground states can be used to measure *geometric properties* of the underlying manifold. More specifically, we constructed models whose ground states can be used to find the *shortest paths* between two given points.

There are some open questions waiting for answers to fully understand the physics of the model introduced in 4.1.3. For example, in SET systems, quasiparticles carry a fractional charge under the symmetry group. For instance, in FQHE states, anyons carry a fraction of the electron charge. This phenomenon, known as symmetry fractionalization, is ubiquitous in symmetry-enriched topological phases [61]. The mechanisms behind *subsystem-symmetry fractionalization* are already under investigation [62]. Further studies are needed to understand how these mechanisms would apply to the model shown in section 4.1.3.

The models of 4.2 encode geometrical properties of the manifold in their ground states. One may ask then how to use these models in *quantum computing*. It is possible to use the Hamiltonian (4.2.60) as a *quantum algorithm* to find the shortest path between two points in *adiabatic quantum computing* [63]. However, it is an open question whether such quantum algorithm outperforms the classical ones. Further investigation is also needed to find out if it is possible to construct a quantum circuit algorithm analog to (4.2.60).

Finally, the formalism of Abelian higher gauge theories has proved to be a very clear path to learn about topological order in $(D+1)d$. From this formalism, we were able to compute the proper topological dependency of the ground state degeneracy and of the entanglement entropy in a general manner, without resorting to concrete examples. The next steps in the

understanding of topological order in $(D + 1)d$ through this formalism would be to consider general *non-Abelian* groups. Fusion and braiding of non-Abelian quasiparticles are important characteristics of topological order. In $2D$, fusion and braiding essentially classify all possible topological phases through modular unitary tensor categories. Thus, to understand the mechanisms of fusion and braiding in higher dimensions would give us a much deeper knowledge on the nature of topological phases.

Appendix A

Homology and homological algebra

Throughout the text we made extensive use of algebraic topology concepts such as chain complexes and homology groups. To make this work as self-contained as possible, in this appendix we briefly review some basic notions of simplicial homology and cohomology. For more details, we refer to [44].

A.1   Simplicial complexes

Let $v_0, v_1, ..., v_r$ be geometrically independent points in $\mathbb{R}^n$, where $n \geq r$. That is, no $(r-1)$-dimensional hyperplane contains all $r+1$ points. The *oriented r-simplex* σ^r is the smallest convex set in $\mathbb{R}^n$ containing the $r+1$ points $v_0, ..., v_r$. It is given by

$$\sigma^r = \left\{ x \in \mathbb{R}^n | x = \sum_{i=0}^{r} c_i v_i, c_i \geq 0, \sum_{i=0}^{r} c_i = 1 \right\} \tag{A.1.1}$$

and denoted as

$$\sigma^r = (v_0, v_1, ..., v_r). \tag{A.1.2}$$

Examples of simplexes are given in figure A.1.1.

The order in which the vertices appear defines the orientation of the r-simplex. For example, the 1-simplex $\sigma^1 = (v_0 v_1)$ can be understood as an oriented line segment from v_0 to v_1. The opposite $-\sigma^1 = (v_1 v_0)$ is understood as the line segment from v_1 to v_0. Even permutations of the vertices in a r-simplex don't change its orientation, while odd permutations of it vertices do change its orientation to the opposite one.
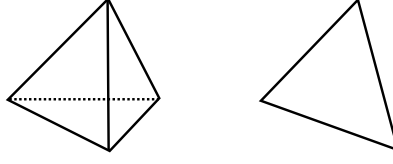
Figure A.1.1: Example of a 3-simplex (tetrahedron) and a 2-simplex (triangle).

For $q \leq r$, a *q-face* σ^q of a r-simplex σ^r is a q-simplex made of $q + 1$ points $(v_{i_0}, ..., v_{i_q})$ chosen from the points $(v_0, ..., v_r)$ defining the r-simplex σ^r. For example, a triangle or a link are faces of a 3-simplex (tetrahedron). We write $\sigma^q \leq \sigma^r$ if σ^q is a face of σ^r.

Let K be a set of a finite number of simplexes. We say that K is a *simplicial complex* if for any simplex $\sigma \in K$ and any of its faces $\sigma' \leq \sigma$, $\sigma' \in K$, and if for any two simplexes $\sigma, \sigma' \in K$, either $\sigma \cap \sigma' = \emptyset$ or there is a common face between σ and σ'. We denote $K_n \subset K$ the set of n-simplices only. From equation (A.1.1), we can always embed K into $\mathbb{R}^n$. The geometrical realization of K in $\mathbb{R}^n$, denoted by $|K|$, is a subset of $\mathbb{R}^n$ known as a *polytope*. A topological space M which is homeomorphic to a polytope $|K|$ is said to be a *triangulable space*. The simplicial complex $|K|$ is then the *triangulation* of M.

A.2   Homology of simplicial complexes

We define the *r-chain group* $C_r(K)$ of a simplicial complex K to be the free Abelian group generated by the oriented r-simplexes in K. If $r > \dim K$, $C_r(K) = 0$. If there are I_r r-simplexes in K, an element $c \in C_r(K)$, called an *r-chain*, is expressed as

$$c = \sum_{i=1}^{I_r} c_i \sigma_i^r, \tag{A.2.1}$$

where $c_i \in \mathbb{Z}$. The group structure is given by defining the sum of two r-chains $c, c' \in C_r(K)$ to be

$$c + c' = \sum_i (c_i + c_i') \sigma_i^r. \tag{A.2.2}$$

Let σ^r be an oriented r-simplex. The *boundary* $\partial_r \sigma^r$ of σ^r is the $(r-1)$-chain given by

$$\partial_r \sigma^r = \sum_{i=0}^r (-1)^i (v_0 v_1, ..., \hat{v}_i...v_r), \tag{A.2.3}$$

114

where the hat in $\hat{v}_i$ indicates that the vertex v_i is omitted in the simplex. For example,

$$\partial_2(v_0 v_1 v_2) = (v_1 v_2) - (v_0 v_2) + (v_0 v_1).$$

The boundary of an r-simplex is the geometrical boundary of the simplex. For example, the boundary of a 2-simplex are the links that form the triangle. Given this definition, we can regard ∂_r as an operator acting over r-simplexes. If we state that ∂_r acts over r-chains $c \in C_r(K)$ as

$$\partial_r c = \sum_i c_i \partial_r \sigma_i^r, \tag{A.2.4}$$

we can regard $\partial_r : C_r(K) \to C_{r-1}(K)$ as a *boundary operator* taking r-chains to $(r-1)$-chains. Clearly, the boundary operator is a group homomorphism.

Given a n-dimensional simplicial complex K, there is a sequence of free Abelian groups and homomorphisms

$$0 \xrightarrow{i} C_n(K) \xrightarrow{\partial_n} C_{n-1}(K) \xrightarrow{\partial_{n-1}} ... \xrightarrow{\partial_1} C_0(K) \xrightarrow{\partial_0} 0 \tag{A.2.5}$$

where $i : 0 \hookrightarrow C_n(K)$ is the inclusion map and 0 is regarded as the trivial group with only the unit element $0 \in C_n(K)$. This sequence is called the *chain complex* associated to K.

Let $c \in C_r(K)$ be a r-chain. If c is such that

$$\partial_r c = 0, \tag{A.2.6}$$

then, c is called an r-*cycle*. The r-cycles are thus elements of the r-chain group that have no boundary. They form a subgroup $Z_r(K) \subset C_r(K)$, the r-cycle group. By definition, $Z_r(K) = \ker\partial_r$.

Let $c \in C_r(K)$ be a r-chain. If there is a $(r+1)$-chain $c' \in C_{r+1}(K)$ such that

$$c = \partial_{r+1} c', \tag{A.2.7}$$

then c is called a r-*boundary*. The r-boundaries are thus elements of the r-chain group that are boundary of a higher dimensional chain. They form a subgroup $B_r(K) \subset C_r(K)$, and clearly $B_r(K) = \mathrm{im}\partial_{r+1}$.

Let $\partial_r : C_r(K) \to C_{r-1}$ and $\partial_{r+1} : C_{r+1}(K) \to C_r(K)$ be boundary maps. The composite

map $\partial_r \circ \partial_{r+1} : C_{r+1}(K) \to C_{r-1}(K)$ is a zero map, taking any $c \in C_{r+1}(K)$ to $(\partial_r \circ \partial_{r+1})c = 0$. In fact, let $\sigma^{r+1} = (v_0, ..., v_{r+1})$ be a oriented $(r+1)$-simplex. We have that

$$\partial_r(\partial_{r+1}\sigma^{r+1}) = \partial_r \sum_{i=0}^{r+1}(-1)^i(v_0...\hat{v}_i...v_{r+1})$$

$$= \sum_{i=0}^{r+1}(-1)^i \left(\sum_{j=0}^{i-1}(-1)^j(v_0...\hat{v}_j...\hat{v}_i...v_{r+1}) + \sum_{j=i+1}^{r+1}(-1)^{j-1}(v_0...\hat{v}_i...\hat{v}_j...v_{r+1}) \right)$$

$$= \sum_{j<i}(-1)^{i+j}(v_0...\hat{v}_j...\hat{v}_i...v_{r+1}) - \sum_{j>i}(-1)^{i+j}(v_0...\hat{v}_i...\hat{v}_j...v_{r+1}) = 0.$$

It follows that the r-boundary group $B_r(K)$ is a subgroup of the r-cycle group $Z_r(K)$, i.e.,

$$B_r(K) \subset Z_r(K). \tag{A.2.8}$$

In fact, any element $c \in B_r(K)$ is such that there exists $c' \in C_{r+1}(K)$ such that $c = \partial_{r+1}c'$. Thus, $\partial_r c = \partial_r(\partial_{r+1}c') = 0$, which means that c is also an element of $Z_r(K)$. This fact agrees with our intuition that a boundary of some object has no boundary. The elements of $Z_r(K)$ that are not boundaries of some higher dimensional object can be used to characterize the topology of a space.

Let K be a n-dimensional simplicial complex. The *rth homology group* $H_r(K), 0 \leq r \leq n$, associated to K is given by

$$H_r(K) = Z_r(K)/B_r(K) = \ker\partial_r/\mathrm{im}\partial_{r+1} \tag{A.2.9}$$

That is, $H_r(K)$ is the set of equivalence classes of r-cycles that are not boundaries of $(r+1)$-chains, i.e.,

$$H_r(K) = \{[c]|c \in Z_r(K)\},$$

where the equivalence classes $[c]$ are defined through the equivalence relation $c\ c'$ if $c - c' \in B_r(K)$. That is, two r-cycles are equivalent if they differ by a r-boundary. Homology groups are *topological invariants* of manifolds [64, 65]. This means that homeomorphic manifolds have isomorphic homology groups.

A.3 Cohomology of simplicial complexes

Cohomology theory is constructed by *dualizing* the algebraic structure of homology theory. Let K be a n-dimensional simplicial complex. Let $C_r(K)$ be a r-chain group and let G be an Abelian group. We define a r-*cochain* c^* as a homomorphism $c^* : C_r(K) \to G$. The evaluation of c^* on a r-chain $c \in C_r(K)$ is denoted by

$$c^*(c) = \langle c^*, c \rangle \in G.$$

The set $C^r(K) = \mathrm{Hom}(C_r(K), G)$ of r-cochains has a natural group structure. The group $C^r(K)$ is called the r-*cochain group*.

Associated to the boundary operator $\partial_r : C_r(K) \to C_{r-1}(K)$, we can canonically define the *coboundary operator* $d^{r-1} : C^{r-1}(K) \to C^r(K)$ as

$$\langle c^*, \partial_r c \rangle = \langle d^{r-1} c^*, c \rangle , \tag{A.3.1}$$

for any $c \in C_r(K), c^* \in C^{r-1}(C)$. Given this definition, it is straightforward to check that

$$d^r \circ d^{r-1} = 0. \tag{A.3.2}$$

The coboundary operator allows us to define the sequence of free Abelian groups

$$\dots \xleftarrow{d^{r+1}} C^{r+1}(K) \xleftarrow{d^r} C^r(K) \xleftarrow{d^{r-1}} C^{r-1}(K) \xleftarrow{d^{r-2}} \dots \tag{A.3.3}$$

called the *cochain complex* associated to the simplicial complex K. Therefore, we can define groups analogous to the r-cycle and r-boundary groups $Z_r(K)$ and $B_r(K)$.

Let $c^* \in C^r(K)$ be a r-cochain. If

$$d^r c^* = 0, \tag{A.3.4}$$

then c^* is called a r-*cocycle*. The set of r-cocycles $Z^r(K) = \ker d^r$ is a subgroup of $C^r(K)$ called the r-*cocycle group*.

Let $c^* \in C^r(K)$ be a r-cochain. If there exists $b^* \in C^{r-1}(K)$ such that

$$c^* = d^{r-1}b^*, \tag{A.3.5}$$

then c^* is called a *r-coboundary*. The set of r-coboundaries $B^r(K) = \mathrm{im}d^{r-1}$ is a subgroup of $C^r(K)$ called the *r-coboundary group*.

Following the same reasoning of section A.2, we can show that $B^r(K) \subset Z^r(K)$. Therefore, we can define the *rth cohomology group with coefficients in G* associated to K as

$$H^r(K) = Z^r(K)/B^r(K) = \mathrm{ker}d^r/\mathrm{im}d^{r-1}. \tag{A.3.6}$$

A.4 Homological algebra

In what follows, we will give a brief review on the algebraic structure used in the construction of Abelian higher gauge theories. In particular, we are interested in discussing the properties of maps between chain complexes.

An *abstract chain complex* $(C_\bullet, \partial_\bullet)$ is a sequence of Abelian groups $\{C_n\}_{n\in\mathbb{Z}}$ and group morphisms $\partial_n : C_n \to C_{n-1}$ such that the composition $\partial_{n-1} \circ \partial_n = 0$. In a similar fashion, an *abstract cochain complex* $(C^\bullet, d^\bullet)$ is a sequence of Abelian groups $\{C^n\}_{n\in\mathbb{Z}}$ and group morphisms $d^n : C^n \to C^{n+1}$ such that $d^{n+1} \circ d^n = 0$ for all $n \in \mathbb{Z}$.

Given an abstract chain complex $(C_\bullet, \partial_\bullet)$, we can define homology groups as

$$H_n(C) = \mathrm{ker}\partial_n/\mathrm{im}\partial_{n+1}. \tag{A.4.1}$$

Likewise, given an abstract cochain complex $(C^\bullet, d^\bullet)$, we define cohomology groups as

$$H^n(C) = \mathrm{ker}d^n/\mathrm{im}d^{n-1}. \tag{A.4.2}$$

Different cell or simplicial complexes with the same homology and cohomology groups can be associated to a manifold, since homology and cohomology groups yield topological invariants.

Let $(C_\bullet, \partial_\bullet)$ and $(C'_\bullet, \partial'_\bullet)$ be two abstract chain complexes. A *p-map* $f : (C_\bullet, \partial_\bullet) \to (C'_\bullet, \partial'_\bullet)$ is a sequence of morphisms $f_n : C_n \to C'_{n-p}$, for $p \in \mathbb{Z}$. The set of all p-maps, denoted $\mathrm{hom}(C, C')^p$ is an Abelian group under the operation $(f+g)_n = f_n + g_n$. It is straightforward

to check that

$$\hom(C, C')^p = \prod_n \mathrm{Hom}(C_n, C'_{n-p}).$$

Let $\hom(C, C')^p$ be the set of all p-maps. Let $\delta^p : \hom(C, C')^p \to \hom(C, C')^{p+1}$ be the group morphism defined by

$$(\delta^p f)_n = f_{n-1} \circ \partial_n - (-1)^p \partial'_{n-p} \circ f_n,$$

for $f \in \hom(C, C')^p$. We have that $\delta^{p+1} \circ \delta^p = 0$, and thus $(\hom(C, C')^\bullet, \delta^\bullet)$ is an abstract cochain complex. The cohomology groups associated to this abstract cochain complex are given by

$$\mathrm{H}^p(C, C') = \ker \delta^p / \mathrm{im} \delta^{p-1}. \tag{A.4.3}$$

A theorem due to Brown [45] states that these cohomology groups are related to the homology and cohomology groups of the abstract chain complexes $(C_\bullet, \partial_\bullet)$ and $(C'_\bullet, \partial'_\bullet)$ through an isomorphism, i.e.,

$$\mathrm{H}^p(C, C') \cong \prod_n H^n(C, H_{n-p}(C')), \tag{A.4.4}$$

where $H^n(C, H_{n-p}(C'))$ are cohomology groups of $(C_\bullet, \partial_\bullet)$ with coefficients in the homology groups of $(C'_\bullet, \partial'_\bullet)$.

We can also construct abstract chain complex using duals of Abelian groups. All irreducible representations r of an Abelian group G are 1-dimensional and form an Abelian group $\hat{G}$. These irreducible representations are completely specified by the group morphism $\chi_r : G \to U(1)$, defined by $\chi_r(g) = \mathrm{Tr}\,(r(g))$, the character of r. The group $\hat{G}$ can be thought of as the group $\mathrm{Hom}(G, U(1))$ due to the correspondence $r \leftrightarrow \chi_r$. Given a moprhism f between finite Abelian groups, there is a dual morphism $\hat{f}$ defined by $r \mapsto \hat{f}(r) = r \circ f$, such that $\chi_{\hat{f}(r)} = \chi_r \circ f$ (see [66, 67] for more details).

Thus, given the Abelian group $\hom(C, C')^p$ and an arbitrary element $f \in \hom(C, C')^p$, we define its dual group $\hom(C, C')_p$ as the set of maps $s : \hom(C, C')^p \to U(1)$, $f \mapsto s(f) = \chi_s(f)$. Since there is a natural pairing between dual elements, we can define a boundary operator $\delta_p : \hom(C, C')_p \to \hom(C, C')_{p-1}$ as follows: let $m \in \hom(C, C')_p$ and $f \in \hom(C, C')^{p-1}$.

We define δ_p to be such that

$$\langle \delta_p m, f \rangle = \langle m, \delta^{p-1} f \rangle, \tag{A.4.5}$$

or equivalently,

$$\chi_{\delta_p m}(f) = \chi_m(\delta^{p-1} f).$$

It is straightforward to check that $\delta_p \circ \delta_{p-1} = 0$, and thus $(\hom(C, C')_p, \delta_p)$ is an abstract chain complex.

Appendix B

2-Groups, crossed modules and higher gauge theories

To generalize gauge theories, higher gauge theories use algebraic structures that generalize gauge groups to higher dimensions, in a sense we will describe shortly. In this appendix, we briefly review these higher dimensional algebraic structures. More specifically, we review basic notions of the theory of crossed modules and strict 2-groups. Then, we briefly review how to construct higher gauge theories using 2-groups and how the Abelian higher gauge theories of chapter 3 are a generalization to D-dimensions of a particular example of a higher gauge theory in 3-dimensions.

B.1 Groups as 1-dimensional algebraic structures

Let G be a group. We introduce a graphical notation to represent its elements and operations as follows: each group element $g \in G$ is represented by a curve starting and ending at the same point, i.e.,

$$g \in G \mapsto \quad \bullet \quad \overset{g}{\frown} \quad \bullet \qquad (B.1.1)$$

Group multiplication is thus the result of going through two loops in sequence and considering it as a new loop:

$$\overset{g}{\curvearrowright} \bullet \overset{h}{\curvearrowright} \bullet = \bullet \overset{gh}{\curvearrowright} \bullet \qquad\qquad\qquad \text{(B.1.2)}$$

The inverse of a group element is given by a loop going in the reverse direction:

$$\overset{g^{-1}}{\curvearrowright} \bullet = \bullet \overset{g}{\curvearrowleft} \bullet \qquad\qquad\qquad \text{(B.1.3)}$$

And the group unit $e \in G$ is given by the trivial loop

$$\overset{e}{\curvearrowright} \bullet = \bullet \qquad\qquad\qquad \text{(B.1.4)}$$

Since the group structure, given by its elements and operations, can be captured and represented by curves, we say that it is a *1-dimensional algebraic structure*. Based on this notion, one could try to generalize groups to a higher dimensional algebraic structure by using a set G with two different group structures. The extra structure could thus be assigned to surfaces enclosed by curves. Thus, the element $\alpha \in G$ could be represented as

$$\alpha \in G \mapsto \bullet \,\, \alpha \,\, \bullet \qquad\qquad\qquad \text{(B.1.5)}$$

which we call a *bigon*. Denoting by $*$ and by concatenation the two different operations coming from the two different group structures of G, we have that

$$\bullet \,\, \alpha \,\, \bullet \,\, \beta \,\, \bullet = \bullet \,\, \alpha * \beta \,\, \bullet \qquad\qquad\qquad \text{(B.1.6)}$$

and

$$(B.1.7)$$

These multiplications imply a natural consistency relation comming from the geometrical description, given by

$$(B.1.8)$$

where $u = (\alpha * \beta)(\gamma * \delta) = (\alpha\gamma) * (\beta\delta)$. This condition is the associativity in two dimensions. In fact, for the case where we have two group structures, for this condition to be satisfied, both groups must be equal and Abelian [28, 68]. This is why if we want to build non-trivial 2-dimensional algebraic structures, we must go beyond groups.

B.2   Crossed modules and 2-groups

Let G_1, G_2 be groups. A *crossed module* G is a quadruple G = $(G_1, G_2.\partial, \triangleright)$, where $\partial : G_2 \to G_1$ is a group morphism and $\triangleright : G_1 \times G_2 \to G_2$ is a group action of G_1 on G_2 such that, for any $g \in G_1, \alpha, \beta \in G_2$,

$$\partial(g \triangleright \alpha) = g\partial(\alpha)g^{-1}, \tag{B.2.1}$$

$$\partial(\beta) \triangleright \alpha = \beta\alpha\beta^{-1}. \tag{B.2.2}$$

Crossed modules were introduced in the context of homotopy theory [69]. A simple example of crossed module is given by a group $G_1 = G$, a normal subgroup $G_2 = N \subset G$, the trivial morphism $\partial = \mathrm{id}_G$ and the action by conjugation $g \triangleright h = ghg^{-1}$. Another simple example is given if we take G_1 and G_2 Abelian groups, the trivial group action and any morphism $\partial : G_2 \to G_1$.

The idea is to use crossed modules to label bigons to construct a non-trivial 2-dimensional algebraic structure. Given a crossed module $\mathsf{G} = (G_1, G_2, \partial, \triangleright)$, we define

$$(g, \alpha) \in G_1 \times G_2 \mapsto \quad \bullet \quad \overset{g}{\underset{h = \partial(\alpha)^{-1}g}{\alpha}} \quad \bullet \tag{B.2.3}$$

The path labelled by $s(g, \alpha) = g$ is called the *source*, and the one labelled by $t(g, \alpha) = \partial(\alpha)^{-1}g$ is called the *target*. The element (g, α) maps the path $s(g, \alpha)$ to the path $t(g, \alpha)$. In particular, if $\alpha = 1$, the bigon is the trivial surface mapping g to itself. Thus, recalling our definition of a group element as a loop, we can make the connection

$$\bullet \overset{g}{\longrightarrow} \bullet \quad = \quad \bullet \overset{g}{\underset{g}{1}} \bullet \tag{B.2.4}$$

To have a non-trivial 2-dimensional algebraic structure, bigons labelled by crossed module elements must be able to bypass the arguments given in [28, 68]. Thus, we define the horizontal composition as

$$\bullet \overset{g}{\underset{\partial(\alpha)^{-1}g}{\alpha}} \bullet \overset{h}{\underset{\partial(\beta)^{-1}h}{\beta}} \bullet \quad = \quad \bullet \overset{gh}{\underset{\partial(\alpha)^{-1}g\partial(\beta)^{-1}h}{\gamma}} \bullet \tag{B.2.5}$$

where $\gamma = (g \triangleright \beta)\alpha$. We denote this product as $(g, \alpha) * (h, \beta) = (gh, (g \triangleright \beta)\alpha)$. The vertical composition is only defined for bigons $(g, \alpha), (h, \beta)$ with matching sources and targets $t(g, \alpha) = s(h, \beta)$. It is defined as

$$\begin{matrix} \bullet \overset{g}{\underset{h}{\alpha}} \bullet \\ \bullet \overset{}{\underset{\partial(\beta)^{-1}h}{\beta}} \bullet \end{matrix} \quad = \quad \bullet \overset{g}{\underset{\partial(\alpha\beta)^{-1}g}{\alpha\beta}} \bullet \tag{B.2.6}$$

Note that since $h = \partial(\alpha)^{-1}g$, $\partial(\beta)^{-1}h = \partial(\alpha\beta)^{-1}g$. We denote this product as $(g, \alpha)(h, \beta) =$

$(g, \alpha\beta)$.

These operations are well-defined and it is straightforward to check that they respect the source and targets implied by the diagrams. The identities for these products are given by

$$g(g, \alpha) = (g, 1)(g, \alpha) = (g, \alpha), \tag{B.2.7}$$

$$1 * (g, \alpha) = (1, 1) * (g, \alpha) = (g, \alpha), \tag{B.2.8}$$

and the vertical inverse is given by

$$(g, \alpha)^{-1} = (\partial(\alpha)^{-1}g, \alpha^{-1}). \tag{B.2.9}$$

These properties define the 2-dimensional algebraic structure. Vertical and horizontal associativity can me immediately verified, i.e.,

$$(g, \alpha)((h, \beta)(t, \gamma)) = ((g, \alpha)(h, \beta))(t, \gamma), \tag{B.2.10}$$

$$(g, \alpha) * ((h, \beta) * (t, \gamma)) = ((g, \alpha) * (h, \beta)) * (t, \gamma). \tag{B.2.11}$$

The exchange rule of equation (B.1.8), which is the associativity in 2-dimensions, can also be verified. In fact, this rule is given by

$$((g, \alpha) * (h, \beta))((t, \gamma) * (w, \xi)) = ((g, \alpha)(t, \gamma)) * ((h, \beta)(w, \xi)). \tag{B.2.12}$$

To verify it, let's expand both sides. We have

$$((g, \alpha) * (h, \beta))((t, \gamma) * (w, \xi)) = (gh, (g \triangleright \beta)\alpha)(tw, (t \triangleright \xi)\gamma) = (gh, (g \triangleright \beta)\alpha(t \triangleright \xi)\gamma), \tag{B.2.13}$$

and

$$((g, \alpha)(t, \gamma)) * ((h, \beta)(w, \xi)) = (g, \alpha\gamma)(h, \beta\xi) = (gh, (g \triangleright \beta\xi)\alpha\gamma). \tag{B.2.14}$$

We have that (g, α) and (t, γ) must have matching sources and targets because we are composing these bigons vertically. This means that $t = \partial(\alpha)^{-1}g$, and

$$\alpha(t \triangleright \xi) = \alpha(\partial(\alpha)^{-1} \triangleright (g \triangleright \xi)) = \alpha\alpha^{-1}(g \triangleright \xi)\alpha = (g \triangleright \xi)\alpha.$$

Thus, the exchange rule follows. This was the rule that prevented the 2-dimensional algebraic structure made of two group structures to be non-trivial. Here, we have no such impediment. Using crossed modules, we can construct non-trivial 2-dimensional algebraic structures.

The crossed module $G = (G_1, G_2, \partial, \triangleright)$ defines a *standard 2-group*, which we denote by $\bar{G}$. To define a 2-group in general, we would have to review category theory and the theory of 2-categories. For more details, we refer to [70]. Any strict 2-group is isomorphic to $\bar{G}$ for some crossed module G. In fact, the category of crossed modules is equivalent to the category of strict 2-groups [71].

B.3   Higher gauge theories

Let $G = (G_1, G_2, \partial, \triangleright)$ be a crossed module and let M be a 3-dimensional manifold. Let K be a triangulation of M. That is, $K = K_0 \cup K_1 \cup K_2 \cup K_3$, where K_0 is the set of vertices, K_1 is the set of links, K_2 is the set of triangles and K_3 is the set of tetrahedrons. To construct a 3-dimensional lattice higher gauge theory over this space, we assign elements of G_1 to links $l \in K_1$ and elements of G_2 to triangles $p \in K_2$ through maps

$$f_1 : K_1 \to G_1, l \mapsto f_1(l) \in G_1,$$

$$f_2 : K_2 \to G_2, p \mapsto f_2(p) \in G_2.$$

For consistency, these maps must satisfy the following property [26, 28]: let $v_0, v_1, v_2 \in K_0$ be the vertices of an arbitrary triangle $p = (v_0 v_1 v_2)$. The *higher gauge configurations* f_1, f_2 must be such that

$$\partial(f_2((v_0 v_1 v_2)))^{-1} f_1((v_0 v_1)) f_1((v_1 v_2)) f_1((v_0 v_2))^{-1} \in \ker(\triangleright). \qquad \text{(B.3.1)}$$

The Hilbert space of this theory is thus given by these higher gauge configurations. That is, each basis state $|f\rangle \in \mathcal{H}$ of the Hilbert space is labelled by a higher gauge configuration. The inner product is defined to be the canonical inner product $\langle f | f' \rangle = \delta(f, f')$. The Hilbert space $\mathcal{H}$ cannot be written as a tensor product of local Hilbert spaces, due to the constraint (B.3.1) connecting degrees of freedom at links with degrees of freedom at triangles.

In usual gauge theory, there is the notion of the holonomy of a curve, which are related to the curvature of the gauge connection [46]. In a lattice gauge theory, the holonomy of a curve is

given by the product of degrees of freedom associated to links along the curve. The holonomy of a curve is invariant under gauge transformations. In the higher gauge theory setting, however, due to the relation between link degrees of freedom and triangle degrees of freedom, we must introduce the notion o *fake 1-holonomy* [26, 25, 28], which is truly invariant under 2-gauge transformations. For a triangle $p = (v_0 v_1 v_2) \in K_2$, the fake 1-holonomy is given by

$$h_p^1(f) = \partial(f_2((v_0 v_1 v_2)))^{-1} f_1((v_0 v_1)) f_1((v_1 v_2)) f_1((v_0 v_2))^{-1}. \tag{B.3.2}$$

The 1-holonomy realizes the parallel transport between two points. In a 2-group, we have also the notion of the transport of a curve along a surface, given by the bigon picture. In higher gauge theory, thus, we can also define a *2-holonomy*, associated to the parallel transport of a curve along a surface. Let $t = (v_0 v_2 v_2 v_3) \in K_3$ be a tetrahedron. The 2-holonomy is defined as [26, 28, 25]

$$h_t^2(f) = (f_1((v_0 v_1)) \triangleright f_2((v_1 v_2 v_3))) f_2((v_0 v_1 v_3)) f_2((v_0 v_2 v_3))^{-1} f_2((v_0 v_1 v_2))^{-1}, \tag{B.3.3}$$

and it is also 2-gauge invariant. To define 2-gauge transformations is a complex subject and we refer to [26, 28, 25] for further details.

Given these notions of a lattice higher gauge theory in 3-dimensions, one can construct a Hamiltonian model whose ground state is topological and extends the notions of Quantum Double Models to dimensions greater than two [26, 28]. Note that this construction is made with an arbitrary crossed module G. If we take the particular example of G being the crossed module with G_1 and G_2 as finite Abelian groups and the action $\triangleright : G_1 \times G_2 \to G_2$ as the trivial group action given by $(g, \alpha) \mapsto \alpha$, we have some simplifications. First, since the kernel of $\triangleright$ is G_1, we have that the product in (B.3.1) belongs to G_1, and thus no intricate relations between degrees of freedom at links and triangles exists. The Hilbert space can thus be written as the product of local ones:

$$\mathcal{H} = \bigotimes_{l \in K_1} \mathcal{H}_l \bigotimes_{p \in K_2} \mathcal{H}_p.$$

If we consider the chain groups generated by the triangulation K, higher gauge configurations f are maps between Abelian groups. Note that we can build a trivial chain complex $0 \to G_2 \xrightarrow{\partial} G_1 \to 0$ using the crossed module G. Thus, the maps defining the higher gauge configurations are just *chain maps* between chain complexes. Then, it follows that the higher

gauge theory constructed here is equivalent to the one in 3.2.3. This suggests a way to construct an Abelian higher gauge theory in any dimension D by considering D-dimensional chain complexes and group chain complexes as was done in chapter 3. Therefore, the Abelian higher gauge theory of chapter 3 is a generalization to any dimension D of a particular case of the 2-gauge theory in 3-dimensions introduced in [26, 28].

Appendix C

Fractons

Fracton models have as its main physical properties the presence of quasiparticles with mobility restrictions and a ground state degeneracy that grows exponentially with system size. The ground states of fracton models are locally indistinguishable from one another. In this appendix, to give an example of fracton phases of matter, we review the *X-cube model* [30].

C.1 The model

Consider a cubic lattice in $3D$ with spin-1/2 degrees of freedom located at its links. The Hamiltonian of the X-cube model is given by

$$H_X = -\sum_c A_c - \sum_{v,\mu} B_v^{(\mu)}, \tag{C.1.1}$$

where A_c is the product of σ^x over all links of the cube c and $B_v^{(\mu)}$, $\mu = xy, yz, xz$, is the product of σ^z over all links that touch the vertex v and belong to the plane μ. The action of A_c and $B_v^{(\mu)}$ is exemplified in figures C.1(a) and C.1(b), respectively.

C.2 Fracton properties

It can be shown that the operators A_c e $B_v^{(\mu)}$ are such that $A_c^2 = (B_v^{(\mu)})^2 = \mathbb{1}$ and that they commute for all cube c, vertex v and plane μ. Thus, the Hamiltonian is exactly solvable. The
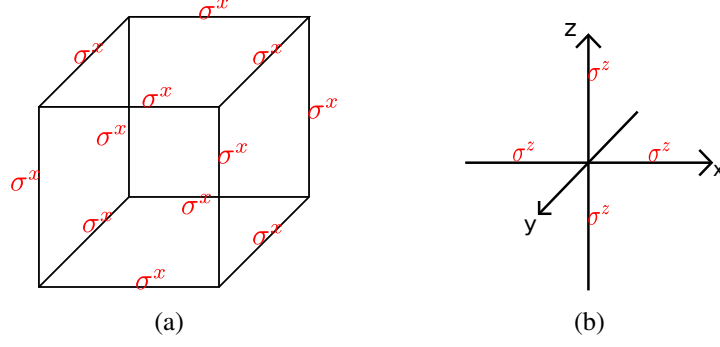
Figure C.1.1: (a) Action of A_c over an elementary cube. (b) Action of $B_v^{(xz)}$ over a vertex.

ground states of the system $|\psi\rangle$ are such that

$$A_c |\psi\rangle = |\psi\rangle , \ B_v^{(\mu)} |\psi\rangle = |\psi\rangle ,$$

for all cube c, vertex v and plane μ. The state

$$|\psi_0\rangle = \prod_c (\mathbb{1} + A_c) |0\rangle ,$$

where $|0\rangle$ is the state where every spin of the lattice is in the $|+1\rangle$ state is clearly a ground state. Therefore, the Hamiltonian H_X is frustration free.

In [30], it was shown that, if the cubic lattice has dimensions $L \times L \times L$, the subspace of ground states has dimension

$$GSD = 2^{6L-3},$$

and that ground states cannot be distinguished from each other through local measurements. Thus, it is considered that the system has topological order.

The excitations of the system are states $|\phi\rangle$ such that

$$A_c |\phi\rangle = - |\phi\rangle ,$$

and/or

$$B_v^{(\mu)} |\phi\rangle = - |\phi\rangle ,$$

for some cube c and/or some vertex v and plane μ. By applying at some link l the operator σ_l^z at the ground state $|\psi_0\rangle$, we construct an excited cube state, i.e., $|\phi\rangle = \sigma_l^z |\psi_0\rangle$, where $A_c |\phi\rangle = - |\phi\rangle$. The state $|\phi\rangle$ has four quasiparticles located at the four cubes that share the link
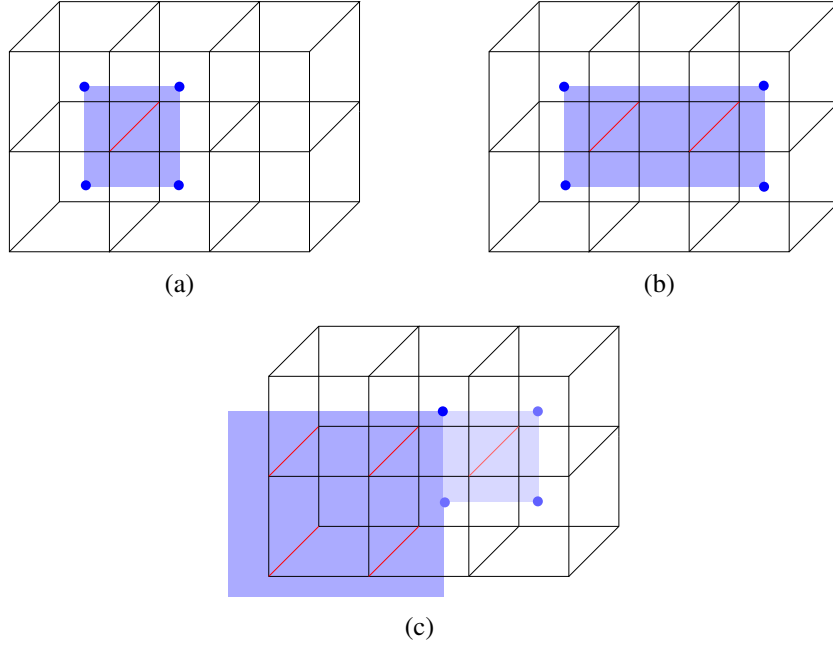
130

Figure C.2.1: (a) The state $|\phi\rangle = \sigma_l^z |\psi\rangle$, where we represent the presence of a σ^z operator at a link as a red link piercing a dual blue plaquette. The cube excitations are represented by blue dots. (b) By applying σ^z at a parallel link, we move two excitations without creating a new one. (c) If we try to move a single excitation, we create three new ones. Since this costs energy, fractons tend to remain immobile.

l. Note that, if we apply $\sigma_{l'}^z$ over $|\phi\rangle$, where l' is a link that is parallel to l, we move a pair of excitations to nearby cubes. However, quasiparticles cannot be moved individually. The cube excitations are completely immobile *fractons*. This is exemplified in figure C.2.1.

Now, by applying σ_l^x in some link l of the state $|\psi_0\rangle$, we obtain the excited state $|\phi\rangle = \sigma_l^x |\psi_0\rangle$ such that $B_v^{(\mu)} |\phi\rangle = - |\phi\rangle$, for two planes μ in which l is located. For example, in figure C.2.2, we represent the link l over which σ^x acts as a red link. The resulting state is an excited state of $B_v^{(xy)}$ and $B_v^{(xz)}$ at two vertices. The excitation of $B_v^{(xy)}$ is represented as a red dot, while the excitation of $B_v^{(xz)}$ is given by a green dot. We thus have in figure C.2(a) a pair of quasiparticles at each excited vertex. By applying σ^x at a link nearby l as in figure C.2(b), we move the pair of excitations in a straight line without energy cost. Nevertheless, if we try to move the pair of quasiparticles in a perpendicular direction, as in figure C.2(c), we create an extra excitation, represented by a yellow dot. Thus, excitations of $B_v^{(\mu)}$ also have mobility restrictions.

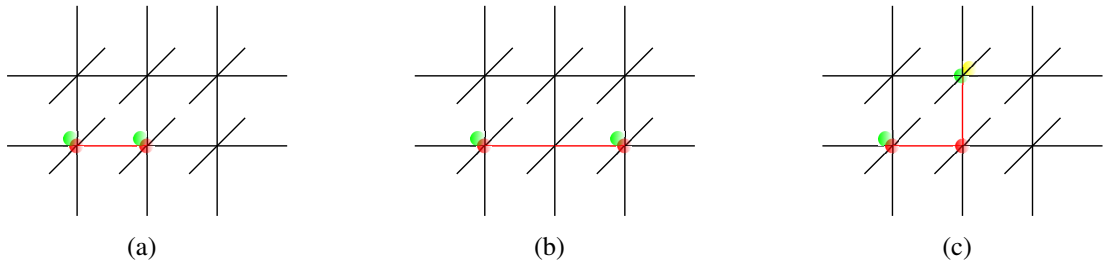Figure C.2.2: (a) The state $|\phi\rangle = \sigma_l^x |\psi\rangle$, where we represent the presence of an operator σ^x at a vertex as a red vertex. The vertex excitations are represented by colored circles. (b) By applying σ^x at a neighbour link, we move two excitations without creating a new one. (c) However, if we try to move the pair in a perpendicular direction, an extra excitation is created.

Bibliography

[1] Juan Pablo Ibieta-Jimenez, Marzia Petrucci, L. N. Xavier, and Paulo Teotonio-Sobrinho. Topological entanglement entropy in d-dimensions for abelian higher gauge theories. *Journal of High Energy Physics*, 2020(3):1–44, 2020.

[2] J. P. Ibieta-Jimenez, L. N. Queiroz Xavier, M. Petrucci, and P. Teotonio-Sobrinho. Fractonlike phases from subsystem symmetries. *Physical Review B*, 102(4):045104, 2020.

[3] Lev Landau. The theory of phase transitions. *Nature*, 138(3498):840–841, 1936.

[4] Subir Sachdev. *Quantum Phase Transitions*. Cambridge University Press, 2011.

[5] Daniel C. Tsui, Horst L. Stormer, and Arthur C. Gossard. Two-dimensional magnetotransport in the extreme quantum limit. *Physical Review Letters*, 48(22):1559, 1982.

[6] Robert B. Laughlin. Anomalous quantum hall effect: an incompressible quantum fluid with fractionally charged excitations. *Physical Review Letters*, 50(18):1395, 1983.

[7] Daijiro Yoshioka. *The Quantum Hall Effect*, volume 133. Springer Science & Business Media, 2002.

[8] Xiao-Gang Wen. Topological orders in rigid states. *International Journal of Modern Physics B*, 4(02):239–271, 1990.

[9] Xiao-Gang Wen. Colloquium: Zoo of quantum-topological phases of matter. *Reviews of Modern Physics*, 89(4):041004, 2017.

[10] Xiao-Gang Wen and Qian Niu. Ground-state degeneracy of the fractional quantum hall states in the presence of a random potential and on high-genus riemann surfaces. *Physical Review B*, 41(13):9377, 1990.

[11] Xie Chen, Zheng-Cheng Gu, and Xiao-Gang Wen. Local unitary transformation, long-range quantum entanglement, wave function renormalization, and topological order. *Physical Review B*, 82(15):155138, 2010.

[12] Jens Eisert, Marcus Cramer, and Martin B. Plenio. Colloquium: Area laws for the entanglement entropy. *Reviews of Modern Physics*, 82(1):277, 2010.

[13] Alexei Kitaev and John Preskill. Topological entanglement entropy. *Physical Review Letters*, 96(11):110404, 2006.

[14] Michael Levin and Xiao-Gang Wen. Detecting topological order in a ground state wave function. *Physical Review Letters*, 96(11):110405, 2006.

[15] A. Yu. Kitaev. Fault-tolerant quantum computation by anyons. *Annals of Physics*, 303(1):2–30, 2003.

[16] Chetan Nayak, Steven H. Simon, Ady Stern, Michael Freedman, and Sankar Das Sarma. Non-abelian anyons and topological quantum computation. *Reviews of Modern Physics*, 80(3):1083, 2008.

[17] Andrej Mesaros and Ying Ran. Classification of symmetry enriched topological phases with exactly solvable models. *Physical Review B*, 87(15):155115, 2013.

[18] Yuan-Ming Lu and Ashvin Vishwanath. Classification and properties of symmetry-enriched topological phases: Chern-simons approach with applications to z 2 spin liquids. *Physical Review B*, 93(15):155121, 2016.

[19] Maissam Barkeshli, Parsa Bonderson, Meng Cheng, and Zhenghan Wang. Symmetry fractionalization, defects, and gauging of topological phases. *Physical Review B*, 100(11):115147, 2019.

[20] Meng Cheng, Zheng-Cheng Gu, Shenghan Jiang, and Yang Qi. Exactly solvable models for symmetry-enriched topological phases. *Physical Review B*, 96(11):115107, 2017.

[21] John B. Kogut. An introduction to lattice gauge theory and spin systems. *Reviews of Modern Physics*, 51(4):659, 1979.

[22] M. A. Levin and X. G. Wen. String-net condensation: A physical mechanism for topological phases. *Phys. Rev. B*, 71:045110, 2005.

[23] Pavel Etingof, Shlomo Gelaki, Dmitri Nikshych, and Victor Ostrik. *Tensor categories*, volume 205. American Mathematical Soc., 2016.

[24] John C. Baez and Aaron D. Lauda. Higher-dimensional algebra v: 2-groups. *arXiv preprint math/0307200*, 2003.

[25] John C. Baez and Urs Schreiber. Higher gauge theory. *arXiv preprint math/0511710*, 2005.

[26] Alex Bullivant, Marcos Calçada, Zoltán Kádár, Paul Martin, and Joao Faria Martins. Topological phases from higher gauge symmetry in 3+ 1 dimensions. *Physical Review B*, 95(15):155118, 2017.

[27] Hudson Kazuo Teramoto Mendonça. *Teorias de 2-gauge e o invariante de Yetter na construção de modelos com ordem topológica em 3-dimensões*. PhD thesis, Universidade de São Paulo, 2017.

[28] Ricardo Costa de Almeida. *Topological order in three-dimensional systems and 2-gauge symmetry*. PhD thesis, Universidade de São Paulo, 2017.

[29] C. Chamon. Quantum glassiness in strongly correlated clean systems: an example of topological overprotection. *Phys. Rev. Lett.*, 94:040402, 2005.

[30] S. Vijay, J. Haah, and L. Fu. Fracton topological order, generalized lattice gauge theory, and duality. *Phys. Rev. B*, 94:235157, 2016.

[31] R. M. Nandkishore and M. Hermele. Fractons. *Ann. Rev. Cond. Matt. Phys.*, 10:295–313, 2019.

[32] J. Haah. Local stabilizer codes in three dimensions without string logical operators. *Phys. Rev. A*, 83:042330, 2011.

[33] Michael Pretko, Xie Chen, and Yizhi You. Fracton phases of matter. *International Journal of Modern Physics A*, 35(06):2030003, 2020.

[34] Salman Beigi, Peter W. Shor, and Daniel Whalen. The quantum double model with boundary: condensations and symmetries. *Communications in Mathematical Physics*, 306(3):663–694, 2011.

[35] Miguel Jorge Bernabé Ferreira, Pramod Padmanabhan, and Paulo Teotonio-Sobrinho. 2d quantum double models from a 3d perspective. *Journal of Physics A: Mathematical and Theoretical*, 47(37):375204, 2014.

[36] Yuting Hu, Yidun Wan, and Yong-Shi Wu. Twisted quantum double model of topological phases in two dimensions. *Physical Review B*, 87(12):125114, 2013.

[37] Jiannis K. Pachos. *Introduction to topological quantum computation*. Cambridge University Press, 2012.

[38] Alexei Yu. Kitaev, Alexander Shen, Mikhail N. Vyalyi, and Mikhail N. Vyalyi. *Classical and quantum computation*. Number 47. American Mathematical Soc., 2002.

[39] Miguel Jorge Bernabé Ferreira. *Teorias de gauge e modelos topológicos (anyons e ordem topológica)*. PhD thesis, Universidade de São Paulo, 2016.

[40] Shawn X. Cui, Dawei Ding, Xizhi Han, Geoffrey Penington, Daniel Ranard, Brandon C. Rayhaun, and Zhou Shangnan. Kitaev's quantum double model as an error correcting code. *Quantum*, 4:331, 2020.

[41] Juan Pablo Ibieta-Jimenez. *Entropia topológica de emaranhamento em teorias de Higher Gauge Abelianas*. PhD thesis, Universidade de São Paulo, 2019.

[42] Javier Ignacio Lorca Espiro. *Sobre o estado fundamental de teorias de n-gauge abelianas topológicas*. PhD thesis, Universidade de São Paulo, 2017.

[43] R. Costa de Almeida, J.P. Ibieta-Jimenez, J. Lorca Espiro, and P. Teotonio-Sobrinho. Topological order from a cohomological and higher gauge theory perspective. *arXiv preprint arXiv:1711.04186*, 2017.

[44] A. Hatcher. *Algebraic Topology*. Cambridge University Press, 2002.

[45] Ronald Brown. Cohomology with chains as coefficients. *Proceedings of the London Mathematical Society*, 3(3):545–565, 1964.

[46] Mikio Nakahara. *Geometry, Topology and Physics*. CRC press, 2003.

[47] C. Xu and J. E. Moore. Strong-weak coupling self-duality in the two-dimensional quantum phase transition of p+ip superconducting arrays. *Phys. Rev. Lett.*, 93:047003, 2004.

[48] C. Xu and J. E. Moore. Reduction of effective dimensionality in lattice models of super-conducting arrays and frustrated magnets. *Nucl. Phys. B*, 716:487–508, 2005.

[49] H. Yan. Hyperbolic fracton model, subsystem symmetry, and holography. *Phys. Rev. B*, 99:155126, 2019.

[50] H. Yan. Hyperbolic fracton model, subsystem symmetry, and holography. ii. the dual eight-vertex model. *Phys. Rev. B*, 100:245138, 2019.

[51] R. J. Baxter. *Exactly solved models in statistical mechanics*. Elsevier, 2016.

[52] G. K. Savvidy and F. J. Wegner. Geometrical string and spin systems. *Nucl. Phys. B*, 413:605–613, 1994.

[53] D. Espriu and A. Prats. Dynamics of the two-dimensional gonihedric spin model. *Phys. Rev. E*, 70:046117, 2004.

[54] D. Espriu and A. Prats. On gonihedric loops and quantum gravity. *J. Phys. A: Math. Gen.*, 39:1743, 2006.

[55] D. J. Williamson, Z. Bi, and M. Cheng. Fractonic matter in symmetry-enriched $u(1)$ gauge theory. *Phys. Rev. B*, 100:125150, 2019.

[56] Samuel Frederick Edwards and Phil W Anderson. Theory of spin glasses. *Journal of Physics F: Metal Physics*, 5(5):965, 1975.

[57] Alexei Kitaev. Anyons in an exactly solved model and beyond. *Annals of Physics*, 321(1):2–111, 2006.

[58] Eric Rowell, Richard Stong, and Zhenghan Wang. On classification of modular tensor categories. *Communications in Mathematical Physics*, 292(2):343–389, 2009.

[59] Xiao-Gang Wen. A theory of 2+ 1d bosonic topological orders. *National Science Review*, 3(1):68–106, 2016.

[60] Han Ma, A. T. Schmitz, S. A. Parameswaran, Michael Hermele, and Rahul M. Nandkishore. Topological entanglement entropy of fracton stabilizer codes. *Physical Review B*, 97(12):125101, 2018.

[61] Xie Chen. Symmetry fractionalization in two dimensional topological phases. *Reviews in Physics*, 2:3–18, 2017.

[62] David T. Stephen, José Garre-Rubio, Arpit Dua, and Dominic J. Williamson. Subsystem symmetry enriched topological order in three dimensions. *Physical Review Research*, 2(3):033331, 2020.

[63] Tameem Albash and Daniel A. Lidar. Adiabatic quantum computation. *Reviews of Modern Physics*, 90(1):015002, 2018.

[64] Joseph J Rotman. *An introduction to algebraic topology*, volume 119. Springer Science & Business Media, 2013.

[65] James R Munkres. *Elements of algebraic topology*. CRC press, 2018.

[66] Jean-Pierre Serre. *Linear Representations of Finite Groups*, volume 42. Springer, 1977.

[67] William Fulton and Joe Harris. *Representation Theory: a First Course*, volume 129. Springer Science & Business Media, 2013.

[68] B. Eckmann and P. J. Hilton. Group-like structures in general categories i multiplications and comultiplications. *Mathematische Annalen*, 145(3):227–255, 1962.

[69] John H. C. Whitehead. Combinatorial homotopy i. *Bull. Amer. Math. Soc*, 55(3):213–245, 1949.

[70] J. C. Baez and J. Huerta. An invitation to higher gauge theory. *Gen. Rel. Grav.*, 43:2335–2392, 2011.

[71] G. Janelidze. Internal crossed modules. *Georgian Mathematical Journal*, 10(1):99–114, 2003.